Effects of Inorganic Ambient Particle Type Mimics on the Differential Expression of a Pro-Inflammatory Mediator by A549 Cells *In Vitro*

by

Michael Ndukauba Eleghasim
B.Sc., University of Nigeria, Nsukka, 1998
M.A.Sc., Memorial University of Newfoundland, 2004.

THESIS SUBMITTED IN PARTIAL FULFILLMENT OF
THE REQUIREMENTS FOR THE DEGREE OF

MASTER OF SCIENCE

In the
Department
of
Chemistry

SIMON FRASER UNIVERSITY

2007

APPROVAL

Name: Ndukauba Michael Eleghasim

Degree: Master of Science

Title of Thesis: Effects of Inorganic Ambient Particle Type Mimics on the Differential Expression of a Pro-Inflammatory Mediator by A549 Cells In Vitro

Examining Committee:

Chair — Dr. Ross H. Hill
Professor, Department of Chemistry

Dr. George R. Agnes
Senior Supervisor
Professor, Department of Chemistry

Dr. David J. Vocadlo
Supervisor
Assistant Professor, Department of Chemistry

Dr. Melanie A. O'Neill
Supervisor
Assistant Professor, Department of Chemistry

Dr. Christopher J. Kennedy
Internal Examiner
Associate Professor, Department of Chemistry

Date Defended/Approved: July 5, 2007

ABSTRACT

This research examined the differential expression of intercellular adhesion molecule (ICAM)-1 by human lung alveolar epithelial cells (A549) following 18-hour incubation with less than 100 particles comprising 1-16 inorganic compounds. ICAM-1 induction is known to indicate potential health problems. Particles were created using an alternating current (ac) trap. The particles were used to address questions at the interface between atmospheric chemistry and lung cell biology. Particles that had diameters of 6.8, 3.8, and 2.6 μm, showed that the 2.6 μm size caused the highest ICAM-1 expression. When aluminium nitrate, iron nitrate, zinc nitrate, and lead nitrate were systematically added to PT-5, PT-6, PT-7, and PT-8, it was found that lead nitrate caused the most differential ICAM-1 expression on A549 cells. Particles comprising NaCl, in different physical states indicated that particles of NaCl plus carbon possessed the greatest pro-inflammation potential, suggesting that particle's physical state was important to ICAM-1 expression.

Keywords: particle mimics; A549 cells; ICAM-1; ac trap; levitation

DEDICATION

To my parents: Benjamin and Comfort Eleghasim.

ACKNOWLEDGEMENTS

The completion of this thesis owes a lot to very many people whose help and support inspired and sustained me. I must thank my senior supervisor, Dr. G. R. Agnes for providing me the opportunity to work in his laboratory as well as supporting me throughout the research. I am also grateful to the members of my supervisory committee: Dr. D. J. Vocadlo and Dr. M. A. O'Neill for their advice and suggestions.

My appreciation also goes to the members of Agnes' research group. In particular, to Allen Haddrell for training me on particle levitation, cell culturing, and immunocytochemistry. I sincerely thank Linda Pinto for her help with cell culturing. The support of my entire family is greatly acknowledged.

I am grateful to Simon Fraser University (SFU), the British Columbia Lung Association, the Canadian Foundation for Climate and Atmospheric Sciences (CFCAS), and the Natural Science and Engineering Research Council of Canada (NSERC) for funding this research.

TABLE OF CONTENTS

LIST OF FIGURES

LIST OF TABLES

LIST OF ABBREVIATIONS AND SYMBOLS

A549	Human lung alveolar epithelial cells
ac	Alternating current
BSA	Bovine serum albumin
CD-18	Cluster determinant-18
CD-54	Cluster determinant-54
dc	Direct current
EDB	Electrodynamic balance
EHC-93	Environmental health centre-93
fmol	Femtomole
FBS	Fetal bovine serum
g	Gram
GM-CSF	Granulocyte macrophage-colony stimulating factor
h	Hour
Hz	Hertz
kV_{0-P}	kilovolts (zero to peak)
IgG	Immunoglobin G
ICAM-1	Intercellular adhesion molecule-1
L	Litre
LB	Lamellar body
LFA-1	Leukocyte function associated antigen-1
M	Mole per litre
mm	Millimetre
mL	Millilitre
mg	Milligram
MEM	Minimal essential medium
min	Minute
MIP-1	Mitogen inflammatory protein-1
MIP-2	Mitogen inflammatory protein-2

MVB	Multi-vesicular body
nm	Nanometre
N	Normality
NF-κB	Nuclear factor-κB
PBS	Phosphate buffered saline
PIP	Pro-inflammation potential
PM	Particulate matter
$PM_{2.5}$	Particulate matter with diameter < 2.5 μm
PM_{10}	Particulate matter with diameter ≤ 10 μm
PMN	Polymorphonuclear neutrophil
q	Charge
rpm	Revolution per minute
s	Second
sICAM-1	Soluble intercellular adhesion molecule-1
TBS	Tris-buffered salt
TNF-α	Tumour necrosis factor alpha
V	Volts
V_{p-p}	Volts (peak to peak)
vol	Volume
μg	Microgram
μL	Microlitre
μm	Micrometre
%	Percentage
°C	Degree centigrade

Chapter 1: Particulate air pollution

1.1 Particulate air pollution and impact on the troposphere

The air that sustains life on earth is contained within a region referred to as the troposphere. This region extends from the earth's surface up to about 20 km, and the air in this region is made up of several gases.[1, 2] These gases reported as percent by volume in air include: nitrogen (78 %), oxygen (21 %), argon (0.934 %) carbon dioxide (0.033 %), trace gases, and variable water vapour (~0.001-0.002 %). The composition of these major species in the troposphere has likely not changed significantly over the past several million years.[3]

Air pollution is a worldwide environmental problem that adversely affects public health.[4-7] The problem of air pollution dates back to early human civilization where analysis of lung tissue remains of early humans showed blackening, suggesting smoke poisoning.[8] In the past 200 years, human industrialization has led to a tremendous emission of compounds into the earth's troposphere that have led to reduced air quality or pollution of the atmosphere.[9-11] Air pollution is recognized as a heterogeneous mixture that comprises particulate matter, gases and liquids emitted into the troposphere at concentrations and length of time that can adversely affect humans, animals, plants, and the environment in general.[12]

The beginning of early nineteenth century witnessed uncontrolled combustion of coal as a source of energy.[13] Coal combustion releases several gases.[14-16] One of the most important being sulphur (IV) oxide, as its oxidation from sulphur (IV) oxide to sulphur (VI) oxide results in a form of acid rain.[15] In addition, particulate matter (soot) is a dominant product of coal combustion. [17] Such emissions were involved in air pollution disasters in several parts of the world marked by excess deaths.[18-20]

In addition to the afore-mentioned emissions, today, petroleum-derived products such as gasoline, diesel, and natural gas are used as fuel in high temperature combustion sources for transportation, electricity generation, industrial processes, domestic heating and cooking.[21] Emissions from such sources include carbon monoxide, carbon dioxide, and oxides of nitrogen and sulphur, and soot.[22-24]

Inhalation exposure to polluted air containing particulate matter has been shown through recent epidemiological and toxicological studies to cause lung function decline, aggravate acute and chronic respiratory and cardiovascular diseases, and is responsible for increased frequency of hospital admissions.[25-27] The excess death rates documented air pollution disasters including the London smug , and the Meuse valley fog, can be attributed to aggravation of existing respiratory and/or cardiovascular disease states.[18-20, 28-32] In addition, time series studies indicate that for each increase in particulate matter concentration by 10 $\mu g/m^3$ there is a corresponding

increase in daily respiratory and cardiovascular mortality by 0.21 % and 0.31%.[33]

Early air quality improvement strategies involved using higher grade fuels with lower sulphur content, locating industrial centres away from regions of high population density, and the requirement of taller emission stacks for improved dispersion of emissions.[34] Other measures have included legislation on ambient air quality standards.[35] For instance, the state of California, USA, has very stringent laws regarding pollutant emissions from automobiles.[36]

Despite these abatement measures, increasing world population and economic development have led to considerable industrial growth, urbanization and increased automobile use.[37-40] While these developments are synonymous with maintenance and elevation of standard of living in both developed and developing countries, tremendous amounts of energy are required. This increasing rate of combustion of natural gas, fossil fuel and coal is increasing the rate of pollutants emission.[41-43]

1.2 Particulate matter (PM)

Ambient particulate matter (PM) is a heterogeneous mixture that contains many different fractions including metals in varied states of oxidation, mineral dusts, thousands of different organic compounds, nitric and sulphuric acids and their ammonium salts, and elemental carbon suspended in the troposphere.[44, 45] Particles range in size from ~ 0.002 to ~100 μm in diameter. However, particles in the size domain of ~ 0.002 to ~10 μm are

most relevant with respect to atmospheric chemistry because the larger sizes tend to gravitationally settle rapidly from the troposphere. Size is the most characterized parameter used in describing PM, possibly because it is a readily measured parameter.[2]

1.3 Troposphere sources of particulate matter

Sources of PM found in the troposphere can be categorized simply as: (i) primary sources, and (ii) secondary sources. Particle introduction or formation through both pathways have been observed in numerous parts of the troposphere including the marine boundary layer, arctic regions, forests, and near the tropopause.[46-49] These sources of particles are further described in sub-sections that follow.

1.3.1 Primary sources of particulate matter

These sources emit particles directly into the troposphere. The sources include natural and anthropogenic. The natural sources include volcanic eruption, sea spray, and biological materials. The biological materials include plant fragments, micro-organisms, pollens, and wind-driven suspension of soil or mineral dust.[50-52] Anthropogenic sources include biomass burning, and incomplete combustion of fossil fuels.[53, 54] In addition, primary particles are generated from sources that cause mechanical break-up of large materials by processes that include grinding or crushing.[55, 56] Primary particles tend to have large sizes (eg. 2.5-10 μm) and generally do not agglomerate in the troposphere.[55]

1.3.2 Secondary sources of particulate matter

These particles are produced predominantly as an outcome of oxidative chemical reactions in the troposphere.[55, 56] The formation of secondary particles in the troposphere occurs through condensation or nucleation and requires ions or clusters as nuclei.[57] Homogenous or self-nucleation, and heterogeneous or ion-induced nucleation are two types of mechanisms involved in particle formation in the troposphere. [58]

Homogeneous/self-nucleation is the mechanism involving particle formation directly from gases.[57] For instance, sulphate particles that play an important role in the cooling of the troposphere have been noted to form by this mechanism. For sulphate particle type formation, a binary mechanism involving sulphuric acid-water have been proposed and characterized.[58-61]

Heterogeneous or ion-induced nucleation is another important mechanism for the formation of secondary particles and requires the presence of gaseous ions that serve as nuclei.[57] This mechanism is utilized by sulphuric acid-ammonia-water ternary system during the formation of sulphate particles, and offers a faster rate of particle growth.[62, 63]

1.4 Classification of PM

PM is divided into two broad classes, namely coarse and fine particles. Coarse and fine fractions of PM show differences regarding their sources, chemical composition, and troposphere lifetimes.[2]

1.4.1 Coarse particulate matter ($PM_{2.5}$ - PM_{10})

This refers to PM with a diameter between 2.5 and < 10 μm. The chemical composition of coarse PM often includes crustal-related elements such as aluminium, silicon, calcium, and iron.[64, 65] This fraction also contains pollen grain, lipopolysaccride, and tire wear debris.[66-68] Mechanical processes including grinding, crushing and surface abrasion result in coarse particle introduction to the troposphere.[69] Other sources include evaporation of sea spray, volcanic eruption, and wind-driven or traffic-related suspension of mineral or soil dusts from roads, farming, mining, and construction activities.[70] This size fraction tends to settle on the upper respiratory tract and is readily removed through the mucocilliary clearance mechanism.[71, 72]

1.4.2 Fine particulate matter ($PM_{<2.5}$)

Particles in this category of PM have a diameter that is less than 2.5 μm. This fraction is respirable and can reach the gas-exchange region of the lungs namely, the alveoli.[71, 72] $PM_{2.5}$ often contains nitrates, sulphates, ammonium ion, elemental and organic carbon.[64, 65, 69] Particles constituting this fraction tend to be formed from chemical reactions in the troposphere including homogenous and heterogeneous nucleation.[56] Other formation processes include evaporation of fog and droplets.[64] Studies indicate that soot particles in this size range are generated during the combustion of coal, gasoline, diesel and wood.[73-75] Additionally, high temperature processes in steel mills, as well as products of reactions of oxides of nitrogen, and sulphur constitute other significant contributions to $PM_{2.5}$.[76]

1.5 Human lung epithelial cells and function

The human lungs are always in contact with the external environment and mediate the function of O_2/CO_2 exchange through diffusion.[77, 78] A consequence of this, the lungs necessarily are involved in the body's immune defence mechanism, facilitating the clearance of inhaled noxious substances including micro organisms and particulate matter.[79-81]

The pulmonary alveolar epithelium of the lung is composed of two cell types. They are the membranous type-I, and large, cubiodal type-II cells. Type-I cells overlay most of the alveolar surface while type-II cells are found in alveolar corners.[82] Type-I cells are prone to injury while type-II cells are comparatively more resistant.[82] During alveolar injury, type-II cells proliferate to replenish injured type-I cells.[82-85]

Type-II cells also contain organelles including multivesicular bodies (MVB) that facilitate material transport into lamellar bodies (LB) where they are internalised or endocytosed.[86] The two organelles, namely MVB and LB enable type-II cells to possess endocytic functions.[86] Other functions of type-II alveolar epithelial cells include the synthesis and secretion of surface-active proteins, cytokines and adhesion molecules, including intercellular adhesion molecule (ICAM)-1, that are essential for effecting the lung's inflammatory response to inhaled harmful materials.[87-92] Type-I cells do not possess endocytosic ability because they lack both MVB and LB.[86]

1.6 Inflammation

Inflammation describes a complex array of biological processes utilized by an organism in response to injury or infection caused by pathogenic organisms, toxic molecules or physical damage.[93] Inflammation involves changes in the blood vessels as well as in the connective tissues that are involved in the elimination of harmful stimuli and tissue repair.[94] Inflammation is essential for the survival of an organism since the entire process targets total removal of the harmful external stimulus and healing of damaged tissue.[95] The four physical signs and symptoms of inflammation include redness or rubor, pain or dolor, heat or calor, and swelling or tumor. [95]

Initial attempts to describe mechanisms underlying the signs and symptoms associated with inflammation were made in the nineteenth century. Marchand alluded these signs and symptoms to the accumulation of heat from the heart, accompanied by inflow of blood and mucus.[96] However, it was John Hunter (1728-1793) who observed that the redness associated with inflammation was caused by increased blood flow and blood vessel dilation.

Investigations in the early nineteenth century that contributed to current knowledge of the inflammatory process included the observation that tissue injury triggers inflammation by Virchow (1858). This was followed by a comprehensive explanation of the process of leukocyte immigration by Cohnheim (1839-1884), and the description of phagocytosis as a method of removal of a stimulus by phagocyte cells by Metchnikoff (1845-1916).

Phagocytic cells, including macrophages mediate an early inflammatory response to a harmful stimulus. Removal of a harmful stimulus by macrophages, without the involvement of the skeletal and circulatory systems, is referred to as a localized response.[97] However, when the external stimulus overcomes the innate immune cells normally resident in an organism, a systemic response characterized by a sequence of events is initiated. These events include the activation of the bone marrow resulting in an increased rate of neutrophil release into the circulatory system, and subsequent neutrophil migration from the circulatory system into the tissue to the site of inflammation.[98] Pro-inflammatory mediators, including ICAM-1 and cytokines, are inter-cellular signalling molecules that facilitate these complex events.[99]

1.7 Ambient particle-induced inflammation

The respiratory system is exposed to many atmospheric pollutants including chemical toxins, pathogens and ambient particles. Particles deposited in the upper respiratory track are removed through the mucociliary clearance mechanism.[100-102] Antioxidants such as glutathione are involved in the body's defence against foreign substances including particles that are deposited onto lung epithelium.[103, 104] However, when these inhaled particulates overwhelm the cellular antioxidant defence mechanism, an inflammatory response is induced.[105-107]

Overwhelming the lung's antioxidant defence mechanism by inhaled PM activates resident macrophages.[108, 109] Activated macrophages secrete

various cytokines, including tumor necrosis factor alpha (TNF)-α .[110, 111] TNF-α secretion serves as a signal for transcription nuclear factor-kappa B (NF-κB) activation.[112] NF-κB exists in the cytoplasm of cells as an inactive dimer with two-protein subunits complexed to the I kappa B (IκB) family of inhibitory proteins, namely I kappa B alpha (IκBα).[113, 114] Following activation, Iκβα is degraded by I kappa B alpha kinase (IKK) facilitating NF-κB translocation to the nucleus.[115] Inside the nucleus, NF-κB binds to sites controlling many inflammatory genes including mitogen inflammatory protein-1 (MIP-1), mitogen inflammatory protein-2 (MIP-2), granulocyte-macrophage-colony stimulating factor (GM-CSF) and ICAM-1 leading to their transcription and subsequent protein expression.[116-118] GM-CSF activates neutrophil production by the bone marrow.[119-121]

The concentration gradient set by secreted MIP-1, MIP-2, other cytokines from injured cells activate resting neutrophils and cause their migration towards the injury source.[122] In addition, circulatory neutrophils, through their receptor, the lymphocyte function associated antigen-1 (LFA-1) bind to ICAM-1 expressed on the vascular endothelium enabling it to subsequently enter the tissue and move to the site of inflammation.[123-126]

Inside the tissue, a particle to be eliminated is coated with protein called opsonin secreted by the host enabling its recognizition by neutrophils.[127, 128] Particle recognition by neutrophil marks the onset of phagocytosis.

1.8 Particle phagocytosis

Phagocytosis is the process by which single cells take solid objects into their interior followed by chemical and enzymatic attack.[129] The first step in this process is the formation of vacuole or phagosome around each particle by neutrophils using their plasma membrane.[130] Particle detoxication during phagocytosis is achieved through degranulation,[131] and respiratory burst. [132, 133] Degranulation is the fusion of the granules contained in the neutrophil cytoplasm with the phagosome.[131, 134]

Respiratory burst is a sequence of processes that generate agents that facilitate particle detoxification.[133] The first step in this process involves an increase in oxygen uptake by neutrophils.[135] This oxygen is utilized by the cells to produce superoxide anion radical in a single-electron process as follows[136]:

$$2O_2 + NADPH \longrightarrow 2O_2^{\cdot -} + NADP^+ + H^+.$$

This process is catalyzed by nicotinamide adenine dinucleotide phosphate oxidase (NADPH oxidase) released from the neutrophil cell membrane.[137-139] Neutrophils utilize the synthesized superoxide anion radical as a precursor molecule to generate several other molecules having detoxifying properties essential for the breakdown of the phagocytosed entities through the following mechanisms.[139, 140]

In one mechanism, the superoxide anion radical is converted into hydrogen peroxide by an enzyme called superoxide dismutase as follows [141, 142].

$$2O_2^{\cdot-} + 2H^+ \longrightarrow H_2O_2 + O_2$$

Though hydrogen peroxide has detoxifying characteristics, its potency has been shown to be augmented by myeloperoxidase, an enzyme found in the granules of neutrophils.[142] This enzyme catalyses the reaction of halide ions such as chloride ion (Cl^-), bromide ion (Br^-), and iodide ion (I^-) with hydrogen peroxide to form the respective hypohalide ions as follows[143-146] :

$$X^- + H_2O_2 \longrightarrow XO^- + H_2O$$

where X^- represents Cl^-, Br^-, or I^-. The hypochlorite ion has more detoxifying action than hydrogen peroxide.[143-146]

1.9 A549 cell line and endocytosis

Endocytosis is the process by which eukaryotic cells take up material from outside by invagination of the plasma membrane to form vesicles enclosing the external material. The vesicle is then pinched off from the cell surface so that it lies within the cell.[147] The A549 cell line is derived from type-II cells of lung alveolar epithelium, and is known to endocytose materials.[148] Studies involving polystyrene beads having diameters of 0.5, 1.0, 2.0, and 3.0 μm showed that 0.5 μm size was internalized or endocytosed most by A549 cells.[149] Other studies have shown that the

internalized materials were cycled from the cell surface through the multi-vesicular bodies to the lamellar bodies that have been noted to contain certain lysosomal enzymes.[150] This cell line do not contain organelles like phagocytic vacuoles of leukocytes, and therefore can not phagocytise materials. [151]

1.10 ICAM-1 in inflammation and disease

ICAM-1 is a member of the Ig supergene family and is a transmembrane glycoprotein that performs several important functions. ICAM-1 is an accessory molecule that assists in leukocyte adhesion and migration thereby enhancing the lung's inflammatory response. Studies have demonstrated that interaction between ICAM-1 and lymphocyte function associated antigen-1 (LFA-1) enhance the phagocytic ability of neutrophils.[152] Moreover, ICAM-1/LFA-1 binding has been shown to provide a costimulatory signal for T-cell proliferation and growth.[153, 154] ICAM-1 is also believed to be involved in bacterial clearance. [153, 154, 153, 159]

Other studies have reported a soluble form of ICAM-1 (sICAM-1) in plasma, cerebrospinal fluid and sputum.[155, 156] sICAM-1 has been reported as a receptor for both rhinovirus and coxsackie A13 virus, and it is involved in the prevention of infection associated with these viruses.[157] Other functions of sICAM-1 include binding to red-blood cells infected with malaria.[158]

Lung epithelial cells express ICAM-1, and is increased in response to various stimuli.[92] ICAM-1 is expressed on both type-I and type-II alveolar

epithelial cells. ICAM-1 expression is unregulated in type-I cells, where as in type-II cells, it is regulated and only expressed in response to a stimulus .[159] Though ICAM-1 can be expressed on both type-I and type-II cells; its expression is highest for type-II cells.[91,160] Studies using a human lung alveolar epithelial cell line (A549) which has characteristics of type-II cells, indicate that it does not express ICAM-1 constitutively, but in response to various stimuli .[91,159]

1.11 Introduction to the research

The *in vivo* response of human lungs to inhaled ambient PM was overviewed in previous sections. Environmental health centre-93 (EHC-93) is an urban PM sample collected from outdoor urban air in Ottawa.[44,161] Its chemical composition, with respect to inorganic, organic, soluble and insoluble components, has been well characterized and the size of particles was < 3.0 μm.[44,162] Previous studies utilizing EHC-93 have reported that it caused increased expression, and secretion of pro-inflammatory mediators.[44, 98] Studies involving the soluble fraction of this PM sample have reported increased ICAM-1 expression in alveolar macrophage, and bronchial epithelial cells.[98] Because EHC-93 is a complex heterogeneous mixture, my first objective was to measure the differential expression of ICAM-1 in response to incubation with particles comprising inorganic compounds that mimic the average or bulk composition of EHC-93.

In this project, the lungs' initial response was studied using a lung alveolar epithelial cell line (A549) originally derived from lung carcinoma

patient.[163,164] The pro-inflammation potential (PIP), defined herein as the potential of EHC-93 particle mimics, inorganic compounds only, to cause differential ICAM-1 expression in A549 cells after an 18 h incubation was measured.

1.11.1 Hypothesis and experimental objectives

(i) Particles with sizes that are within the coarse and fine range exist in ambient PM. Particle size is an important physiochemical parameter since it is a primary factor determining the site of particle deposition in the respiratory tract. A hypothesis that particles whose bulk or average inorganic compounds mimic EHC-93 but having different sizes cause differential ICAM-1 expression by A549 cells was proposed. Herein, particles having diameters of 6.8, 3.8, and 2.6 μm whose average or bulk inorganic chemical composition mimic EHC-93 were created and their pro-inflammation potential in A549 cells after an 18 h incubation was measured through differential ICAM-1 expression.

(ii) The results of the studies involving particles having different sizes showed that particles of 2.6 μm in diameter caused the greatest differential expression of ICAM-1. The second question asked was: what is the relative contribution of the inorganic compounds in the particle to the measured ICAM-1 expression? The second hypothesis addresses the possibility that each inorganic compound that was systematically added to each particle type did not cause differential ICAM-1 expression on A549 cells. The objective herein was to measure the pro-inflammation potential (ICAM-1 expression) in

response to incubation with particles having different composition of inorganic compounds.

(iii) While the pro-inflammation potential of specific inorganic compounds contained in particles was investigated, it was found that particles containing NaCl plus carbon caused measurable differential ICAM-1 expression in A549 cells. NaCl is an ubiquitous compound in the troposphere,[165-167] and it exists in both liquid and solid states.[168-170] The third objective of this research was to measure the pro-inflammation potential (differential ICAM-1 expression) by A549 cells in response to particles having varied moles of NaCl and in different physical states. The hypothesis is that particles containing different moles of NaCl and in different physical states do not cause differential ICAM-1 expression in A549 cells.

Chapter 2: Experimental apparatus and methods

2.1 Introduction

This chapter introduces the apparatus, materials and experimental methods used in this study. The principal apparatus used was an ac trap for the creation, and delivery of particle populations to human lung cell cultures. The materials include those for cell culture (A549 cell line) and immunocytochemistry.

2.2 Particle levitation

A definition of levitation is for an object to rise or float in the air in seeming defiance of gravitation.[171] The description of the force (electric, acoustic, optical) used to keep that object suspended in space denotes the levitation technique.[172-178] Particles a few micrometers in diameter have been levitated using time dependent electric fields.[175, 176, 179, 180] On those particles levitated using an electric field, chemical reaction rates were measured.[172-174, 176, 178, 179, 181] Acoustic levitation techniques have been applied to studies of protein crystallization.[177, 182] The history of levitation can be traced to Millikan's oil drop experiment, in which time independent electrostatic forces were applied between two horizontal electrodes permitting temporary suspension of charged oil droplets.[183]

An ac trap was used in this study to create particles. Our interest in this apparatus can be attributed to the relative ease with which particles that mimic ambient particles regarding their chemical composition and size can be created.[184, 185] A schematic diagram of an ac trap is depicted in Figure 2-1. It consists of a pair of parallel ring electrodes and a pair of disc-shaped end cap electrodes, one above and another below the ring electrodes. V_{ac} indicates an alternating current (ac) waveform applied to the ring electrodes. $+V_{dc}$ indicates a positive direct current (dc) potential applied to the top endcap electrode while $-V_{dc}$ indicates a negative direct current potential applied to the bottom endcap electrode (Fig. 2-1).

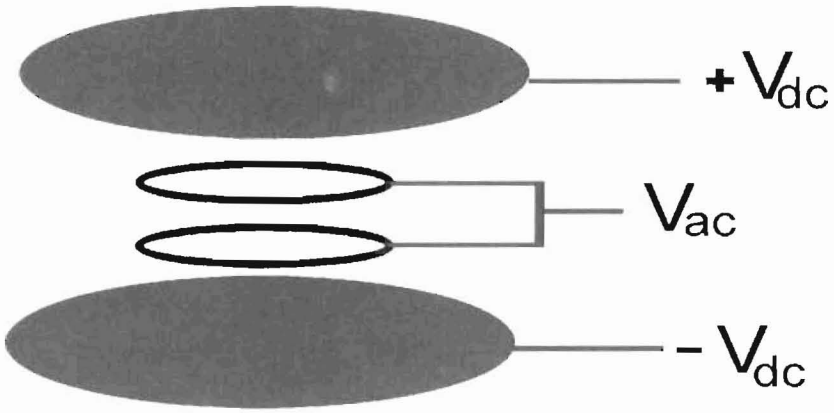

Figure 2-1: A schematic diagram of the ac trap used for particle levitation in this study. The polarity of the dc potential indicated would be used to offset the force of gravity acting on a particle having a net negative charge.

The ac trap was housed in a chamber placed in a biological safety cabinet (Nuaire Inc., Model Nu-425-600. Plymouth, MN, USA). Fig. 2-2 is a schematic diagram showing the electrical connections to an ac trap.

Monodisperse droplet dispensing was achieved by using a commercially available droplet dispenser (MicroFab Technologies Inc., MJ-AB-01-60, TX, USA) that has a nozzle with an internal diameter of 60 μm. The droplet dispenser reservoir was filled with an aliquot of a starting solution to be dispensed using a 10-μL pipette. To dispense a droplet, an electrical signal from the waveform generator of the droplet dispenser caused actuation of a cylindrical piezoceramic element bonded to the outside of the dispenser reservoir. This actuation caused a small volume of liquid to be expelled as a jet from the dispenser nozzle. A direct current (dc) potential applied to the induction electrode caused ion mobility within this liquid jet. The momentum of the jet caused it to separate and collapse to form a droplet. The charge imbalance resulted in each droplet having net elementary charge.

Each droplet passes through a 5-mm diameter hole cut in the induction electrode and into the ac trap. Within the ac trap, a sinusoidal waveform of 4.5 $kV_{0\text{-}P}$ was applied to the ring electrodes during the period of time droplets were being introduced to the trap. During the period of droplet levitation, the evaporation of the volatile components causes the non-volatile components, solutes and dispersed solids in each droplet, to precipitate/coagulate, forming a residue that is referred to as a particle. Particles were removed from the ac trap and directed onto a target, either an 18 mm x 18 mm glass cover slip on which an A549 cell culture had been grown, or a glass slide for optical microscopy, by applying an attractive 500 V dc electric potential to the bottom end cap electrode on which the target had been placed.

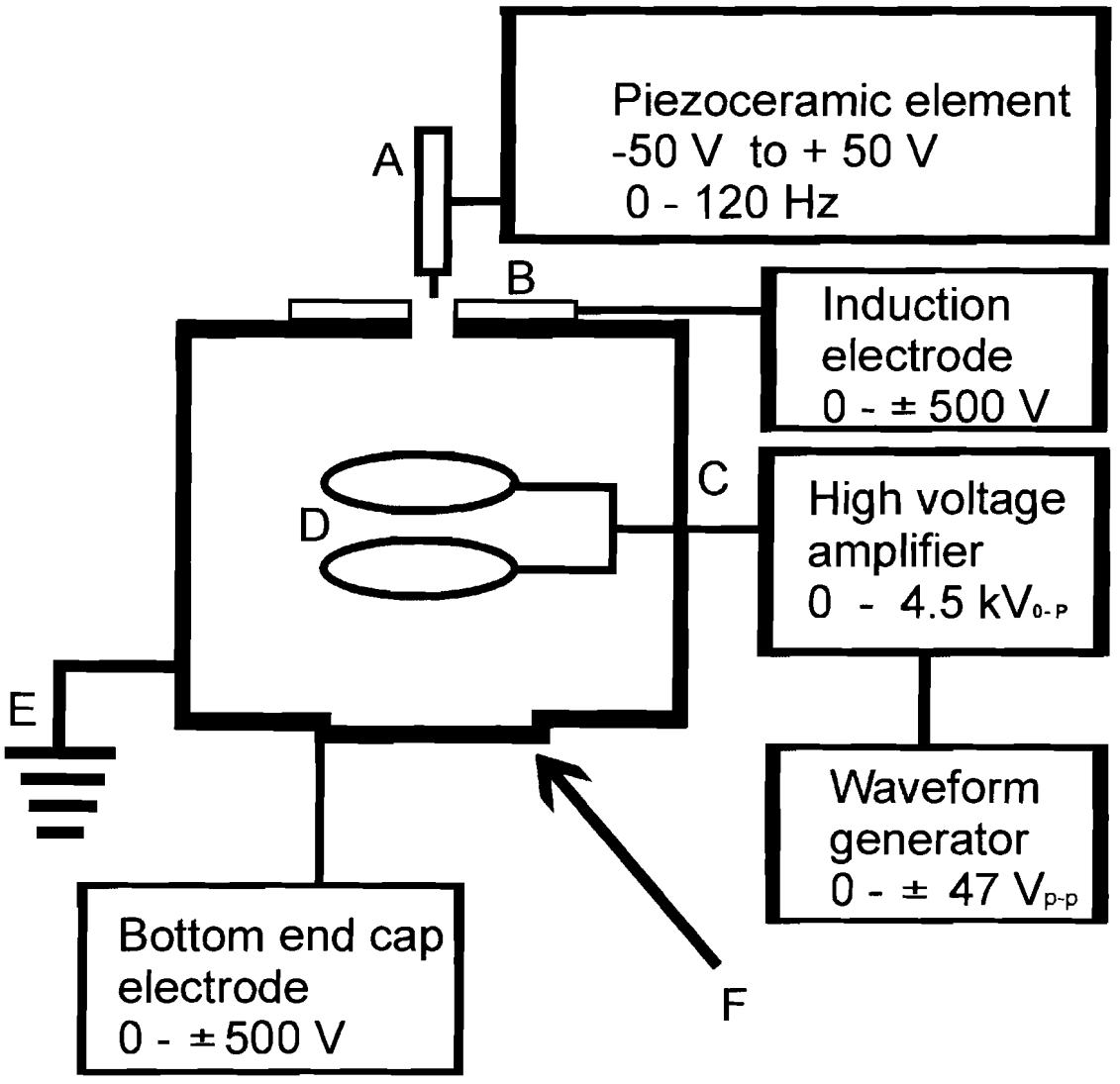

Figure 2-2: **A schematic diagram showing the electrical connections to the levitation apparatus. The components are: (A) Droplet dispenser, (B) Induction electrode, (C) Chamber housing the ac trap, (D) ac trap, (E) Grounded aluminium wire, (F) Bottom end cap electrode. Diagram not drawn to scale.**

2.3 Environmental health center-93 (EHC-93)

This is an urban particulate matter sample collected from outdoor air by the Environmental Health Centre in Ottawa.[44, 161] This PM sample was collected in summer (August) 1992.[186] Its chemical composition regarding metals and non-metals is well characterized (Table 2.1). Its major organic

compounds, mainly polycyclic aromatic hydrocarbons, also have been characterized (Table 2-1).[44, 162] The carbon content of this PM sample was not reported.

Table 2-1: The concentration of metals, non-metals, and organic compounds that have been characterized in EHC-93. Source: Vincent *et al.*, Fundamental and Applied Toxicology, 39, 18-32, 1997.

Metals			
Metal	Concentration (µg/g)	Metal	Concentration (µg/g)
Aluminum	$9.8x10^3$	Manganese	483
Ammonium	104	Nickel	69.6
Arsenic	Not detectable	Sodium	$20.6x10^3$
Barium	295	Strontium	272
Boron	81.2	Tin	$1.2x10^3$
Cadmium	7.3	Titanium	929
Calcium	$109x10^3$	Vanadium	90.4
Chromium	42.3	Zinc	$10.4x10^3$
Cobalt	5.9	Lead	$6.7x10^3$
Copper	845	Magnesium	$7.2x10^3$
Iron	$14.9x10^3$	Molybdenum	4.6
Non-metals			
Non-metal	Concentration (µg/g)	Mon-metal	Concentration (µg/g)
Nitrate	1.93	Sulphate	15.6
Chloride	8.72		
Polycyclic aromatic hydrocarbons (PAH)			
PAH	Concentration (µg/g)	PAH	Concentration (µg/g)
Dibenz(a,c&a,h)anthracene	Not detectable	Chrysene	1.66
Anthracene	0.54	Perylene	0.28
Benzo (a) anthracene	1.10	Prylene	2.11
Benzo (b) fluoranthracene	2.78	Benzo (e) pyrene	1.09
Benzo (k) fluoranthracene	Not detectable	Fluoranthene	2.47
Benzo (a&b) fluorene	0.23	Phenanthrene	1.83
Benzo (ghi) perylene	1.52	Benzo (a) pyrene	0.95
Indeno(1,2,3-cd) pyrene	1.19	Acenaphthene	0.20

2.4 Cell culture

A history of animal cell culture would include Ross Harrison's seminal work on growing nerve fibre cells from explants of neural tissue.[187-189] That work was followed by the discovery of a method for culturing tissues *in vitro* for several months by Alexis Carrel.[190] By 1952, the first human cell line, the human epithelial cell derived from cervical carcinoma (HeLa), were established by Gey and colleagues.[191] More knowledge was added to this new field by the description of attachment factors, and media requirement for cell cultures by Eagle.[192] Other investigations that greatly contributed to the development of this field were methodologies for maintaining differentiated cell cultures.[193] A system for studying normal myogenic cells *in vitro* was introduced by Yaffe.[194] The determination of optimal media supplement requirements for growth of rat neuroblastoma cells was characterized by Eagle.[195]

Tissue culture is now an essential tool in life and related sciences, and the methodologies for it are taught in undergraduate courses. This subsection describes the A549 cell line and the materials utilized in its culture.

2.4.1 A549 cell line

This cell-line was derived from a lung alveolar carcinoma patient.[163] It has characteristics similar to type-II cells of the human lungs.[163] These cells are known to endocytose particles.[196] This cell line is noted to express several cytokines including granulocyte macrophage-colony stimulating factor (GM-CSF) and an adhesion molecule, intercellular adhesion molecule (ICAM)-1.[197]

ICAM-1 expression by these cells is known to be induced by tumor necrosis factor (TNF)-α through the transcription nuclear factor (NF)-κB pathway.[99, 198] ICAM-1 has been referred to as cluster determinant (CD)-54 in the literature.[199-201]

The A549 cells used in this study were provided by Dr. Stephan F. van Eeden (James C Hogg iCAPTURE Centre for cardiovascular and pulmonary research, University of British Columbia, Canada). The number of passages of the cell sample received was not known at the time of their receipt.

Cultures of these cells were grown on 18 mm x 18 mm glass cover slip supports. When growing adhered to the support, these cells have a diameter of 10-15 μm.[202] Cell passaging was performed in a biological safety cabinet. To each 100 mm (diameter) x 20 mm (depth) petri dish containing A549 cell culture, 1 mL of trypsin-ethylenediaminetetraacetic acid (Trypsin-EDTA) solution (Invitrogen Corporation, Burlington, Ont. Canada) was added and incubated for 5 min. After incubation, trypsinised cells were collected using 5 mL of minimal essential medium (MEM) and placed in a 15 mL test tube. This test tube was centrifuged at 1000 revolutions per minute (rpm) for 5 min enabling cell pellet formation. The MEM was drained after centrifugation. Pelleted cells were resuspended with fresh aliquots of MEM. 0.5 mL of MEM containing A549 cells was dispensed onto an 18 mm x 18 mm cover slip placed in each well of a six-well plate containing 2 mL of MEM. Cells were grown to 95 % confluence at 37 °C, 5 % CO_2, and 100 % relative humidity before use. The compositions of solutions introduced in this

paragraph are commonly used in cell culture. These solutions are described later in this chapter.

2.5 India ink

This product (Speedball, Product no. 3328, Statesville, NC, USA), according to the manufacturer, contains the following components (vol/vol): water (75-85 %), carbon black (7-9 %), shellac (6-8 %), ammonium hydroxide (1-2 %), phenol (0.45 %), and ethylene glycol (1.6 %). The carbon black, dispersed ~ 20 nm carbon nanoparticles, was used as the source of carbon in soot-like ambient particle mimics. The use of carbon black facilitated visualization and counting of particles using an optical microscope following their deposition onto A549 cell culture, prior to performing an immunocytochemistry assay. In addition, as will be presented, particles comprising carbon from India ink did not effect significant differential expression of ICAM-1 by A549 cells relative to negative controls.

2.6 Components of the cell culture medium

This subsection describes the materials used in A549 cell culturing and their functions.

2.6.1 Minimal essential medium (MEM)

The composition of MEM has been optimised for the culturing of cells *in vitro*.[203-205] This solution contains essential amino acids, vitamins, glucose and inorganic salts.[206-208] The essential amino acids are required for cell

survival and growth.[207, 209-211] The vitamins are necessary for their roles in facilitating cell differentiation,[212] while the inorganic salts facilitate signal transduction and modulation of membrane potential.[213]

MEM solution was prepared from MEM powder according to instructions provided by the supplier of this material (Sigma-Aldrich, Oakville, Ont, Canada). 9.4 g MEM powder was added to 1 litre of distilled, deionised water. While this solution was stirred, 2.2 g of sodium bicarbonate ($NaHCO_3$) powder was added. The pH of the resulting solution was adjusted to 7.6 with 1 N sodium hydroxide solution. Sodium bicarbonate forms a buffer system with dissolved carbon dioxide that maintains cell culture pH at 7.6 during growth.[213]

Filtration of the MEM was performed in a biological safety cabinet (Forma scientific Inc. # 14567-386, Marietta, OH, USA) using a sterilized cellulose acetate membrane filter having a mean pore size of 0.2 μm. The purpose of this filtration step is to maintain media sterility. Following filtration, the following solutions were added to 1000 mL of MEM solution: 10 mL of L-glutamine, 10 mL of MEM vitamin, and 100 mL of fetal bovine serum (FBS). The function of each component is described below.

2.6.2 L-glutamine

L-glutamine (Invitrogen Corporation, Burlington, Ont, Canada) according to the manufacturer has pH (4.7 - 6.0) and contains 29.8 mg L-

glutamine per mL in 0.85 % sodium chloride. It is required for nucleic acid synthesis, and is a source of energy for the cells.[213]

2.6.3 Minimal essential medium (MEM) vitamin

MEM Vitamin (Invitrogen Corporation, Burlington, Ont, Canada) according to the manufacturer has pH (7.0 - 7.4) and contained vitamin B-complex in 0.85 % saline. These vitamins are required mostly for cell growth, energy production, and synthesis of genetic materials and phospholipids.[192, 214, 215]

2.6.4 Fetal bovine serum (FBS)

FBS solution (Invitrogen Corporation, Burlington, Ont. Canada) contains proteins, growth factors, hormones, amino acids, and minerals.[213] Albumin in FBS serves as a carrier for lipids and minerals. Transferrin detoxifies the medium by binding metals.[208, 216-218] Fetuin in FBS promotes cell attachment and spreading.[214-222]

Growth factors stimulate cell proliferation.[223-226] The hormones are required for cellular uptake of glucose and amino acids.[227-231] Amino acids are precursors for the synthesis of phospholipids.[213] Metals including iron, copper and zinc are cofactors for enzymes.[232]

2.7 Immunocytochemistry assay

Immunocytochemistry involves specific interaction between an antigen and an antibody labelled with flourophores. The function of the flourophore is

to facilitate the detection of the antigen.[233] Early immunocytochemistry studies involved reactions of bacteria proteins (antigens) with organic salts coupled to proteins (antibodies). Those studies found that organic salts did not measurably affect the specificity of the antibodies for the antigens.[234] By 1934, a methodology enabling quantitative antibody study was developed by Heidelberger and colleagues.[235] Heidelberger's work stimulated the interest of Marrak who employed the method to study the nature of antibodies in bacteria and concluded that they were proteins.[236] In 1941, Coons and co-workers repeated Marrack's work but found the intensity of light produced by the proteins too weak to enable the detection of the antigens. This prompted Coons to couple the antibody to anthracene isocyanate, generating what is termed a labelled antibody, denoting a large fluorescence quantum yield of the fluorophore (eg. anthracene isocyanate). That work is regarded as being the start of modern immunocytochemistry.[237] Coons utilized the immunofluorescence technique as a tool for studying the localization of rickettsiae and mumps antigens, following injection of the antigen in mice.[238-240]

These developments as well as the commercial availability of reliable, inexpensive fluorescent microscopes have contributed to immunocytochemistry developing as an indispensable research method that continues to be used in numerous areas of scientific research.[241-243] This method has been used to investigate the expression of placental protein by HeLa cells, and the study of characteristics of A549 cells *in vitro*.[244, 245, 246] A

representation of immunocytochemistry labelling of ICAM-1 on A549 cell culture with primary and secondary antibodies is shown in Fig. 2-3.

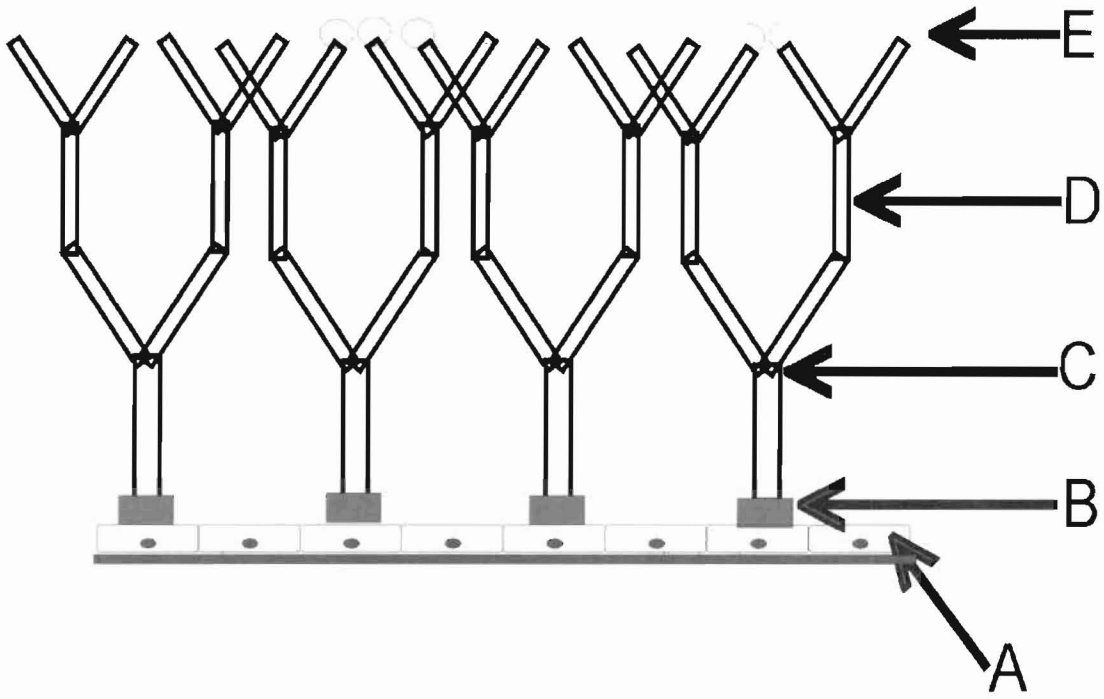

Figure 2-3: **A representation of labelling of ICAM-1 expressed on A549 cell culture with secondary antibody tagged with fluorophore. (A) A549 cell culture, (B) ICAM-1 expressed on A549 cell culture following incubation with particles that was long enough to allow for maximal differential expression of ICAM-1, (C) Primary antibody (mouse-antihuman monoclonal ICAM-1 antibody), (D) Secondary antibody (goat-antimouse conjugated to a fluorophore), (E) Fluorophore (Alexa fluor 546). See text for details. Diagram not drawn to scale.**

The use of immunocytochemistry assay in this study enabled the measurement of ICAM-1 expressed at the site of particle deposition. The materials used for performing immunocytochemistry assay on A549 cell cultures following 18 h incubation with ambient particle mimics are described in the subsection below.

2.7.1 Phosphate buffered saline (PBS) solution

This solution was prepared from PBS salt (Oxoid Ltd., Basingstoke, Hampshire, England) according to the manufacturer's direction as follows. A tablet of the salt was dissolved in 100 mL distilled deionised water, and the resulting solution autoclaved at 115 ^{o}C for 10 minutes. The resulting concentrations of the different salts in PBS were $1.4x10^{-1}$ M NaCl, $2.7\ x10^{-3}$ M KCl, $6.5x10^{-3}$M $Na_2HPO_4.2H_2O$, and $1.5x10^{-3}$ M KH_2PO_4. This solution was used for rinsing the A549 cell culture.

2.7.2 Acetone solution

This solution was used in fixing cell culture. Acetone fixation preserved cellular morphology.[247] The solution was prepared by mixing 1 mL of acetone with 99 mL of distilled deionised water. 1 mL of this solution was used in fixing each 18 mm x 18 mm glass cover slip containing A549 cells.

2.7.3 Tris-buffered salt (TBS) solution

Tris is the abbreviation for tris-(hydroxylmethyl) aminomethane. TBS solution was prepared in the following way. 8.7 g of tris-(hydroxylmethyl) aminomethane was dissolved in 80 mL of distilled deionised water. Another solution was prepared by dissolving 6.05 g NaCl in 80 mL of distilled deionised water. The two solutions were mixed together and diluted to 1 litre. The concentrations of TBS and NaCl in the resulting solution were 0.07 M and 0.10 M. The resulting solution pH was adjusted to 7.6 with 1 N HCl

solution. This solution was used as a pH buffer for the solutions containing both primary and secondary antibodies.

2.7.4 Tris-buffered salt (TBS)/Bovine serum albumin (TBS/BSA) solution

This solution contains TBS/BSA (1:1, vol/vol). The function of the TBS is to maintain solution pH and BSA is a carrier for both primary and secondary antibodies.[248, 249] BSA solution was prepared as follows. 1 mg of BSA (Sigma-Aldrich, A9647-50G, Oakville, Ont., Canada) was dissolved in 100 mL of distilled deionised water.

2.7.5 Serum-free protein block

The serum-free protein block (DakoCytomation Inc., X0909, Carpinteria, CA, USA) according to the manufacturer contains casein in 0.25 % PBS, stabilizing proteins and 0.015 M sodium azide. Casein is a protein from milk, and its role is to reduce non-specific binding,[249] while sodium azide is an antimicrobial agent.

2.7.6 Mouse antihuman monoclonal antibody

The mouse-antihuman monoclonal CD-54 antibody (CALTAG laboratories, Burlingame, # MHCD54 F, CA, USA) served as primary antibody.[123, 250] It is specific for, and binds to human ICAM-1. A solution of this antibody was prepared by mixing 1 μL of 50-μg/0.5 mL of the antibody with 50 μL of TBS/BSA solution (1:1, vol/vol).

2.7.7 Goat antimouse antibody

The goat-antimouse immunoglobin G (IgG) antibody (Invitrogen Detection Technologies, 34779A, Eugene, OR, USA) was the secondary antibody. It is specific for the primary antibody. The secondary antibody is conjugated to a fluorophore, Alexa fluor 546. This fluorophore's optimal excitation wavelength range is 546 ± 5 nm, and its optimal emission wavelength range is 580 ± 15 nm.[251] The detection of fluorescence emission from this fluorophore was interpreted as being attributed to ICAM-1 expressed on an A549 cell culture at that site. The solution of secondary antibody was prepared by mixing 1 μL of 2 mg/mL of the antibody with 100 μL of TBS/BSA solution (1:1, vol/vol).

2.7.8 Human tumor necrosis factor-α (TNF-α)

Human TNF-α (Sigma-aldrich, T6674-10UG, St. Louis, MO, USA) is known to induce ICAM-1 expression on A549 cells through the activation of NF-κB pathway.[99] 10 μL of 1 mg/mL of TNF-α was introduced into each well of a six-well plate containing 18 mm x 18 mm glass cover slip on which A549 cells were bathed in 2 mL of MEM. (The concentration of TNF-α in the resulting solution was $5x10^{-3}$ mg/mL).

2.7.9 Fluorescence microscopy

An inverted fluorescent microscope (Motic AE30/31, Motic Inc. Ltd, Richmond, BC, Canada) was used for acquisition of fluorescence emission signal intensity at the site of particle deposition. Prior to performing

fluorescence microscopy, each 18 mm x 18 mm cover slip containing A549 cells, labelled with fluorophore-tagged secondary antibody was mounted on a 75 mm x 25 mm microscope glass slide as follows. 0.2 mL of glycerol was spread on a glass slide. The cover slip containing A549 cells was placed on this glass slide and held with nail polish. The glycerol was found to improve the preservation of the cell culture.

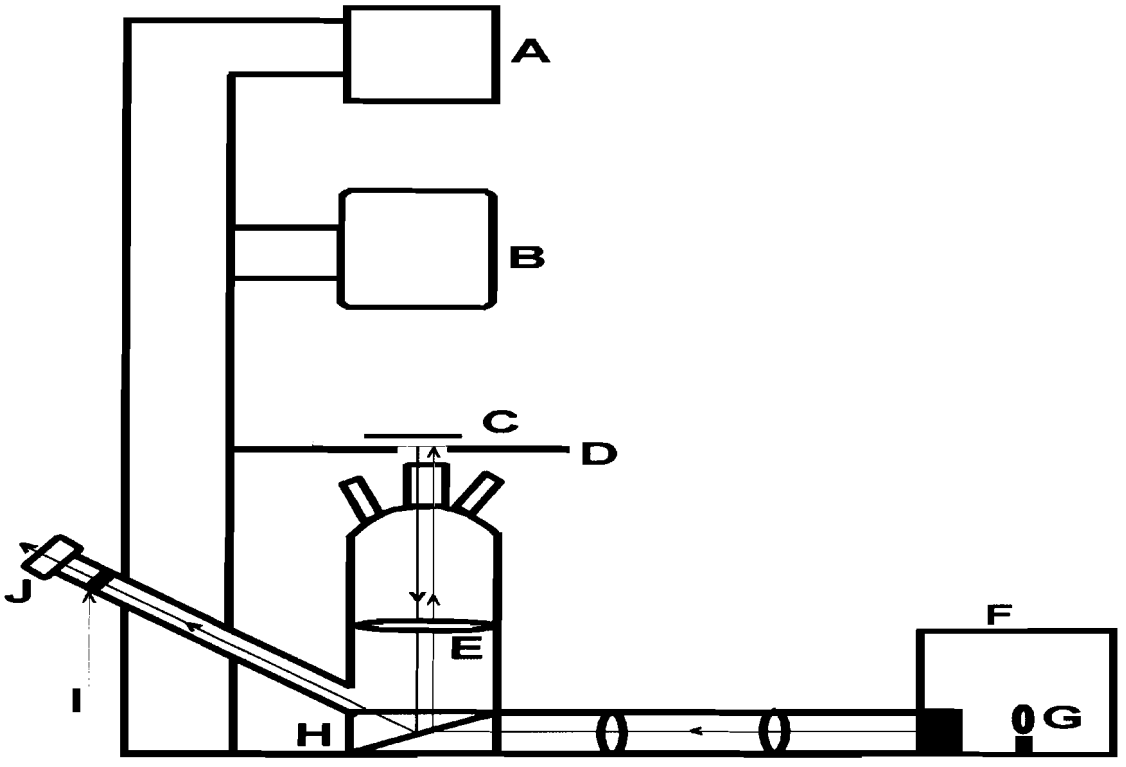

Figure 2-4: **A schematic diagram of an inverted fluorescent microscope with its main components in labels. The components are: (A) Light source for the optical microscope, (B) Condenser for visible light, (C) A549 cell culture fixed onto a glass slide mounted on the specimen stage, (D) Specimen stage, (E) Condenser for fluorescence emission, (F) Fluorescent lamp housing, (G) Fluorescent lamp, (H) Epi-fluorescent filter block, (I) Barrier filter, (J) Eyepiece. Diagram not drawn to scale.**

Each glass slide containing A549 cell culture was mounted on the microscope specimen stage. Light from the optical microscope's light source was focused on the glass slide through a condenser. The light was used to locate the site of particle deposition on cell culture through the field-of-view of the eyepiece.

Following the location of particle deposition site, the microscope's fluorescence module was used to obtain fluorescence emission signals from the deposition site within the cell cultures. Photons from the fluorescence excitation lamp are focused on the epi-fluorescent filter block that selects and passes photons of a particular wavelength range (eg. those photons that can be absorbed by the fluorophore). Fluorescence emission from the specimen's fluorophore are collimated, and then sent to the epi-fluorescent filter. The fluorescence emission is passed through a barrier filter that removes any residual excitation light, before passing through an eyepiece for observation.

Chapter 3: The preparation of <100 particles per trial having the same mole fraction of sixteen inorganic compounds at diameters of 6.8, 3.8, or 2.6 μm followed by their deposition onto human lung cells (A549) with measurement of the relative downstream differential expression of ICAM-1

3.1 Context

Particle size, often categorized by a particle's diameter, is an important parameter determining the deposition site on the respiratory tract upon inhalation. However, ambient particles are more often than not, irregular in shape. Regardless, the purpose of this study was to query the effect of particles having the same mole fraction composition, but different sizes. This chapter, sections 3-2 to 3-7 was published as a special issue on aerosols/microparticle in the international journal of mass spectrometry (Eleghasim, M.N.; Haddrell, A.E.; van Eeden, S. F.; and Agnes. G. R. Int. J. Mass. spect. **2006**, 258, 134-141). Note, not published were figure 3-2, and table 3-2.

My role in the work that went into the manuscript included the designing of the chemical composition of the particles; the characterization of diameter of particles, the measurement of ICAM-1 expressed on A549 cell cultures following incubation with particles. I also wrote the manuscript.

3.2 Abstract

The characterization of particulate matter suspended in the troposphere (PM_{10}) based on size is an important basis for assessing the extent of their adverse effects on human health. The relevance of such assessments is anticipated to be significantly improved through the continued development of tools that can identify the chemical components within individual ambient particles, and the injury that they cause. We used recently reported methodology to create mimics of ambient particle types of known size and chemical composition that are levitated within an ac trap. The ac trap uses an electric field to levitate particles that have a net elementary charge, and as such, the ac trap is a mass-to-charge filter. The ac trap was used to levitate populations of particles where the size of particles in any given population could be altered. The levitated particles are delivered direct from the ac trap to human lung cells (A549), *in vitro*, with downstream measurement of differential expression of intercellular adhesion molecule (ICAM)-1 and counting of the number of particles actually delivered to the culture using an optical microscope. In this study, the chemical composition of the ambient particle mimics was restricted to inorganic compounds whose relative abundance was purposely designed to mimic the average abundance in Environmental Health Centre-93 (EHC-93) particles. The sizes of the multi-compound particle types prepared were 6.8 ± 0.5 μm, 3.8 ± 0.3 μm, 2.6 ± 0.2 μm (mean ± SD). Particles of carbon were used as a control. In any given experiment, a known number of particles, but always <100, of a given size,

were deposited onto a small region of an A549 cell culture. Following an 18 h incubation period and anti-body labelling of ICAM-1, the fluorescence emission from a 1.07 mm^2 area of the cell culture centred at the site of particle deposition was acquired. The relative differential expression of ICAM-1 was greatest for multi-compound particle type having diameters of 2.6 ± 0.2 μm for which as few as ~15 particles deposited onto the culture resulted in maximal ICAM-1 expression, whereas with multi-compound particle types having diameters of 6.8 ± 0.5 μm, it was necessary to deposit >50 particles in order to effect comparable ICAM-1 expression. This data set indicates that for multi-compound particle types comprised of the same mole fraction of inorganic compounds and of sizes within the course fraction of PM_{10}, the 2.6 μm particle type was the most potent with respect to effecting differential expression of ICAM-1.

3.3 Introduction

Epidemiological studies positively correlate ambient particle concentrations to increased frequency of hospital admissions.[252-256] It is speculated that inflammation, ranging in severity from localized within lung tissue to systemic is the biological connection linking ambient particle exposure to the pathogenesis of respiratory and cardiovascular diseases.[257-262] Regulations specify exposure limits to particulate matter with aerodynamic diameters less than 10 μm (PM_{10}) and 2.5 μm ($PM_{2.5}$) respectively.[263-265] Small reductions in ambient particulate matter concentrations achieved

through reasonable and attainable strategies are predicted to yield substantial returns with respect to reduced health care cost.

While it is understood from aerodynamic modelling studies that fine fraction ambient particles ($PM_{2.5}$) penetrate deep into the alveolar region of the respiratory tract, and coarse fraction of ambient particles ($PM_{2.5}$ - < PM_{10}) tend to be most important for the upper region of the airway,[266] it is not yet well characterized what actual particle chemical composition causes the most injury.[267-270] Further complicating this issue is that the chemical compositions of various size fractions vary based on source, tropospheric processing, and season.[271] This has been an impetus for developing tools to characterize the chemical composition of individual ambient particles. The challenges in contributing new knowledge in this area are formidable, as evidenced by the number of studies that report different conclusions regarding a single known component of ambient particle types, such as endotoxin from gram-negative bacteria.[272-274]

Prior studies performed by other investigators have used particle models, including polystyrene beads, titanium dioxide, and carbon black to mimic various particulate matter size fractions.[275, 276] However, the chemical composition of such models of ambient particles might not be relevant mimics of actual ambient particles. In contrast, other toxicology studies have used actual ambient particles collected from the troposphere.[277] A chemically well characterized sample of ambient particles, now referred to as Environmental Health Centre-93 (EHC-93), is an example of a heterogeneous population of

particles being used in toxicology studies in which the whole particle, and its soluble and insoluble fractions have been characterized.[44, 98, 278] EHC-93 comprised metals, inorganic compounds,[45, 161] and organic compounds with 99 % of its size fraction being <3 μm.[279] Studies involving EHC-93 report the mass of particles introduced to a cell culture, but not the actual size and number of particles interacting with any given cell. Also, the chemical composition of the individual particles in EHC-93 are not characterized, so it is difficult to extrapolate from those studies what individual particle compositions are most significant with respect to their role in causing tissue inflammation. Such information could be important with respect to effecting rational strategies to reduce emissions of the specific compounds identified as being most significant in particulate air pollution. With respect to addressing these issues of particle chemistry, we have reported a laboratory apparatus that enables the design of multi-component particles that mimic those found, or speculated to exist in the troposphere, and deposit those particles directly onto human lung cells, *in vitro.*

Ambient particles of different sizes are likely to have different chemical composition, but within the same size fraction, it is probable that there are particle types having similar composition. To learn the extent of the relative injury reported by a cell culture in response to incubation with different sizes of a given particle type, we chose to prepare particles having a chemical composition similar to the bulk, or average, inorganic composition of EHC-93. The relative inflammation reported by cells in these experiments was

quantified based on the differential expression of the pro-inflammatory membrane glycoprotein, intercellular adhesion molecule (ICAM)-1.

The clearance of inhaled particles from the respiratory tract has been shown to be mediated by the respiratory epithelium whose action constitutes one of the body's inflammatory responses.[280] Recent studies have shown this inflammatory mechanism involves the recruitment and migration of leukocytes, mainly neutrophils, through the endothelium to the site of inflammation.[153] The leukocyte recruitment and migration requires the surface expression of an adhesive glycoprotein, (ICAM)-1, which interacts with LFA-1 on neutrophils.[281, 282]

A hypothesis that particles whose bulk or average inorganic compounds mimic EHC-93 but having different sizes cause differential expression of ICAM-1 by A549 cells was proposed. Herein, particles having diameters of 6.8, 3.8, and 2.6 μm but whose average or bulk inorganic compound composition mimics EHC-93 were created and deposited onto A549 cells. Following 18 h incubation, the pro-inflammation potential (differential expression of ICAM-1) on A549 cells was measured.

3.4 Materials and methods

3.4.1 Starting solutions

Each of the particle types created and used consisted of the dissolved solids, and black carbon, that had been introduced to each of the starting solutions used.

The procedure for the preparation of a multi-compound starting solution first required the preparation of single component stock solutions using reagent grade compounds. Aliquots from the single component stock solutions were combined to yield what is referred to as the multi-compound starting solution (Table 3-1).

Table 3-1: The concentrations of inorganic compounds in stock solutions from which multi-compound starting solutions were prepared.

Inorganic compound	Concentration (M)	Inorganic compound	Concentration (M)
$CaSO_4$	$6.5x10^{-5}$	$MgSO_4 \cdot 7H_2O$	$5.4x10^{-2}$
$BaSO_4$	$3.7x10^{-7}$	$Al_2(SO_4)_3 \cdot 18H_2O$	$6.7x10^{-2}$
$SrSO_4$	$3.6x10^{-4}$	$FeSO_4 \cdot 7H_2O$	$4.9x10^{-2}$
$Cr_2(SO_4)_3 \cdot H_2O$	$1.5x10^{-4}$	$CoSO_4 \cdot 7H_2O$	$1.6x10^{-5}$
$3CdSO_4 \cdot 8H_2O$	$3.6x10^{-5}$	$Zn(NO_3)_2 \cdot 6H_2O$	$2.9x10^{-2}$
$CuSO_4 \cdot 5H_2O$	$2.4x10^{-3}$	$Ni(NO_3)_2 \cdot 6H_2O$	$2.2x10^{-4}$
$VOSO_4 \cdot 2H_2O$	$3.3x10^{-4}$	$Mn(NO_3)_2 \cdot 4H_2O$	$1.6x10^{-3}$
Na_2SO_4	$1.7x10^{-1}$	$PbCl_2$	$2.1x10^{-5}$

The amount of carbon in EHC-93 is not reported in the literature,[44, 162] however, previous studies have indicated that carbon generally constitutes approximately 10 % by mass of particulate matter.[283] That result was used to establish the mass of carbon black in India ink added to the multi-compound

starting solution. To this solution, India ink (Speedball, Product no.3328, Statesville, NC, USA) was added as the source of black carbon. 3.0 mL of India ink, calculated to contain ~0.45 g carbon black, was added to 6.50 mL of multi-compound solution. The India ink facilitated visualization and counting of the multi-compound particles deposited onto each cell culture prior to performing immunocytochemistry assay. Serial dilution of the multi-compound starting solution to which carbon black had been added was performed as indicated in preparing other multi-compound solutions having lower ionic strength.

Three set of starting solutions consisting of India ink in distilled deionised water were prepared as follows. 3 mL of India ink calculated to contain ~0.45 g was made up to 9.5 mL. 0.5 mL aliquots were diluted with 7.5 mL, 12.5 mL, and 25.0 mL of distilled deionised water. The particles prepared using these starting solutions are referred to as carbon black particle types. Note that these particle types differ in chemical composition relative to soots released in the exhaust of high temperature combustion sources.

3.4.2 Cell culture

The human lung alveolar epithelial cells (A549) were provided by Dr. Stephan F. van Eeden (James C Hogg iCAPTURE centre for cardiovascular and pulmonary research, University of British Columbia, Canada). The cells were derived originally from a lung alveolar carcinoma patient, and has the characteristics of type-II cells of the human lung alveolar epithelium.[163] These cells have been used extensively in studies of particulate matter-induced

responses via ICAM-1 expression.[184, 198, 284] Cells were seeded onto a 18 mm x 18 mm glass cover slip placed in each well of a 6-well culture plate containing 2 mL of minimal essential medium (MEM), supplemented with 10 % heat inactivated fetal bovine serum (FBS) (vol/vol), 1 % L-glutamine (vol/vol), and 1 % MEM vitamin solution (vol/vol). Cells were grown to 95 % confluence at 37 °C, 5 % CO_2 and 100 % relative humidity.

Cell cultures that served as positive controls contained 2 mL of growth medium to which 10 µL of 1 mg mL^{-1} of tumor necrosis factor alpha (TNF)-α (Sigma-Aldrich, T6674-10UG, Oakvillle, ON, Canada) in water was added. [285, 286] Cell cultures that served as negative controls were bathed in 2 mL growth medium only. A549 cells incubated with different numbers of carbon particles served as another control. These controls were incubated under the same conditions as cell cultures dosed with test particles.

3.4.3 Droplet dispensing

Each particulate mimic was derived from a monodisperse droplet dispensed from a droplet dispenser loaded with a starting solution. The dispensed droplets were trapped in an ac trap and levitated while the volatile solvent evaporated causing the dissolved solids to precipitate.[184, 287]

To prepare particles of varying sizes, 0.5 mL aliquots of the multi-compound starting solutions were taken and diluted with 7.5, 12.5, and 25.0 mL of distilled deionised water, to generate secondary multi-compound

solutions that had ionic strengths of 0.103 M, 0.092 M and 0.045 M respectively. The concentrations of the inorganic compounds are indicated in Table 3-2.

The levitation chamber that housed the ac trap was placed in a biological safety cabinet (Nuaire Inc., Model Nu-425-600, Plymouth, MN, USA). A schematic diagram of the ac trap with the major components indicated is shown in Fig. 3-1A. The droplet dispenser that has a nozzle with an internal diameter of 60 μm (MicroFab Technologies Inc., MJ-AB-01-60, Plano, TX, USA) was filled with an aliquot of a starting solution using a 10 μL pipette. To dispense a droplet, the waveform generator for the droplet dispenser was programmed to dispense a set number of droplets at a set frequency. The electrical signals from this waveform generator were used to actuate a cylindrical piezoceramic element bonded to the outside of the droplet dispenser reservoir and caused a small volume of liquid to be ejected from the dispenser nozzle as a jet (Fig. 3-1B). Care was exercised to ensure monodisperse droplet dispensing.

A 200 V dc potential applied to an induction electrode positioned 2 mm below the droplet dispenser nozzle caused charge imbalance within the liquid jet. The momentum of the jet caused it to separate and collapse to form a droplet, and the charge imbalance in the jet resulted in each droplet having a net charge. Droplets were dispensed downwards into the ac trap that was used to levitate the droplets.

Table 3-2: The concentrations of inorganic compound in secondary starting solution for droplet dispensing. 0.5 mL aliquots of the multi-compound starting solutions were diluted with: (A) 7.5 mL, (B) 12.5 mL, and (C) 25.0 mL distilled deionised water to give secondary starting solutions for droplet dispensing. The solutions were used in dispensing droplets for the creation of particles having diameters of:(A) 6.8 µm, (B) 3.8 µm, and (C) 2.6 µm.

Inorganic compound	Concentration of compound in secondary starting solutions that were directly delivered into the droplet dispenser (M)		
	A	B	C
$CaSO_4$	$1.1x10^{-6}$	$6.7x10^{-7}$	$3.4x10^{-7}$
$BaSO_4$	$1.0x10^{-10}$	$6.2x10^{-11}$	$3.1x10^{-11}$
$SrSO_4$	$1.4x10^{-7}$	$8.6x10^{-8}$	$4.3x10^{-8}$
$Cr_2(SO_4)_3 \cdot H_2O$	$1.6x10^{-7}$	$9.3x10^{-8}$	$4.7x10^{-8}$
$3CdSO_4 \cdot 8H_2O$	$9.1x10^{-9}$	$5.5x10^{-9}$	$2.7x10^{-9}$
$CuSO_4 \cdot 5H_2O$	$4.1x10^{-6}$	$2.4x10^{-6}$	$1.2x10^{-6}$
$VOSO_4 \cdot 2H_2O$	$7.7x10^{-7}$	$4.6x10^{-7}$	$2.3x10^{-7}$
Na_2SO_4	$9.7x10^{-4}$	$5.8x10^{-4}$	$2.9x10^{-4}$
$MgSO_4 \cdot 7H_2O$	$2.0x10^{-4}$	$1.2x10^{-4}$	$6.1x10^{-5}$
$Al_2(SO_4)_3 \cdot 18H_2O$	$3.1x10^{-4}$	$1.8x10^{-4}$	$9.2x10^{-5}$
$FeSO_4.7H_2O$	$1.7x10^{-4}$	$9.9x10^{-5}$	$4.9x10^{-5}$
$CoSO_4 \cdot 7H_2O$	$1.8x10^{-9}$	$1.1x10^{-9}$	$5.4x10^{-10}$
$Zn(NO_3)_2 \cdot 6H_2O$	$5.8x10^{-5}$	$3.5x10^{-5}$	$1.8x10^{-5}$
$Ni(NO_3)_2 \cdot 6H_2O$	$3.4x10^{-8}$	$2.0x10^{-8}$	$1.0x10^{-8}$
$Mn(NO_3)_2 \cdot 4H_2O$	$1.8x10^{-6}$	$1.1x10^{-6}$	$5.4x10^{-7}$
$PbCl_2$	$7.1x10^{-8}$	$4.3x10^{-8}$	$2.1x10^{-8}$

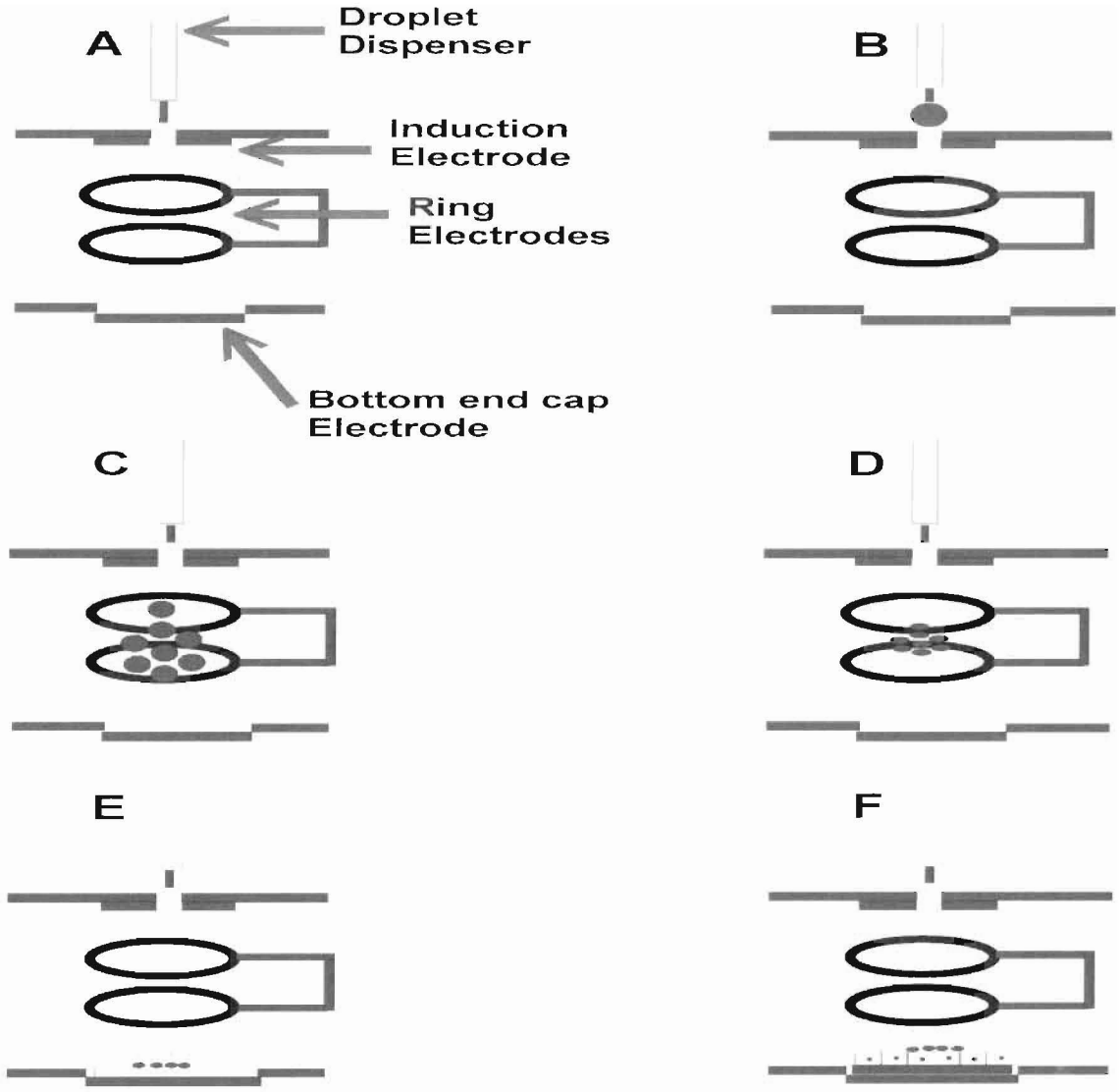

Figure 3-1: A representation of the levitation apparatus used in the creation and deposition of particles onto two different surfaces. (A) A schematic diagram of an ac trap with the major components indicated. A 10 µL aliquot of a multi-compound starting solution was used to load the internal reservoir of the droplet dispenser. (B) Dispensing of a droplet, (C) Levitation of a population of droplets while its volatile solvents evaporated, (D) Levitation of the resultant particles formed by the precipitation of the dissolved solids present in the droplets, (E) Particle deposition onto a glass slide for size characterization using optical microscopy, (F) Particle deposition onto a A549 cell culture. Note that any one cell was typically only in contact with one particle. Diagram not drawn to scale.

3.4.4 Particle levitation in an ac trap and measurement of particle diameter

The ac trap used is an imperfect electrodynamic balance (EDB). The ac trap has many similarities to a Paul trap; also known as a three dimensional quadrupole ion trap mass spectrometer,[288] and as such, the ac trap is a mass-to-charge filter.[180, 289] The frequency of the ac trap was adjusted, in conjunction with the ionic strength of the multi-compound starting solution, or also the concentration of carbon black in other starting solutions described in section 3.4.1, to effect levitation of particle populations having different sizes.

The droplets dispensed from the droplet generator passes into the ac trap through a 5-mm diameter hole cut on the induction electrode (Fig. 3-1C). Within the ac trap, a sinusoidal waveform of 4.5 $kV_{0\text{-}P}$ and frequency of 10 Hz, applied to the ring electrodes established an electric field that enabled the droplets to be levitated in air. The volatile components evaporated within seconds from the levitated droplet causing the non-volatile components in each droplet to precipitate and coagulate as a spherical particle (Fig. 3-1D). The actual distribution of the compounds in these particles has not been characterized. Though the motion of the levitated droplets/particles is collisionally dampened because of the high pressure at which these experiments were performed (1 atm), it is necessary to maintain the magnitude of the dimensionless parameter q for a trapped droplet/particle approximately constant. The q-value for a charged object trapped by an electric field relates to the droplet/particle mass-to-charge value to the square

of the ac waveform frequency in addition to other factors describing the dimensions of the electrodes. In practice, manually increasing the frequency of the ac waveform applied to the ring electrodes of the ac trap during the period over which volatile solvent evaporates from the levitated droplets allows crude tracking of the loss of mass from the levitated droplet. Imperfect electrode dimensions that introduce higher order fields, and collisional pressure dampening of the levitated particle, are key factors that enable the retention of a population of levitated droplets with each droplet having its own different mass-to-charge value in the ac trap during the period over which volatile solvent evaporates from each droplet. The end frequency necessary to maintain a population of particles levitated was dependent on the resulting size of the particle that in turn depended on the ionic strength of the multi-compound solution from which the original droplet was dispensed. For multi-compound particle types that were 6.8, 3.8, and 2.6 μm diameters, the final ac frequency was 510, 810, and 910 Hz, respectively.

Following the formation of these particles, an attractive 500 V dc potential applied to the bottom electrode of the ac trap facilitated the removal of the particles from the trap. In one phase of the experiment, particles removed from the ac trap were collected on 75 mm x 25 mm glass slides (Fig. 3-1E) and the diameters of the roughly spherical-shaped particles measured using a calibrated optical microscope.

3.4.5 Particle deposition onto A549 human lung epithelial cell culture

The procedure and conditions in the ac trap described above for the dispensing of droplets and subsequent levitation of particles, whose diameters were characterized, was used without alteration for particles that were deposited onto A549 cell cultures. Upon levitation of a population of 5 to 100 particles, a culture of A549 cells was prepared as follows. First, each 18 mm x 18 mm glass cover slip supporting a monolayer of A549 cells was removed from the well of a six well plate, and drained for 2 s. The cover slip was placed on a 75 mm x 25 mm glass slide (Surgipath Inc., #00375, Winnipeg, MN, Canada). The glass slide was then placed on a mount that sat on the bottom electrode. A 500 V dc potential applied to the bottom electrode established an attractive force that enabled the particles to be removed from the EDB and impact onto the cell culture positioned directly below the ring electrodes of the ac trap (Fig. 3-1F). After the deposition of the particles, the 18 mm x 18 mm glass cover slip was immediately transferred into a 35 mm (diameter) x 10 mm (depth) tissue culture petri dish (Sarstedt Inc. Model #28658-0468, Newton, NC, USA) and incubated at 5 % CO_2, 37 °C, and 100 % relative humidity for 18 hrs.

3.4.6 Immunocytochemistry assay

After an 18-h incubation period, an antibody assay was performed in a biological safety cabinet as follows. The monolayer of A549 cells was twice

rinsed with 1 mL Phosphate-Buffered Saline (PBS) solution. The cell culture was then fixed with 1 mL of 1 % acetone solution, allowed to stand for 10 min, and afterwards discarded. Thereafter, cells were rinsed with 1 mL of PBS, and 1 mL of tris-buffered salt (TBS) solution prior to treatment with serum-free protein block. Each 18 mm x 18 mm cover slip containing A549 cell culture was treated with 95 µL serum-free protein block, reported by the manufacturer as having 0.25% casein in PBS, stabilizing proteins and 0.015 M sodium azide (DakoCytomation Inc., X0909, Carpinteria, CA, USA) for 30 min. Followed by treatment with 95 µL of 50 µg/0.5 mL solution of mouse-antihuman monoclonal CD-54 primary antibody (Caltag Laboratories, LMHCD54F, Burlingham, CA, USA) for 1 h.

After the 1 h treatment with the primary antibody, the cell culture was rinsed with 1 mL of TBS solution and then treated with 95 µL of 2 mg/mL solution of goat-antimouse secondary antibody solution conjugated to Alexa Fluor 546 (Invitrogen Detection Technologies, 34779A, Eugene, OR, USA) for 30 min. At the end of 30 min treatment with the secondary antibody, the cell culture was rinsed four times with TBS solution. Following 18 h incubation, the controls were labelled as described herein using immunocytochemistry assay. Each 18 mm x 18 mm cover slip was mounted on a 75 mm x 25 mm glass slide prior to performing fluorescence microscopy and image analysis.

3.4.7 Fluorescence microscopy and analysis of acquired images

All images of fluorescence emission from the fluorescently tagged antibodies bound to ICAM-1 expressed on A549 cells were collected with an inverted fluorescence microscope equipped with an epi-fluorescence filter block (filter block model MG-1, Epi-Fl, microscope model AE31, Motic Instruments Inc., Richmond, BC, Canada). The deposition site scan is defined as a 1.07 mm^2 circular area centered over the site of particle deposition from which fluorescence emission was collected. Differential ICAM-1 expression was calculated based on the fluorescence emission signal intensity at each pixel in each scan of a cell culture using Image J software (Research Services branch, National Institute of Health, Bethesda, MD, USA) and the numerical values of the pixel signals were summed using Microsoft Excel. The summed ICAM-1 expression is reported as a percent of total signal intensity relative to A549 cell cultures treated with TNF-α as the positive control.[184] The fluorescent signal emission from fluorophore-tagged secondary antibody of goat-antimouse antibody bound to ICAM-1 expressed on A549 cell culture after 18 h incubation is indicated in Figure 3-2.

Figure 3-2: **Fluorescence emission signal from fluorophore-tagged secondary antibody of goat-antimouse bound to ICAM-1 expressed on A549 cell culture after 18 h incubation: (A) Negative control, (B) Carbon particles, (C) 2.6 μm particle, (D) 6.8 μm particles, (E) Tumour necrosis factor-alpha (TNF-α). The scale bar in panel (E) is 15 μm and is valid for all images.**

3.5 Results

3.5.1 Characterization of particle diameter

Ac traps have been used in many studies involving the levitation of droplets containing inorganic compounds.[290] In this work, multi-compound containing droplets were captured in the ac trap and levitated for 5 s or less, allowing the dissolved solids to precipitate. The multi-compound particles thus formed were then deposited onto a glass cover slip. Photomicrographs of each size of these particles as viewed using an optical microscope are presented in Fig. 3-3A, panels i-iii. The average diameter of each particle type

generated from the multi-compound starting solution having ionic strengths of 0.103 M, 0.092 M and 0.045 M were 6.8 ± 0.5 μm, 3.8 ± 0.3 μm, 2.6 ± 0.2 μm, respectively (mean ± SD). The relative sizes of these particles are depicted in bar-graph format in Fig. 3-4, and their per particle mass in Fig. 3-5. Not shown are images of carbon black particle types that were similarly characterized. Representative photomicrographs of these same particle sizes following their deposition onto A549 cell cultures and an incubation period of 18-hr are shown in Fig. 3-3B, panels i-iii.

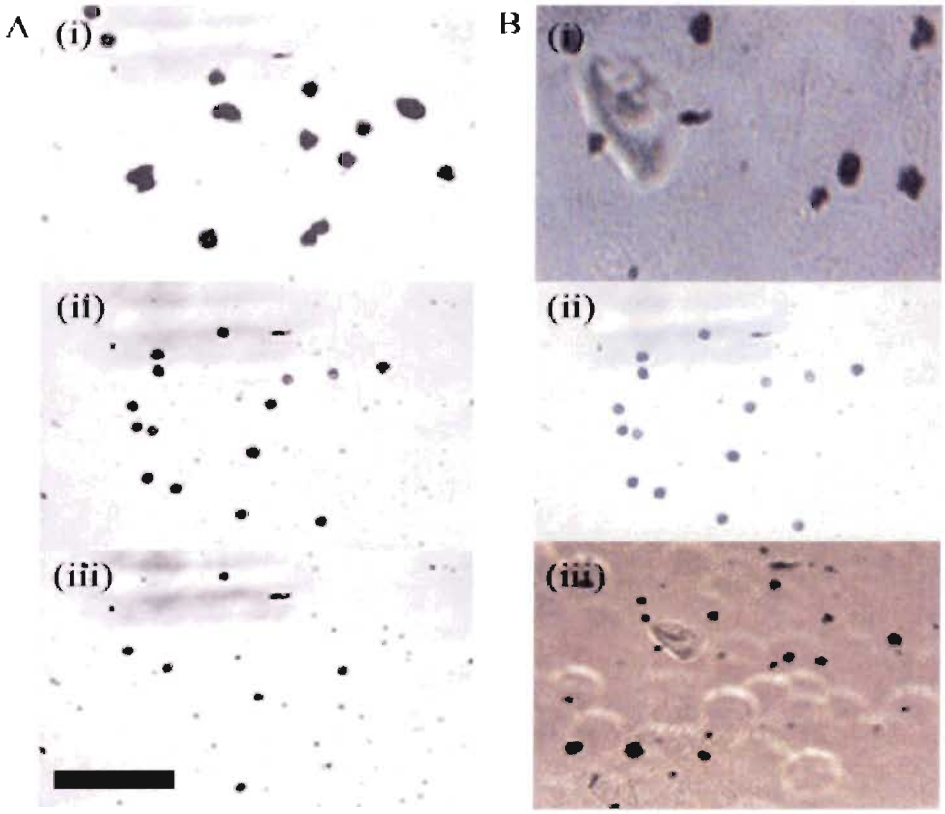

Figure 3-3: Representative images of multi-compound particles types that were deposited onto glass slides for size characterization via calibrated optical microscopy. The average diameters were: (i) 6.8 ± 0.5 μm, (ii) 3.8 ± 0.3 μm, (iii) 2.6 ± 0.2 μm. (B) Representative images of multi-compound particles types that had been deposited onto A549 cell cultures and visualized following 18 h incubation period. The scale bar in panel A (iii) is 15 μm

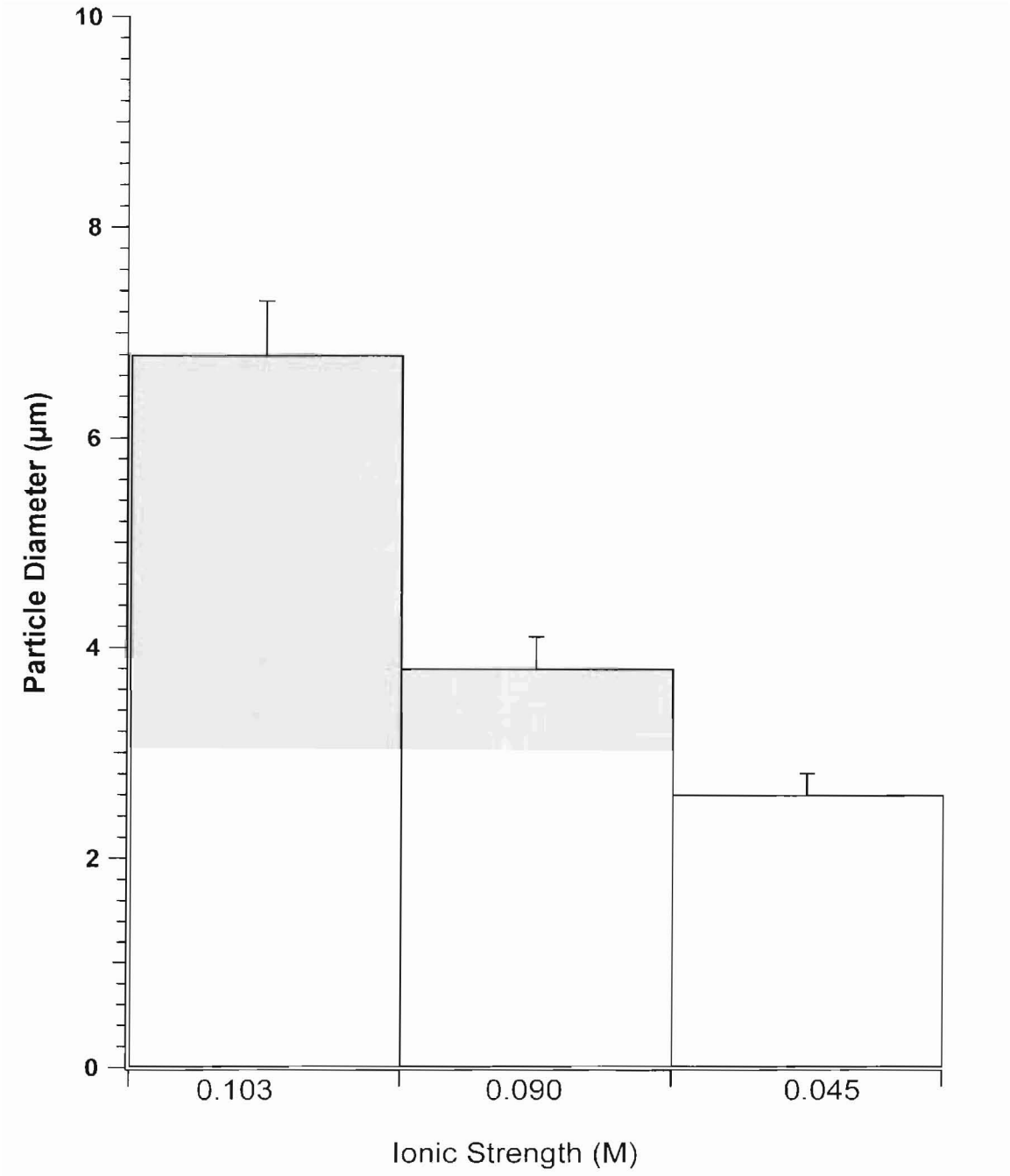

Figure 3-4: **Bar graph representation of the diameters of the multi-compound particles formed as a function of the ionic strength of the multi-compound secondary starting solutions.**

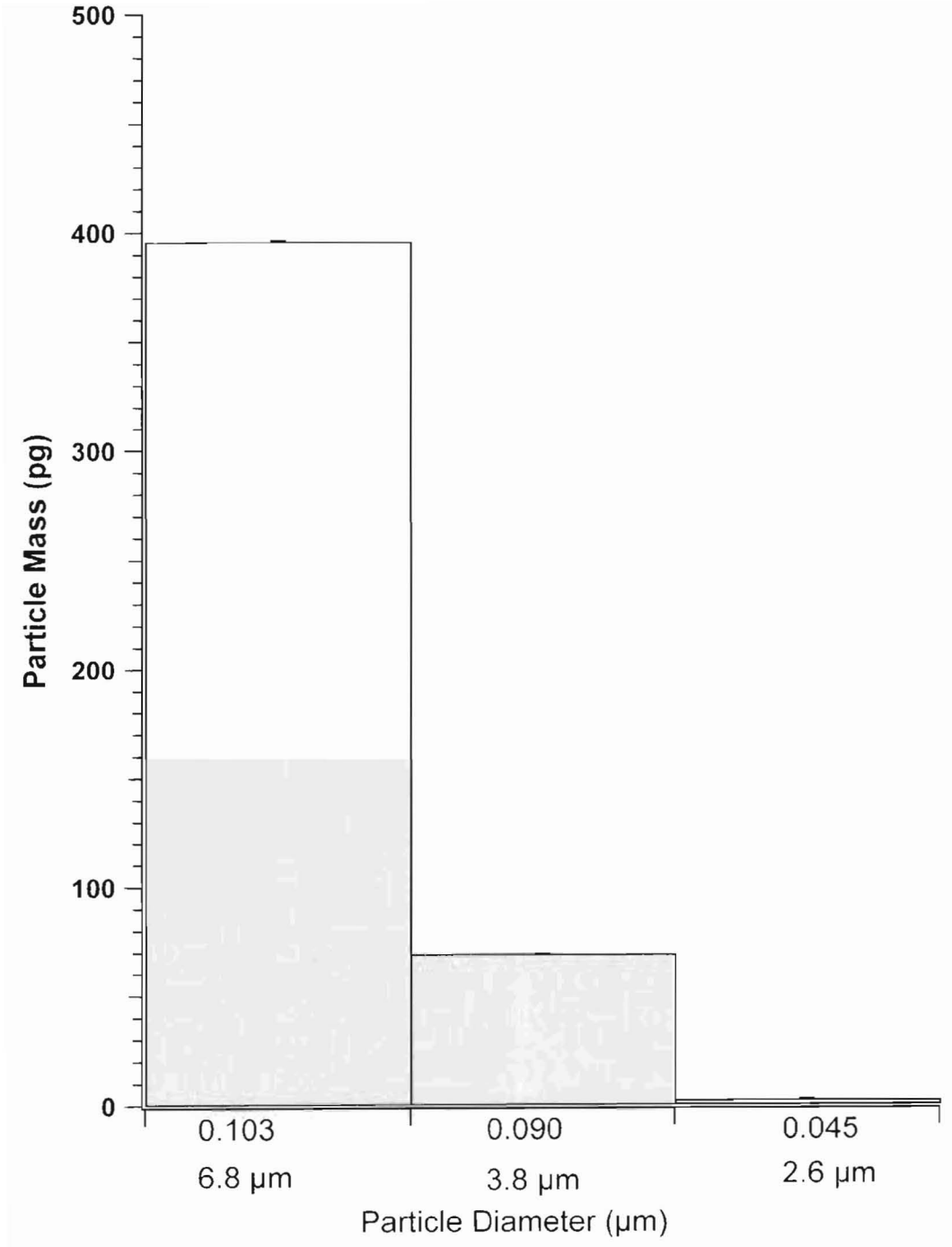

Figure 3-5: **Bar graph representation of the mass of inorganic compounds in each size of the multi-compound particle type created.**

3.5.2 Inflammation potential of a multi-compound inorganic particle type using particle diameters of 6.8, 3.8, and 2.6 µm.

The apparatus used to create and deliver particles to cultures in these dose-response experiments allows us to know the number, size, and composition of the particles deposited. With respect to the cellular response, the injury monitored was limited to the quantitative measurement of the differential expression of a single pro-inflammatory mediator, ICAM-1. The expression of ICAM-1 in all test cultures was normalized using the positive control. The cultures used as negative controls were also normalized to the positive controls and the relative expression of ICAM-1 measured in those was ~0.4.

Each data point in figure 3-6 to 3.8 is the fluorescence signal intensity measured at the site of particle deposition, and that value is taken as the differential expression of ICAM-1 relative to the positive control from each experiment. The data showing the fluorescence from cultures dosed with elemental carbon particles that were themselves 6.8, 3.8, and 2.6 µm in diameter are plotted as open symbols in figure 3-6 to 3-8. The elemental carbon particles did not cause measurable differential expression of ICAM-1 in A549 cells relative to the negative control. Clearly, the addition of the inorganic compounds, in the relative quantities indicated in Table 3-2, to carbon black to create a multi-compound particle type resulted in differential expression of ICAM-1.

The relative fluorescence signal intensity data from cell cultures following immunocytochemistry, indicative of the relative ICAM-1 expression, were fitted to least squares linear regressions as a function of the number and as the mass of multi-compound particle types delivered. The value of the slopes to these fits is presented in bar-graph format in Figure 3-9 to 3-10, and the error bars indicate the error in the fitted slope. The magnitude of the numerical values for the slope of the least squares linear fits are interpreted as the pro-inflammation potential (ICAM-1) for a given particle size.

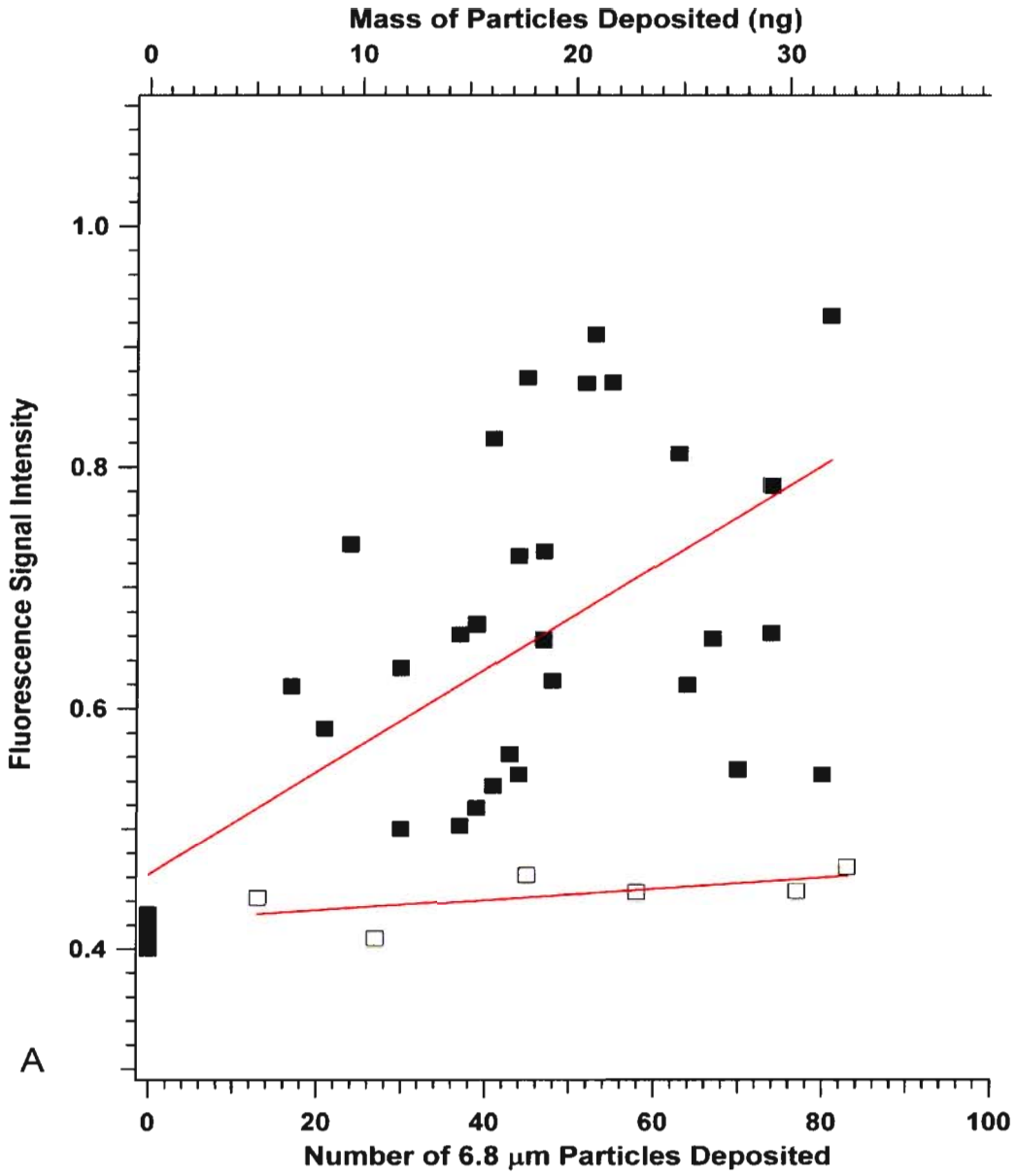

Figure 3-6: **Relative fluorescence signal intensity of ICAM-1 expressed on A549 cell culture after 18 h incubation with particle having nominal diameter of 6.8 μm. Bottom x-axis represents the number of particles deposited to the cell culture. Top x-axis represents the mass of particles delivered. Filled symbols represent multi-compound particles, and open symbols represent carbon particles. The fluorescence signal intensity was collected from 1.07 mm^2 circular area centred over the site of particle deposition. The R^2 coefficient from the linear least square fit to the fluorescence signal versus the number of particles deposited (filled symbols) was: (A) 0.6502.**

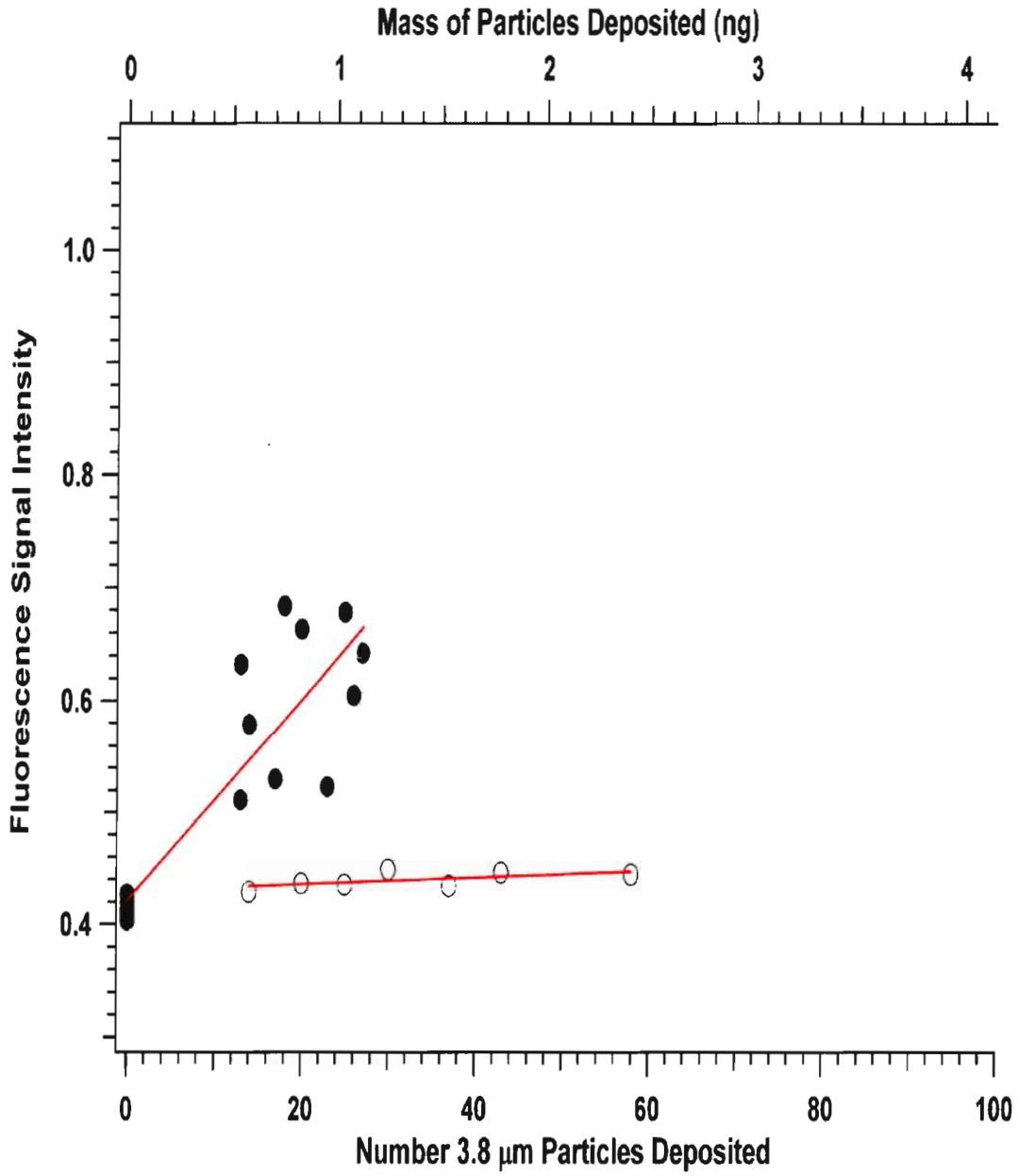

Figure 3-7: **Relative fluorescence signal intensity of ICAM-1 expressed on A549 cell culture after 18 h incubation with particle having nominal diameter of 3.8 μm. Bottom x-axis represents the number of particles deposited to the cell culture. Top x-axis represents the mass of particles delivered. Filled symbols represent multi-compound particles, and open symbols represent carbon particles. The fluorescence signal intensity was collected from 1.07 mm^2 circular area centred over the site of particle deposition. The R^2 coefficient from the linear least square fit to the fluorescence signal versus the number of particles deposited (filled symbols) was: (B) 0.6265.**

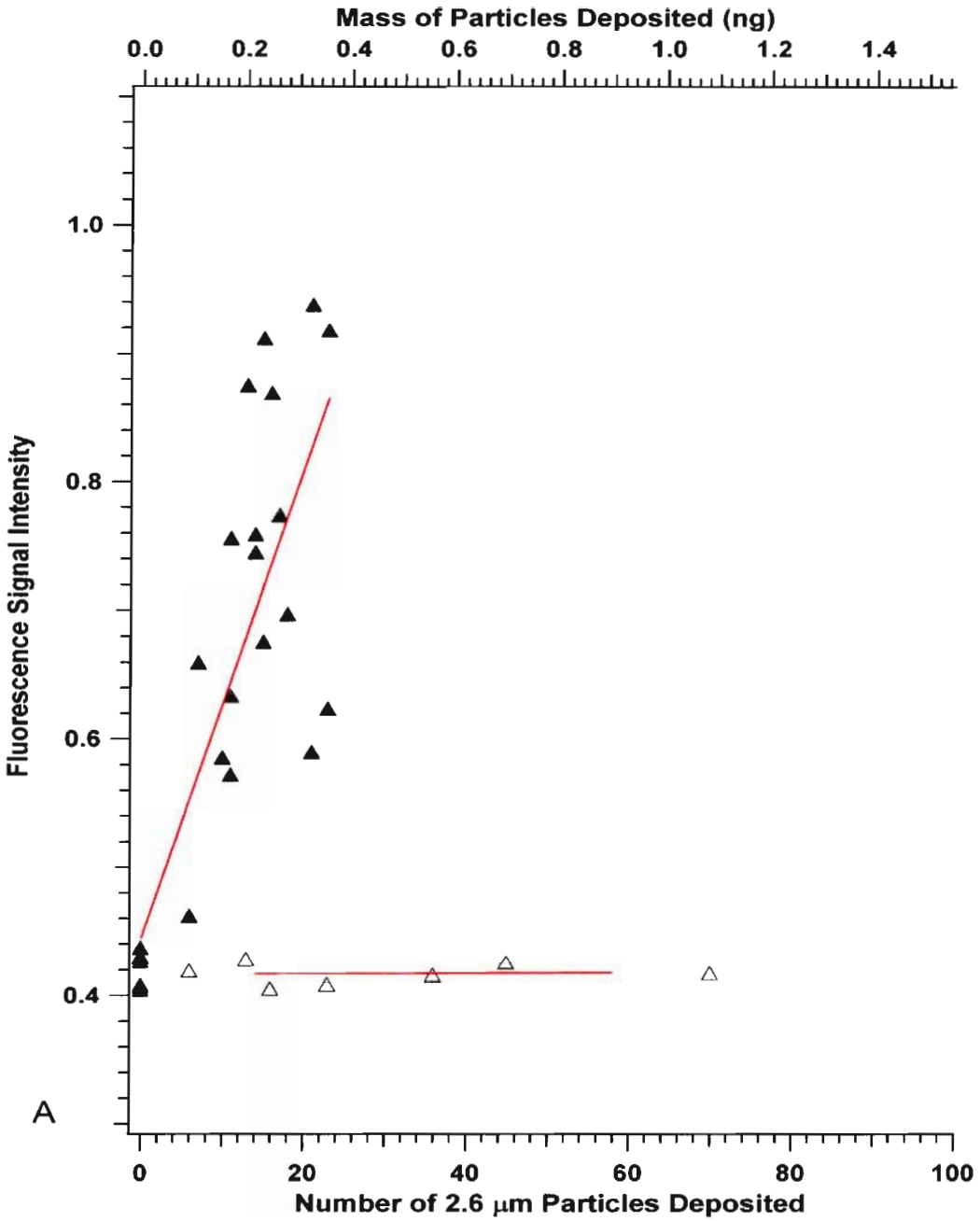

Figure 3-8: **Relative fluorescence signal intensity of ICAM-1 expressed on A549 cell culture after 18 h incubation with particle having nominal diameter of 2.6 μm. Bottom x-axis represents the number of particles deposited to the cell culture. Top x-axis represents the mass of particles delivered. Filled symbols represent multi-compound particles, and open symbols represent carbon particles. The fluorescence signal intensity was collected from 1.07 mm^2 circular area centred over the site of particle deposition. The R^2 coefficient from the linear least square fit to the fluorescence signal versus the number of particles deposited (filled symbols) was: (C) 0.7901.**

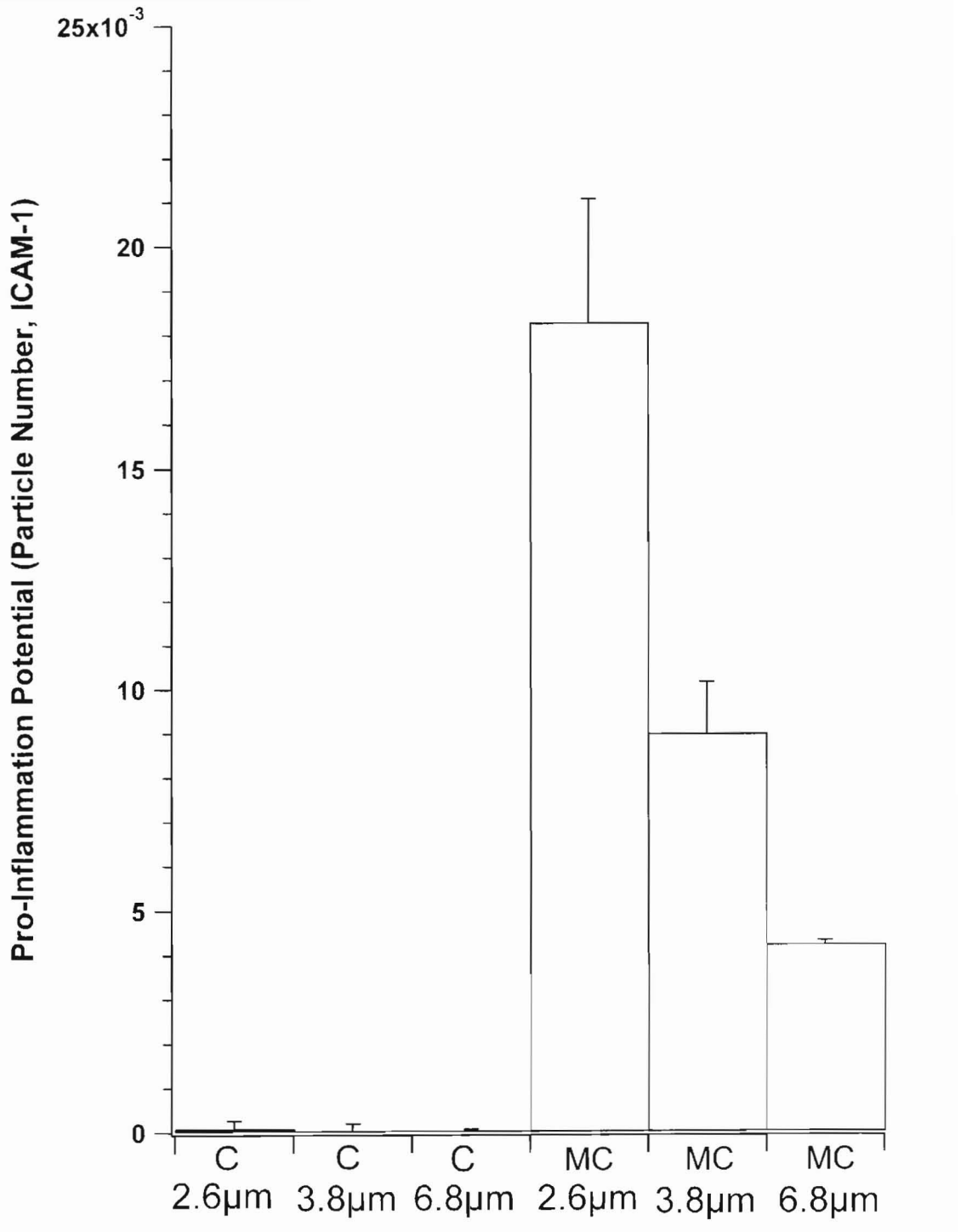

Figure 3-9: **Pro-inflammation potential (PIP) represented in terms of differential expression of ICAM-1 by A549 cells in response to 18 h incubation with particles of carbon, or multi-compound (MC) particles having indicated diameters in micrometers. The PIP is presented as a function of number of particles deposited onto the cell cultures.**

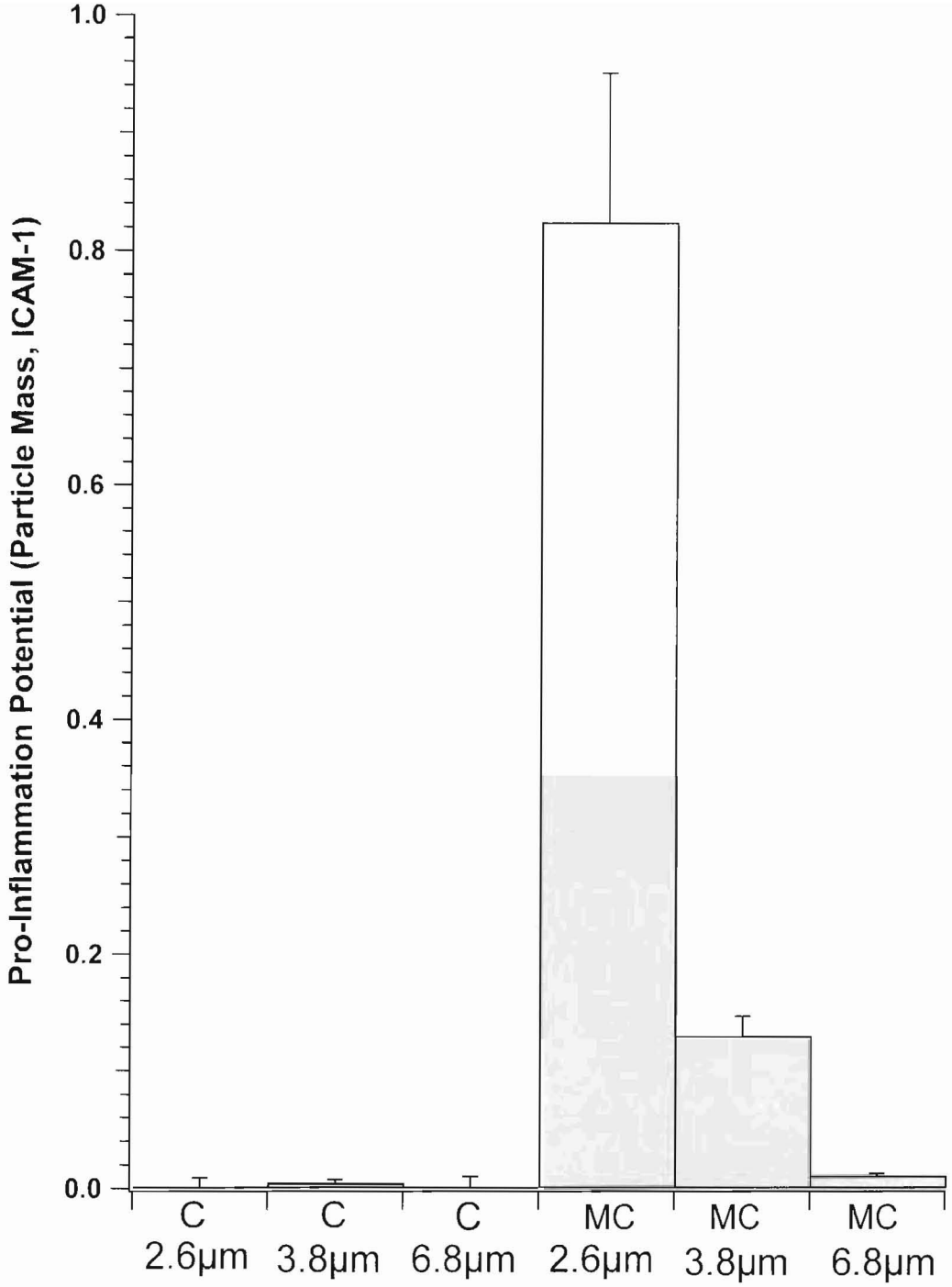

Figure 3-10: **Pro-inflammation potential (PIP) represented in terms of differential expression of ICAM-1 by A549 cells in response to 18 h incubation with particles of carbon(C), or multi-compound (MC) particles having indicated diameters in micrometers. The PIP is presented as a function of mass of particles deposited onto the cell cultures.**

3.6 Discussion

This study utilized an ac apparatus and associated methodology with which questions at the interface between atmospheric particle chemistry and lung cell biology can be addressed. For example, the data generated with this infrastructure allows the data to be presented in a format that enables inter-comparison between composition, number, and size of particles actually delivered to cell cultures for the purpose of identifying which components on different ambient particle types are most significant with respect to causing adverse effects on human health. Clearly, the type (e.g. chemical composition), size, and number of particles delivered to a culture are significant factors in characterizing the relative injury, in vivo, caused by ambient particle types. Our results indicate that particles having varying sizes but the same bulk inorganic chemical composition effected a different level of injury to A549 cells based on the measured differential ICAM-1 expression. As few as ~15 multi-compound particles of diameter 2.6 μm caused significant ICAM-1 expression whereas with 6.8 μm diameter particles having the same mole fraction of multiple compounds >50 such particles were required to initiate an appreciably significant response. Moreover, different sizes of a control particle type, carbon black, were measured to have induced no differential expression of ICAM-1 relative to the negative controls. The correlation reported for the differential ICAM-1 expression due different particle sizes reported herein is weak.

Prior studies have indicated that the fine fraction particles (i.e. $PM_{2.5}$) were more toxic than coarse fraction ambient particles (i.e. $PM_{2.5}$ - < PM_{10}). [291, 292] This could simply be due to more favourable particle-cell interaction (i.e. rate of endocytosis) for the smaller particle size studied, and not a function of particle chemical composition. The extent to which the varied compounds contribute to toxicities of coarse and fine fractions of ambient particles following inhalation exposure is not well understood, as significant differences exist between coarse and fine fractions regarding their sources, chemical compositions, atmospheric life times and temporal variability. The question remains, what particle physicochemical properties contribute most significantly to the observed inflammation following inhalation exposure to particulate matter of varying size fractions? Particulate matter has been shown to generally contain numerous chemical components that include elemental carbon, metals, inorganic compounds and organic compounds.[2] Furthermore, coarse fraction particulate matter contains endotoxin, and several studies have suggested that these particle types are significant contributors to particulate air pollution. While conclusions should not be drawn at this stage regarding the role of chemical components on fine versus coarse fraction ambient particles and their potency with respect to causing tissue injury, hypotheses can however be formulated to address this issue regarding particulate air pollution using the apparatus and associated methodology described herein. Note that the results presented involved particles within the coarse fraction of ambient particles. An extension of this

data set using the same multi-element particle types into the fine fraction of ambient particles could be informative because for such particles sizes the particle-cell interactions could be less dissimilar, and particle surface area or surface area of reactive sites on a particle could be important.[267]

A hypothesis regarding nanoparticle toxicity postulates that their surface area could be a very important factor in determining the extent of the injury that they cause.[293] In order for our data to have been in agreement with that nanoparticle surface-area hypothesis, a similar relative injury caused on a per particle surface area basis would have had the ICAM-1 expression caused by a single 6.8 μm diameter particle being approximately similar to that caused by a calculated 7 particles of 2.6 μm diameter. This was not what was observed, and therefore these results on coarse fraction ambient particle types ($PM_{2.5}$ - < PM_{10}) should not be extrapolated to the nanometer size regime. When quantitative dose-response methodology has been developed to the extent that particles of size within the $PM_{2.5}$ classification can be used and the relative cellular injury inter-compared, a test of the nanoparticle surface area hypothesis for fine fraction ambient particles ($PM_{2.5}$) could be performed.

3.7 Conclusion

A particle levitation apparatus and associated methodology was used to design a multi-compound particle type that was created at different sizes within the coarse fraction of PM_{10} but all with the same chemical composition that represented the bulk inorganic composition of EHC-93. Based on the

number of multi-compound particles deposited, particles of 2.6 μm in diameter were respectively, 2 and 4 times more potent in causing cellular up-regulation of ICAM-1 than particles of 3.8 and 6.8 μm in diameter in terms of number of particles deposited. The same data, evaluated based on the mass of particulate material delivered to a culture, indicated that the 2.6 m diameter particle type was, respectively, 6 and 80 times more potent in terms of effecting cellular up-regulation of ICAM-1 versus the 3.8 and 6.8 μm diameter particles. These results illustrate there is need to have detailed knowledge of particle composition, number and size of particulate matter delivered to tissue in order to more accurately evaluate potential health outcomes associated with inhalation exposure to ambient particles.

CHAPTER 4: The differential expression of ICAM-1 by A549 cells, *in vitro*, in response to incubation with < 100 particles prepared by systematic addition of inorganic compounds at different mole fractions

4.1 Context

An alternating current (ac) trap and associated levitation methodology was used to create single- and multi-compound inorganic particles. These particles were deposited onto A549 cells and the downstream differential ICAM-1 expression was measured.

4.2 Abstract

Inhalation exposure to ambient particulate matter (PM) causes lung tissue injury. Identification of specific components within ambient PM that are responsible would enhance strategies aimed at improving air quality through restriction of the respective emissions. Herein, an ac trap was used to levitate particles of carbon plus each of $Ca(NO_3)_2$, $Mg(NO_3)_2$, $Sr(NO_3)_2$, and $NaNO_3$, and also multi-compound particles, referred to as particle type (PT)-4,5,6,7,8,13, prepared by systematic addition of inorganic compounds at a constant but different, mole fraction. The numerical value in each particle type refers to the number of different metal nitrate salts in the particle. These particles were deposited onto A549 cells and the downstream differential expression of ICAM-1 was measured. The single-compound particles caused low, but measurable, differential ICAM-1 expression on A549 cells. For the

multi-compound particles: PT-5, PT-6, PT-7, and PT-8, prepared by systematic addition of aluminium nitrate, iron nitrate, zinc nitrate, and lead nitrate, it was found that lead nitrate effected the most differential ICAM-1 expression on A549 cells.

4.3 Introduction

Measurements of the chemical composition of bulk samples of ambient PM have indicated that it is complex in terms of the number different compounds.[294-297] An association between inhalation of metal-rich ambient particles and the pathogenesis of several pulmonary and cardiovascular diseases has been shown.[258, 298] Because of these adverse effects on human health, there is interest in identification of the relative injury that the different compounds known to be present in PM cause.[296, 297] Such knowledge would enhance the implementation of effective emission reduction strategies targeted towards improving air quality.[299-301] For instance, previous inhalation exposure studies involving a particulate matter fraction containing organic compounds have identified polyaromatic hydrocarbons (PAHs) that are linked to increased probability of cancer.[302, 303]

Varying metal concentration have been reported in ambient PM sampled at different locations across the planet.[278, 304, 305] However, the lung's response to specific metal components within ambient PM is not yet fully understood.[306-308] For instance, recent studies indicate that instilled water-soluble components of ambient particles cause pulmonary toxicity.[298, 306, 309] This toxicity was noted to exhibit variation based on what sampled ambient

particles were used.[306, 309] Different metal content, such as zinc, copper, iron, lead, and manganese, in those samples were suggested to be responsible.[310] In addition, it is believed that ambient particles' size and number are two other important physicochemical properties that mediate adverse effects on human health.[185, 260, 311] *In vitro* methodologies that can provide mimicry of ambient particle's physical state, chemical composition, and size are needed to provide new information regarding particulate air pollution.

It is hypothesized that inorganic compounds systematically added to the multi-compound particles did not cause significant differential ICAM-1 expression. To address this hypothesis, an ac trap was used to create particles prepared by systematic addition of inorganic compounds at different mole fraction, and the pro-inflammation potential (differential ICAM-1 expression) by A549 cells was measured.

4.4 Materials and methods

4.4.1 The preparation of starting solutions

The grouping of particles with regard to the inorganic compounds (nitrates) they contained is shown (Table 4-1). Reagent grade inorganic compounds were used in the preparation of single-compound stock solutions. The concentration of each inorganic compound's stock solution is indicated (Table 4-2). The volume of single-compound stock solutions used for preparing single-compound starting solutions is given (Table 4-3). In ambient air, particles are known to contain several inorganic compounds in addition to

such components as black carbon that is emitted during the combustion of biological materials.[312, 313] In all cases, 2.0 mL of India ink, calculated to contain 0.30 g of carbon black was added to these aliquots. These aliquots were diluted to a total volume of 9.5 mL with distilled deionised water.

Each multi-compound starting solution was prepared by combining aliquots of single-compound stock solutions based on the grouping of inorganic compounds indicated in Table 4-1. The volumes of single-compound stock solutions used for preparing multi-compound starting solution were the same for the single component starting solutions, as indicated in Table 4-3. In all cases, 2.00 mL of India ink, calculated to contain 0.30 g of carbon black, was added to each multi-compound starting solution. All multi-compound starting solutions were diluted to a total volume of 9.5 mL with distilled deionised water.

The following solution preparation was used in creating carbon particles that served as a control. 2.0 mL India ink was diluted with 9.5 mL of distilled deionised water.

Table 4-1: The grouping of multi-compound particle types with respect to metals they contained. The numerical value in each particle type refers to the number of different metal nitrate salts in the particle. √ indicates inclusion in the particle type.

Particle type	PT-4	PT-5	PT-6	PT-7	PT-8	PT-13
Ca^{2+}	√	√	√	√	√	√
Sr^{2+}	√	√	√	√	√	√
Na^{+}	√	√	√	√	√	√
Mg^{2+}	√	√	√	√	√	√
Al^{3+}		√	√	√	√	√
Fe^{3+}			√	√	√	√
Zn^{2+}				√	√	√
Pb^{2+}					√	√
Cr^{3+}						√
Cu^{2+}						√
Ni^{2+}						√
Mn^{2+}						√
Co^{2+}						√
NO^{-}_3	√	√	√	√	√	√
C	√	√	√	√	√	√

Table 4-2: The concentrations of single-compound stock solutions.

Inorganic compounds	Stock solution concentration (mol/L)	Inorganic compounds	Stock solution concentration (mol/L)
$Ca(NO_3)_2{\cdot}4H_2O$	$6.5x10^{-5}$	$NaNO_3$	$1.7x10^{-1}$
$Sr(NO_3)_2$	$3.6x10^{-4}$	$Al(NO_3)_3{\cdot}9H_2O$	$6.7x10^{-2}$
$Mg(NO_3)_2$	$5.4x10^{-2}$	$Fe(NO_3)_3{\cdot}9H_2O$	$4.9x10^{-2}$
$Zn(NO_3)_2{\cdot}6H_2O$	$2.9x10^{-2}$	$Cu(NO_3)_2{\cdot}6H_2O$	$2.4x10^{-5}$
$Pb(NO_3)_2$	$2.1x10^{-5}$	$Co(NO_3)_2{\cdot}6H_2O$	$1.6x10^{-5}$
$Cr(NO_3)_3{\cdot}9H_2O$	$1.5x10^{-4}$	$Ni(NO_3)_2{\cdot}6H_2O$	$2.2x10^{-4}$
$Mn(NO_3)_2{\cdot}4H_2O$	$1.6x10^{-3}$		

4.4.2 A549 cell culture

The human lung alveolar epithelial cells (A549) were provided by Dr. Stephan F. van Eeden (James C Hogg iCAPTURE Centre for cardiovascular and pulmonary research, University of British Columbia, Canada). Cells were seeded onto a 18 mm x 18 mm glass cover slip placed in each well of a six-well plate that contained 2 mL minimal essential medium (MEM), supplemented with 10 % heat inactivated fetal bovine serum (FBS) (vol/vol), 1 % MEM vitamin solution (vol/vol), and 1 % L-glutamine (vol/vol). Cells were grown to 95 % confluence at 37 °C, 5 % CO_2, and 100 % relative humidity.

A positive control was cells bathed in 2 mL of MEM and treated with 10 µL of 1 mg/mL of tumour necrosis factor alpha (TNF)-α (Sigma-Aldrich, T6674-10UG) in water. A negative control was cells bathed in 2 mL of growth medium only. Sets of negative control were cultures incubated with different numbers of carbon particles. All of these controls were incubated under the same conditions as cell cultures dosed with test particles.

4.4.3 Droplet dispensing

A 0.5 mL aliquot of the single-, multi-compound starting solutions, and the solutions for carbon particles, were diluted with 12.5 mL of distilled deionised water to make solutions referred to as single- and multi-compound secondary starting solutions. The concentrations of each inorganic compound in the single-and multi-compound secondary starting solutions are stated in Table 4-3.

Figure 4-1A is a schematic diagram of an ac trap with its main components. It is contained within a chamber placed in a biological safety cabinet (Nuaire Inc., Model Nu-425-600, Plymouth, MN, USA). The droplet dispenser has a nozzle with an internal diameter of 60-μm (MicroFab Technologies Inc., MJ-AB-01-60, Plano, TX, USA). The dispenser's reservoir was filled with an aliquot of a secondary starting solution to be dispensed using a 10-μL pipette. The procedure for droplet dispensing is described below.

To dispense a droplet, an electrical signal from the waveform generator for the droplet dispenser was used to actuate a cylindrical piezoceramic element bonded to the outside of the droplet dispenser's reservoir. The actuation of the piezoceramic element caused a small volume of liquid to be expelled as a jet from the dispenser nozzle (Fig. 4-1B). Droplets were generated at a rate of 120 Hz. The droplet-dispensing period was 5 s or less. A 200 V dc potential applied through an induction electrode placed 2 mm below the nozzle of the droplet dispenser caused ion mobility within this jet to effect charge separation. The momentum of the jet caused it to separate and collapse to form a droplet, and the charge separation resulted in each droplet possessing a small net elementary charge. This net charge enabled each droplet to be levitated within an ac trap.[289]

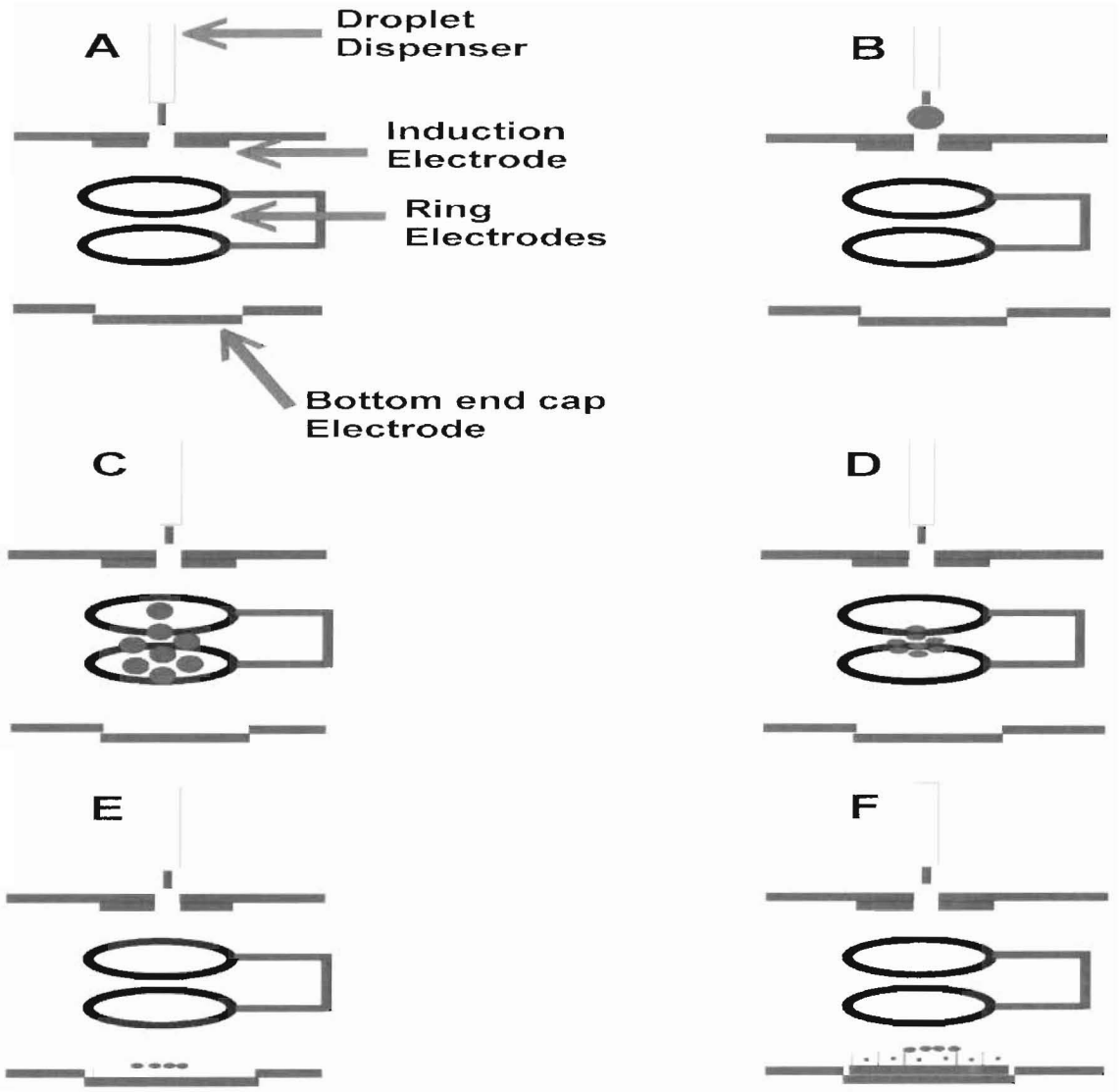

Figure 4-1: A representation of the levitation apparatus used in the creation and deposition of particles onto two different surfaces. (A) A schematic diagram of an ac trap with the major components indicated. A 10 µL aliquot of a multi-compound starting solution was used to load the internal reservoir of the droplet dispenser. (B) Dispensing of a droplet, (C) Levitation of a population of droplets while its volatile solvents evaporated, (D) Levitation of the resultant particles formed by the precipitation of the dissolved solids present in the droplets, (E) Particle deposition onto a glass slide for size characterization using optical microscopy, (F) Particle deposition onto a A549 cell culture. Note that any one cell was typically only in contact with one particle. Diagram not drawn to scale.

Table 4-3: The concentration of each inorganic compound in each of the single- and multi-component secondary starting solutions for droplet dispensing.

Inorganic compounds	Volume used (L)	Concentration of compound in secondary starting solutions delivered directly to the droplet dispenser (M)
$Ca(NO_3)_2{\cdot}4H_2O$	$2.4x10^{-3}$	$6.7x10^{-7}$
$Sr(NO_3)_2$	$6.0x10^{-5}$	$8.6x10^{-8}$
$Mg(NO_3)_2$	$5.4x10^{-4}$	$1.2x10^{-4}$
$NaNO_3$	$8.1x10^{-4}$	$5.8x10^{-4}$
$Al(NO_3)_3{\cdot}9H_2O$	$6.5x10^{-4}$	$1.8x10^{-4}$
$Fe(NO_3)_3{\cdot}9H_2O$	$4.8x10^{-4}$	$9.9x10^{-5}$
$Zn(NO_3)_2{\cdot}6H_2O$	$2.8x10^{-4}$	$3.5x10^{-5}$
$Pb(NO_3)_2$(A)	$1.0x10^{-5}$	$8.8x10^{-10}$
$Pb(NO_3)_2$(B)	$6.0x10^{-5}$	$5.3x10^{-9}$
$Pb(NO_3)_2$(C)	$6.0x10^{-4}$	$4.3x10^{-8}$
$Cr(NO_3)_3{\cdot}9H_2O$	$1.4x10^{-4}$	$9.3x10^{-8}$
$Cu(NO_3)_2{\cdot}6H_2O$	$2.4x10^{-4}$	$2.4x10^{-6}$
$Co(NO_3)_2{\cdot}6H_2O$	$1.6x10^{-5}$	$1.0x10^{-9}$
$Ni(NO_3)_2{\cdot}6H_2O$	$2.2x10^{-5}$	$2.0x10^{-8}$
$Mn(NO_3)_2{\cdot}4H_2O$	$1.6x10^{-4}$	$1.0x10^{-6}$

4.4.4 Particle levitation and deposition onto A549 cell culture

Each dispensed droplet passes through a 5-mm diameter hole cut on the induction electrode into an ac trap. Within the ac trap, each droplet was captured and levitated by the electric field generated by applying a sinusoidal waveform at 4.5 k $V_{0\text{-}P}$ and frequency 10 Hz (Fig. 4-1C) to the ring electrodes of the ac trap. With the droplets captured, the frequency of this waveform generator was manually ramped to 920 Hz. The volatile solvents and water within each droplet quickly evaporated (i.e. within seconds), leaving behind a single residue per droplet that is comprised of the non-volatile solutes contained in each dispensed droplet (Fig. 4-1D). An attractive 500 V dc potential applied to the bottom electrode established an electric field that

facilitated particle removal from the ac trap onto a 75 mm x 25 mm glass slide for optical microscopy (Fig. 4-1E). Each residue was viewed with a calibrated optical microscope. These residues were roughly spherical in appearance, and they are subsequently referred to as a particle (Fig. 4-2). Each particle had a diameter of 2.7 ± 0.5 μm (mean ± SD). The number of femtomoles of the elements contained in each single-compound and multi-compound particle type is indicated in Table 4-4 and 4.5 respectively.

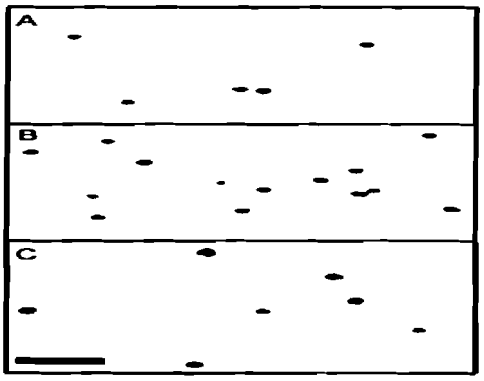

Figure 4-2: Photomicrographs of representative single- and multi-compound particles that were deposited onto a glass slide and the sizes characterized through optical microscopy. Their average diameters were 2.7 ± 0.5 μm. The particles represented are: (A) C + $Ca(NO_3)_2$, (B) PT- 4, (C) PT-13. The scale bar in panel (C) represents 15 μm and it is valid for all images.

With a population of particles levitated (between 5 to < 100 per trial), an A549 cell culture was prepared for particle deposition. The 18 mm x 18 mm glass cover slip containing A549 cells was removed from the well of a 6-well plate. The growth medium was drained for about 2 s. This cover slip was placed on a 75 mm x 25 mm glass slide. The glass slide was positioned on the bottom end cap electrode of the ac trap. An attractive 500 V dc potential

applied to the bottom electrode established the electric field that facilitated particle removal from the ac trap onto the cell culture (Fig. 4-1F). After particle deposition, each glass cover slip was quickly removed from the glass slide and placed in a 35 mm (diameter) x 10 mm (depth) tissue culture petri dish. This petri dish was incubated at 37 ^{o}C, 5 % CO_2 and 100 % relative humidity for 18 hrs.

Table 4-4: The number of femtomoles of each metal nitrate salt contained in single-compound particles.

Particle type	Moles of metals (fmol)	Moles of nitrate (fmol)	Moles of carbon (fmol)
C + $NaNO_3$	262	262	$3.3x10^4$
C + $Ca(NO_3)_2$	0.2	0.4	$3.3x10^4$
C + $Mg(NO_3)_2$	36	72	$3.3x10^4$
C + $Sr(NO_3)_2$	0.03	0.06	$3.3x10^4$
C + $Pb(NO_3)_2$ (A)	$2.7x10^{-4}$	$5.3x10^{-4}$	$3.3x10^4$
C + $Pb(NO_3)_2$ (B)	$1.6x10^{-3}$	$3.2x10^{-3}$	$3.3x10^4$
C + $Pb(NO_3)_2$ (C)	$1.6x10^{-2}$	$3.2x10^{-2}$	$3.3x10^4$

Table 4-5: The number of femtomoles of each element contained in each multi-compound particle type.

Element	PT-4 (fmol)	PT-5 (fmol)	PT-6 (fmol)	PT-7 (fmol)	PT-8 (fmol)	PT-13 (fmol)
Ca^{2+}	$2x10^{-1}$	$2x10^{-1}$	$2x10^{-1}$	$2x10^{-1}$	$2x10^{-1}$	$2x10^{-1}$
Sr^{2+}	$3x10^{-2}$	$3x10^{-2}$	$3x10^{-2}$	$3x10^{-2}$	$3x10^{-2}$	$3x10^{-2}$
Na^{+}	262	262	262	262	262	262
Mg^{2+}	36	36	36	36	36	36
Al^{3+}		41	41	41	41	41
Fe^{3+}			22	22	22	22
Zn^{2+}				10	10	10
Pb^{2+}					1.6×10^{-3}	$1.6x10^{-3}$
Cr^{3+}						$2x10^{-2}$
Cu^{2+}						$7x10^{-3}$
Ni^{2+}						$6x10^{-3}$
Mn^{2+}						$3x10^{-1}$
Co^{2+}						$3x10^{-5}$
NO^{-}_3	336	461	529	556	556	556
C	$3.3x10^4$	$3.3x10^4$	$3.3x10^4$	$3.3x10^4$	$3.3x10^4$	$3.3x10^4$

4.5 Immunocytochemistry assay

Immunocytochemistry assay was used for antibody labelling of ICAM-1 expressed on A549 cells following 18 h incubation with particles. 1 mL of phosphate buffered saline (PBS) solution was used to rinse each 18 mm x 18 mm glass cover slip containing A549 cells twice. 1 mL of 1 % acetone solution was then used to fix the cells for 10 min. The acetone solution was removed by draining. Thereafter, cells were rinsed with 1 mL of PBS, and 1 mL of tris-buffered salt (TBS) solution prior to treatment with serum-free protein block.

The cell culture was next treated with 95 µL of serum-free protein block for 30 min. The serum-free protein block according to the manufacturer contains 0.25 % casein in PBS, stabilizing proteins and 0.015 M sodium azide (DakoCytomation Inc., X0909, Carpinteria, CA, USA). After 30 min, 95 µL of 50 µg/0.5 mL mouse-antihuman monoclonal CD54 (ICAM-1) primary antibody (Caltag Laboratories, LMHCD54F, Burlingham, CA, USA) was added and the cell culture left for 1 h.

The cell culture was rinsed with 1 mL of TBS solution following the 1 h treatment with primary antibody. This was followed by treatment with 95 µL of 2 mg/mL solution of goat-antimouse secondary antibody conjugated to Alexa fluor 546 (Invitrogen Detection Technologies, 34779A, Eugene, OR, USA) for 30 min. Each 18 mm x 18 mm glass cover slip containing A549 cells was rinsed four times with 1 mL of TBS solution. The control cell cultures incubated under the same conditions as cells dosed with test particles for 18

h, were labelled for ICAM-1 using primary and secondary antibodies as described herein. Lastly, each cover slip was mounted on a 75 mm x 25 mm glass slide prior to performing fluorescence microscopy and image analysis.

4.6 Fluorescence microscopy and image analysis

An inverted fluorescent microscope fitted with epi-flourescent filter block (filter block model MG-1, EP-FI, microscope model AE31, Motic instruments Inc., Richmond, BC, Canada) was used for the acquisition of images of fluorescent signal emission from fluorescently labelled goat anti-mouse secondary antibodies bound to ICAM-1 expressed on A549 cells. The acquisition of fluorescent signal emission at the site of particle deposition, indicative of ICAM-1 expression was performed as follows. First, the particle deposition site ($< 0.44\ mm^2$)[287] on each cell culture was located through the field-of-view using the microscope's visible wavelength optics. The microscope's fluorescence module was then used to acquire fluorescent emission signal from a $1.07\ mm^2$ circular area centred over particle deposition site. The optimal excitation wavelength range of the alexa fluor 546 (fluorophore) tagged to secondary antibody of goat-antimouse bound to ICAM-1 was 546 ± 5 nm, and optimal fluorescent signal emission emitted at 580 ± 15 nm.[251] The fluorescent signal intensity of each scan image was used to determine the differential ICAM-1 expression using Image J software (National Institute of Health, Bethesda, MD, USA). Microsoft excel was employed to sum these numerical values as a single signal per culture. The total signal intensity per cell culture, normalised using the fluorescent signal

emission from a cell culture treated with TNF-α, is taken as the differential ICAM-1 expression for each cell culture. The cultures deposited with carbon particles, as well as those used as negative controls were also normalized to the positive controls and the relative expression of ICAM-1 measured in those was ~0.4.

4.7 Results

The numerical value of fluorescence signal intensity of fluorophore-tagged secondary antibody of goat antimouse bound to ICAM-1 expressed on an A549 cell culture is plotted as a function of the number of particles deposited (Fig. 4-3 to 4-9). The data were fitted using a least squares linear regression. The value of the fitted slope for each particle type is referred to as pro-inflammation potential (PIP).

The inorganic compounds comprising single compound particles, $Ca(NO_3)_2$, $Mg(NO_3)_2$, $Sr(NO_3)_2$, $NaNO_3$, PT-4 to PT-13, and $Pb(NO_3)_2$ (A), $Pb(NO_3)_2$ (B), and $Pb(NO_3)_2$ (C) caused measurable ICAM-1 expression on A549 cells (Fig. 4-3 to 4.9). When PT- 4 was prepared from these 4 inorganic compounds, $Ca(NO_3)_2$, $Mg(NO_3)_2$, $Sr(NO_3)_2$, and $NaNO_3$, at the same concentrations as in the single particles, a measurable ICAM-1 expression on A549 cells was also observed (Fig. 4.5A). The PIPs for the respective single compound particles relative to PT-4 are plotted in Fig. 4-10.

The PIP for multi-compound particles, PT-5, PT-6, PT-7, PT-8, and PT-13 are shown in Fig. 4-11. These PIP values showed small increases in differential ICAM-1 expression with the systematic addition of respective inorganic compounds. For instance, the amount of Pb in PT-8 was 1.6 amol, and it caused a measurable level of differential ICAM-1 expression on A549 cells when compared to PT-7, which did not contain Pb. Upon incubation of A549 cells with particles containing only Pb (plus carbon) at same amount as in PT- 8, a comparable extent of differential expression of ICAM-1 was observed (Fig. 4-12).

The relative increase in PIP resulting from the addition of an inorganic compound to each multi-compound particle (PT-5 to PT-8) is indicated in Table 4-6. This increase in PIP for each particle type was normalized to the number of moles of metal added to the multi-compound particle. The result indicated that Pb^{2+} clearly caused the highest normalized PIP.

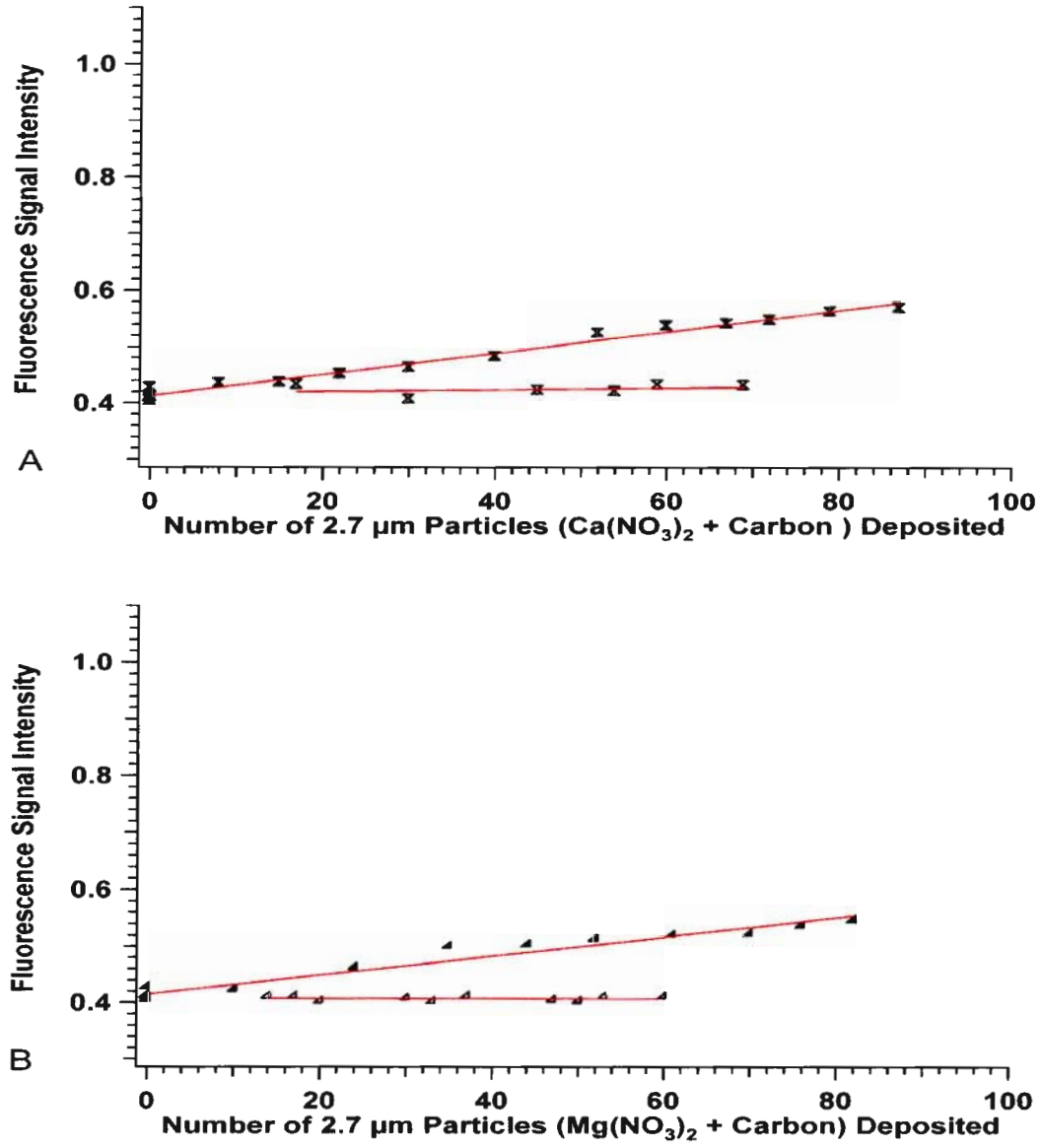

Figure 4-3: **Relative fluorescence signal intensity of ICAM-1 expressed on A549 cell culture after 18 h incubation with particles comprising: (A) calcium nitrate and carbon, and (B) magnesium nitrate and carbon. Bottom x-axis indicates the number of particles deposited onto the cell culture. Filled symbols represent (A) calcium nitrate and carbon, and (B) magnesium nitrate and carbon. Open symbols represent carbon particles. The fluorescence signal intensity was collected from 1.07 mm^2 area centred over the site of particle deposition. The R^2 coefficient from the linear least squares fit to the fluorescence signal intensity versus the number of particles deposited (filled symbols) was: (A) 0.9826, and (B) 0.9628. The mole compositions of these particles were: (A) Ca^{2+} = 0.2 fmol, NO^-_3 = 0.4 fmol, C (India ink) = 3.3 x 10^4 fmol, and (B) Mg^{2+} = 36 fmol, NO^-_3 = 72 fmol, C (India ink) = 3.3 x 10^4 fmol.**

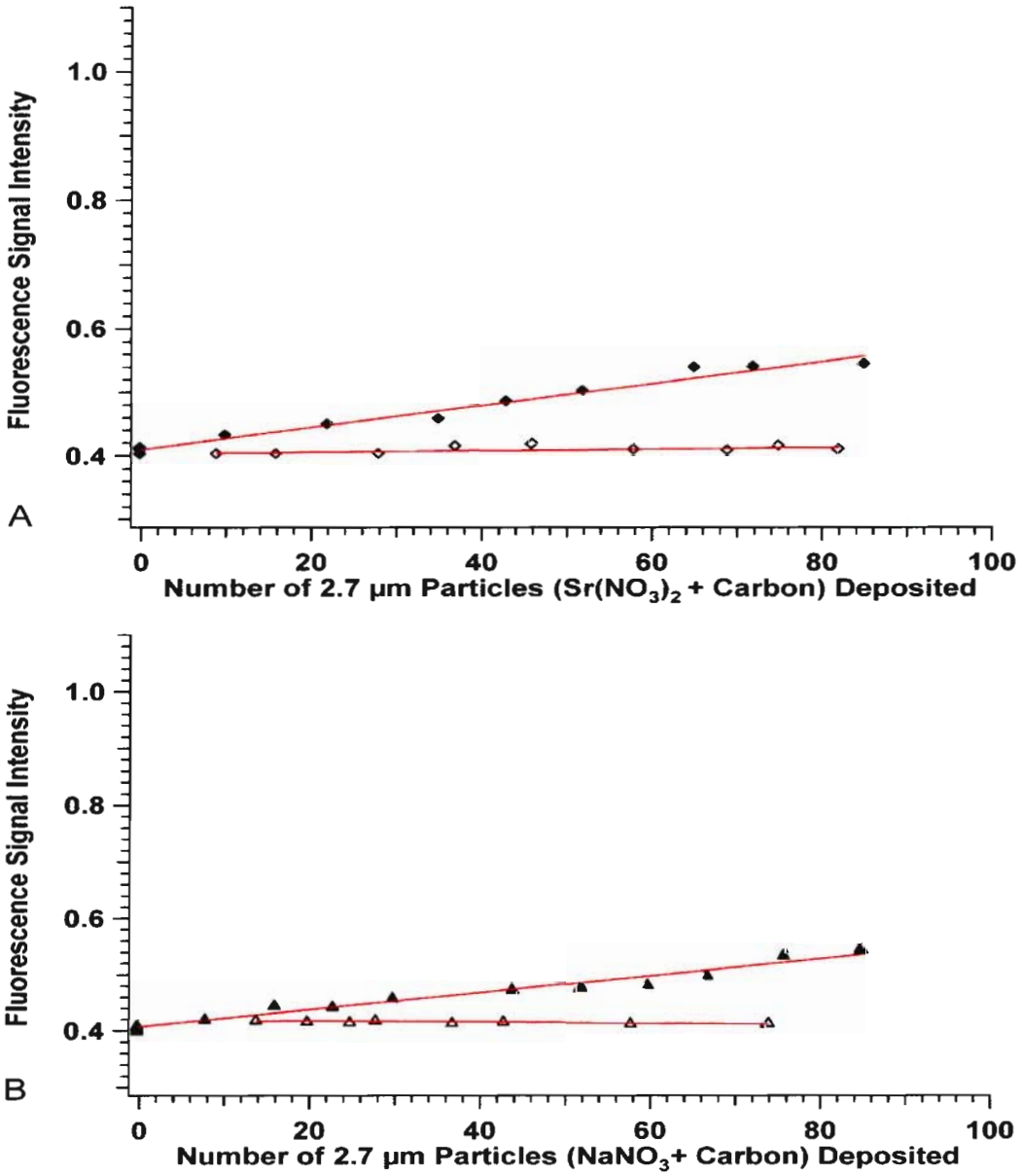

Figure 4-4: **Relative fluorescence signal intensity of ICAM-1 expressed on A549 cell culture after 18 h incubation with particles comprising: (A) strontium nitrate and carbon, and (B) sodium nitrate and carbon. Bottom x-axis indicates the number of particles deposited onto the cell culture. Filled symbols represent (A) strontium nitrate and carbon, and (B) sodium nitrate and carbon. Open symbols represent carbon particles. The fluorescence signal intensity was collected from 1.07 mm^2 area centred over the site of particle deposition. The R^2 coefficients from the linear least squares fit to the fluorescence signal intensity versus the number of particle deposited (filled symbols) was: (A) 0.9788, and (B) 0.9753. The mole compositions of these particles were: (A) Sr^{2+} = 0.03 fmol, NO^-_3 = 0.06 fmol, C (India ink) = 3.3 x 10^4 fmol, and (B) Na^+ = 262 fmol, NO^-_3 = 262 fmol, C (India ink) = 3.3 x 10^4 fmol.**

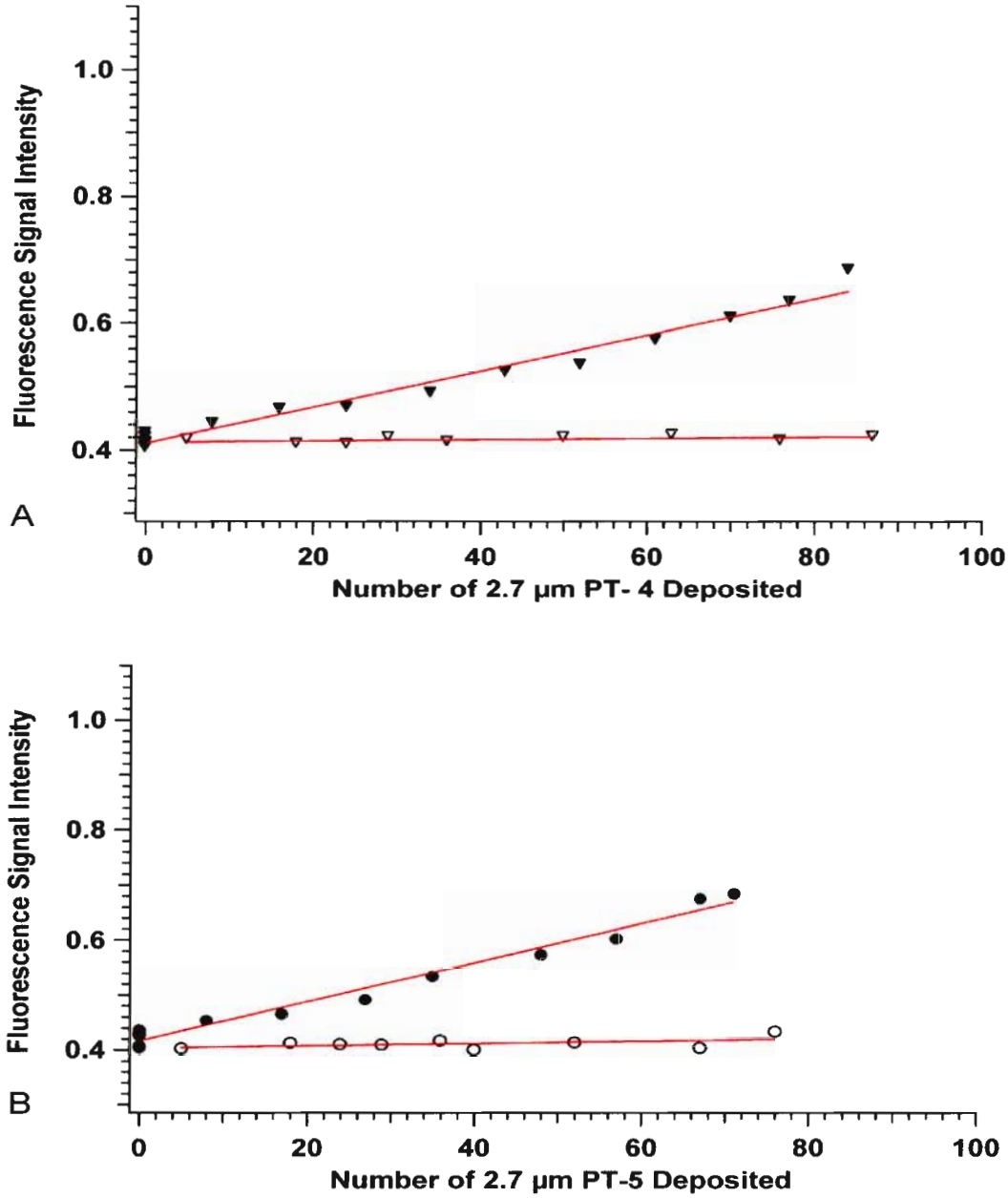

Figure 4-5: **Relative fluorescence signal intensity of ICAM-1 expressed on A549 cell culture after 18 h incubation with: (A) PT- 4, and (B) PT- 5. Bottom x-axis indicates the number of particles deposited onto the cell culture. Filled symbols represent (A) PT-4, and (B) PT-5. Open symbols represent carbon particles. The fluorescence signal intensity was collected from 1.07 mm^2 area centred over the site of particle deposition. The R^2 coefficient from the linear least squares fit to the fluorescence signal intensity versus the number of particles deposited (filled symbols) was: (A) 0.9767, and (B) 0.9768. Refer to table 4-5 for the amounts of metals and non-metals in each particle type.**

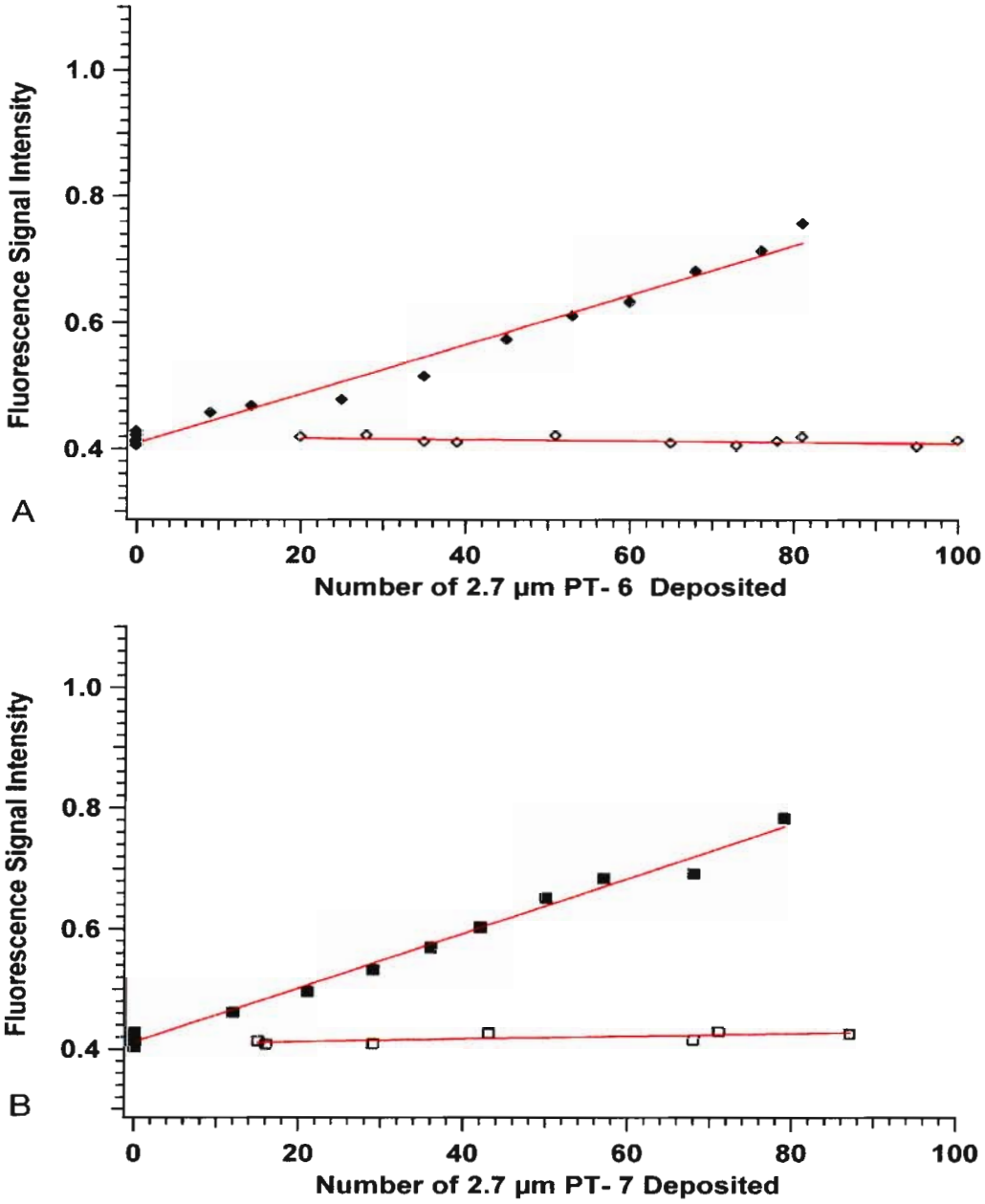

Figure 4-6: **Relative fluorescence signal intensity of ICAM-1 expressed on A549 cell culture after 18 h incubation with: (A) PT- 6, and (B) PT- 7. Bottom x-axis indicates the number of particles deposited onto the cell culture. Filled symbols represent (A) PT- 6, and (B) PT- 7. Open symbols represent carbon particles. The fluorescence signal intensity was collected from 1.07 mm^2 area centred over the site of particle deposition. The R^2 coefficient from the linear least square fit to the fluorescence signal intensity versus the number of particle deposited (filled symbols) was: (A) 0.9839, and (B) 0.9921. Refer to table 4-5 for the amounts of metals and non-metals in each particle type.**

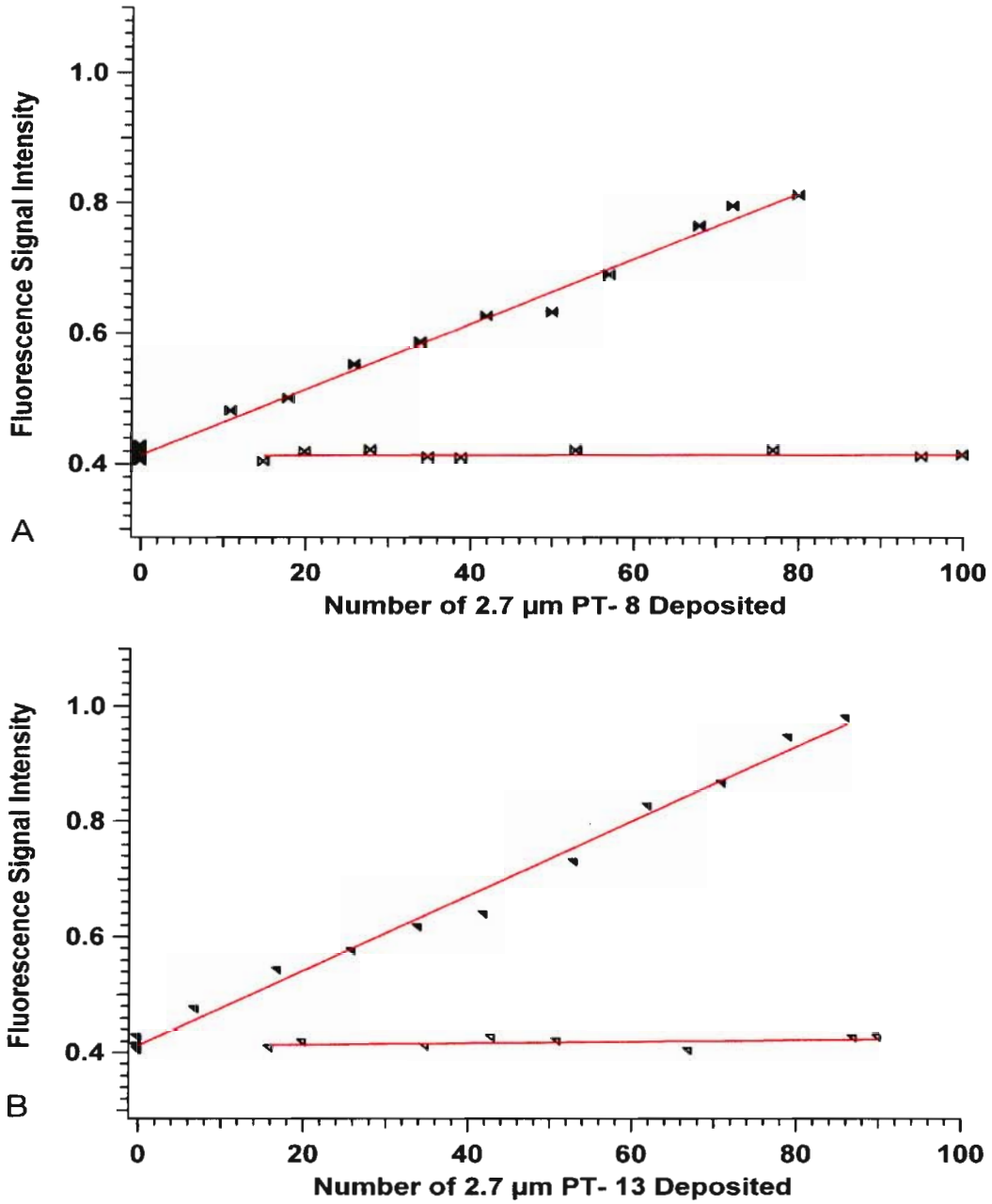

Figure 4-7: **Relative fluorescence signal intensity of ICAM-1 expressed on A549 cell culture after 18 h incubation with: (A) PT- 8, and (B) PT- 13. Bottom x-axis indicates the number of particles deposited onto the cell culture. Filled symbols represent (A) PT- 8, and (B) PT- 13. Open symbols represent carbon particles. The fluorescence signal intensity was collected from 1.07 mm^2 area centred over the site of particle deposition. The R^2 coefficient from the linear least square fit to the fluorescence signal intensity versus the number of particle deposited (filled symbols) was: (A) 0.9939, and (B) 0.9935. Refer to table 4-5 for the amounts of metals and non-metals in individual particle type.**

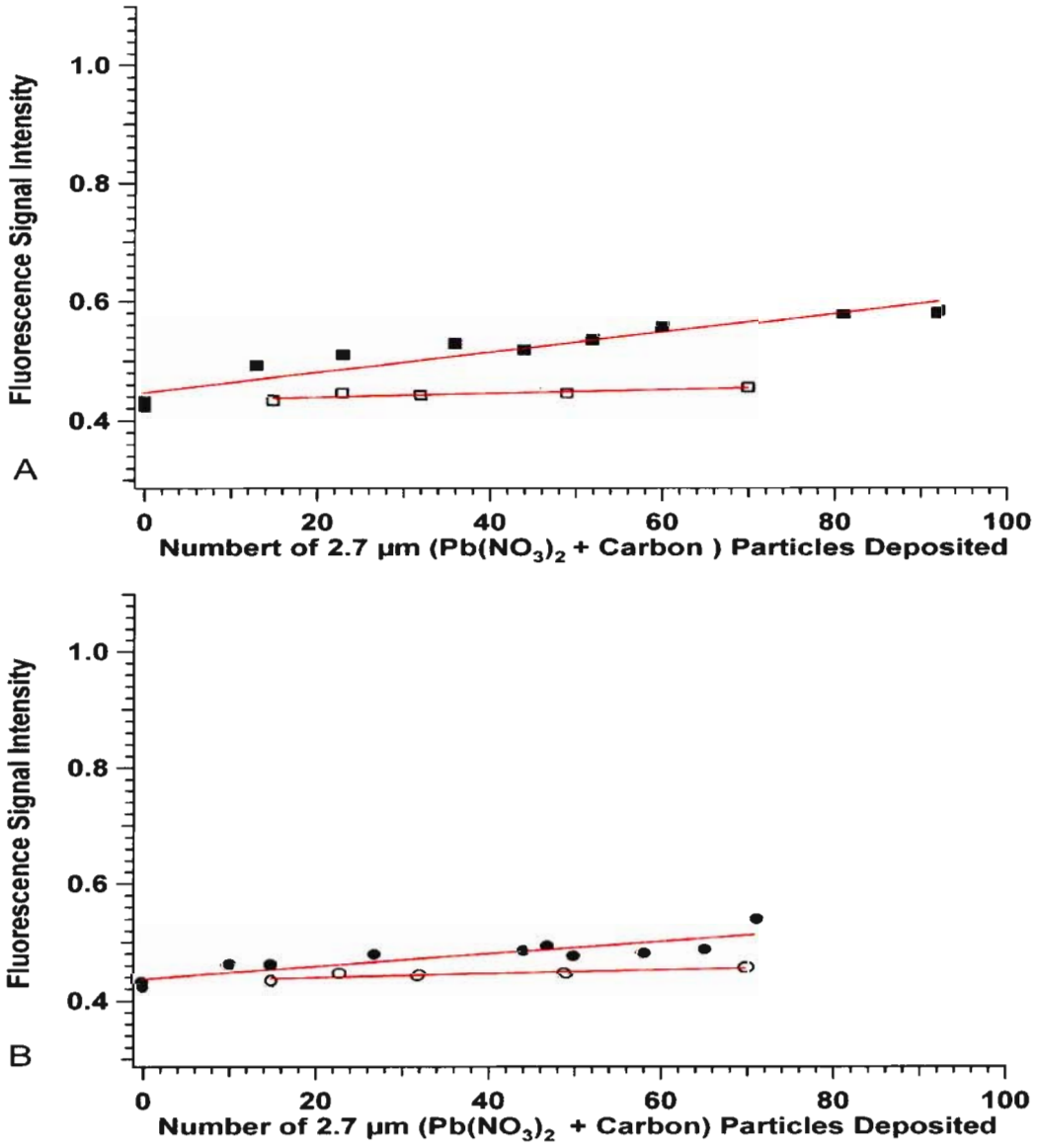

Figure 4-8: **Relative fluorescence signal intensity of ICAM-1 expressed on A549 cell culture after 18 h incubation with single-compound particles comprising lead nitrate and carbon, at different amounts of $Pb(NO_3)_2$. Bottom x-axis indicates the number of particles deposited onto the cell culture. Filled symbols in (A) and (B) represent lead nitrate plus carbon particles. Open symbols represent carbon particles. The fluorescence signal intensity was collected from 1.07 mm^2 area centred over the location of particle deposition. The R^2 coefficient from the linear least squares fit to the fluorescence signals intensity versus the number of particle deposited (filled symbols) was: (A) 0.9084, and (B) 0.7767. The mole composition of these particles were: (A), Pb^{2+} = 0.016 fmol, NO^-_3 = 0.032, fmol, C (India ink) = 3.3 x 10^4 fmol, and (B) Pb^{2+} = 0.0016 fmol, NO^-_3 = 0.0032 fmol, C (India ink) = 3.3 x 10^4 fmol.**

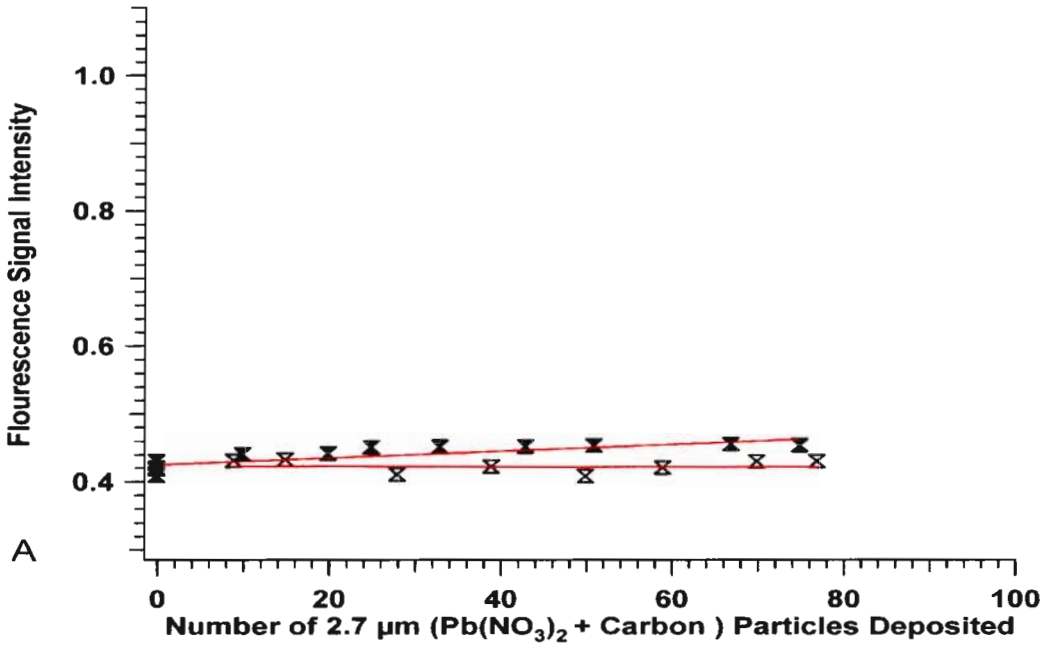

Figure 4-9: **Relative fluorescence signal intensity of ICAM-1 expressed on A549 cell culture after 18 h incubation with single-compound particles comprising lead nitrate and carbon. Bottom x-axis indicates the number of particles deposited onto the cell culture. Filled symbols in (A) represent lead nitrate plus carbon particles. Open symbols represent carbon particles. The fluorescence signal intensity was collected from 1.07 mm^2 area centred over the location of particle deposition. The R^2 coefficient from the linear least square fit to the fluorescence signal intensity versus the number of particle deposited (filled symbols) was: (A) 0.7123. The mole composition of the particles was: (A), Pb^{2+} = 0.00027 fmol, NO^-_3 = 0.00053 fmol, C (India ink) = 3.3 x 10^4 fmol.**

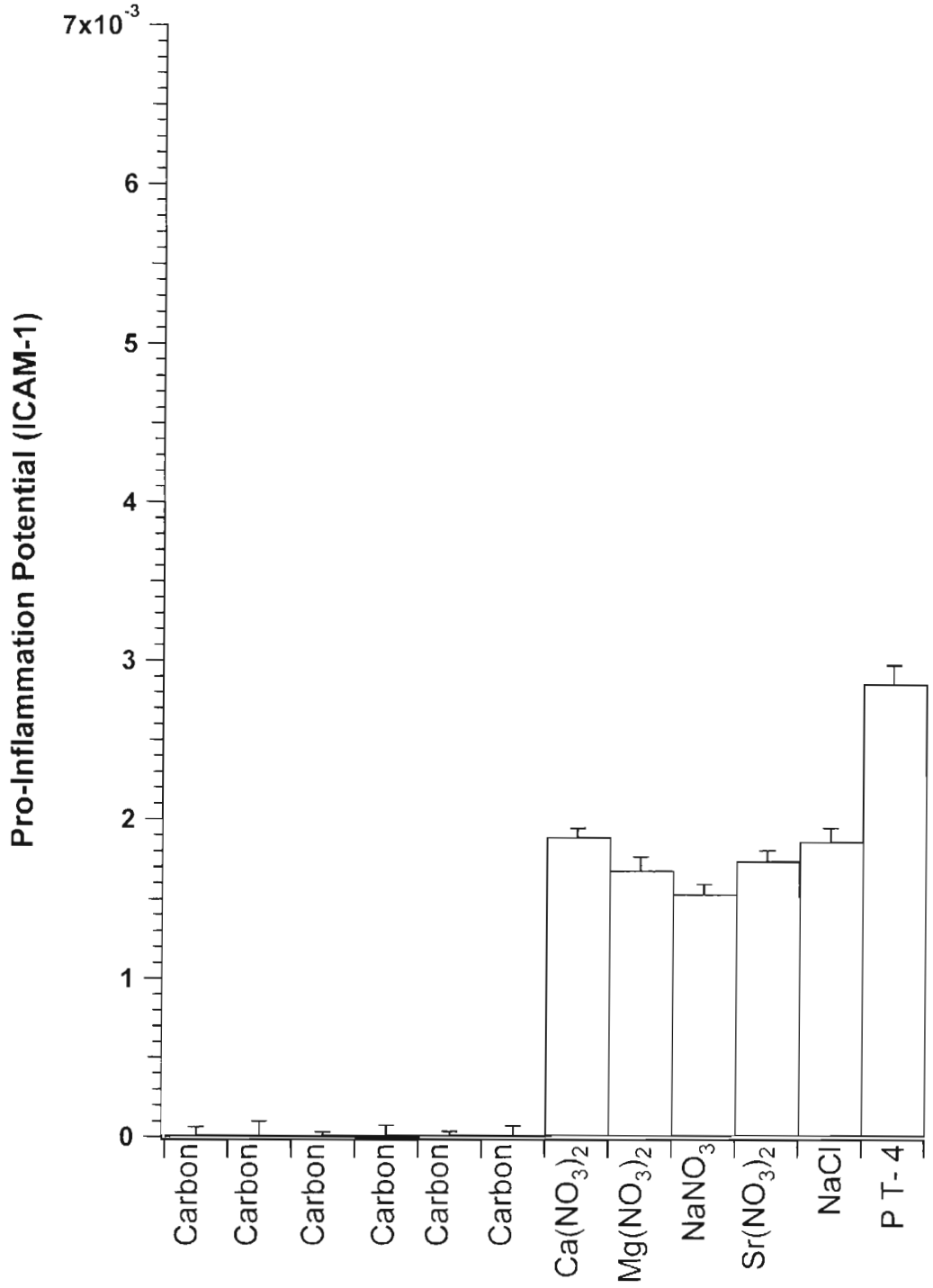

Figure 4-10: **Pro-inflammation potential (PIP) represented in terms of differential expression of ICAM-1 by A549 cells in response to 18 h incubation with carbon, C + $Ca(NO_3)_2$, C + $Mg(NO_3)_2$, C + $NaNO_3$, C + $Sr(NO_3)_2$, C + NaCl particles, or PT- 4.**

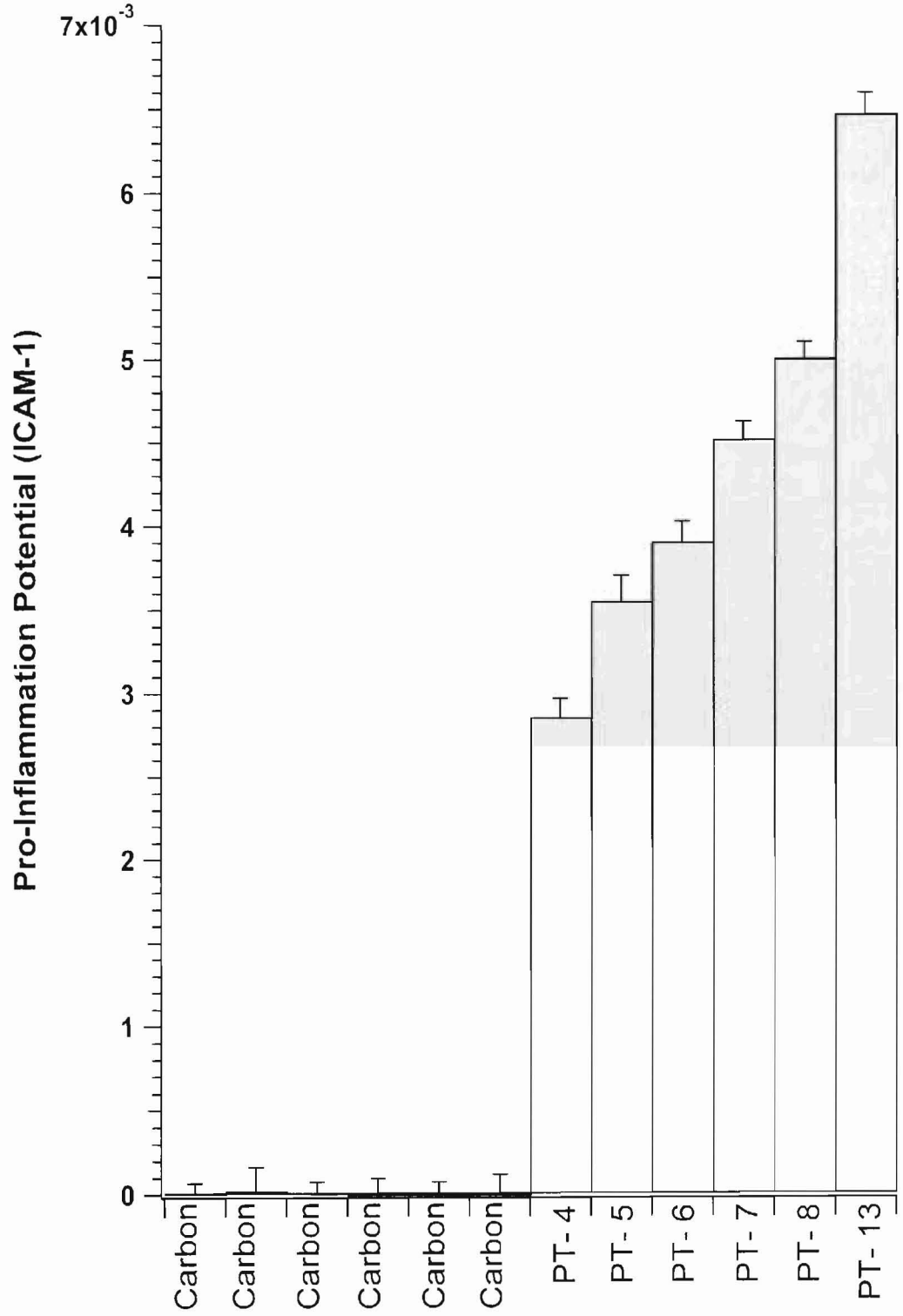

Figure 4-11: **Pro-inflammation potential (PIP) represented in terms of differential expression of ICAM-1 by A549 cells in response to 18 h incubation with carbon particles, PT- 4, PT- 5, PT- 6, PT- 7, PT- 8, or PT- 13.**

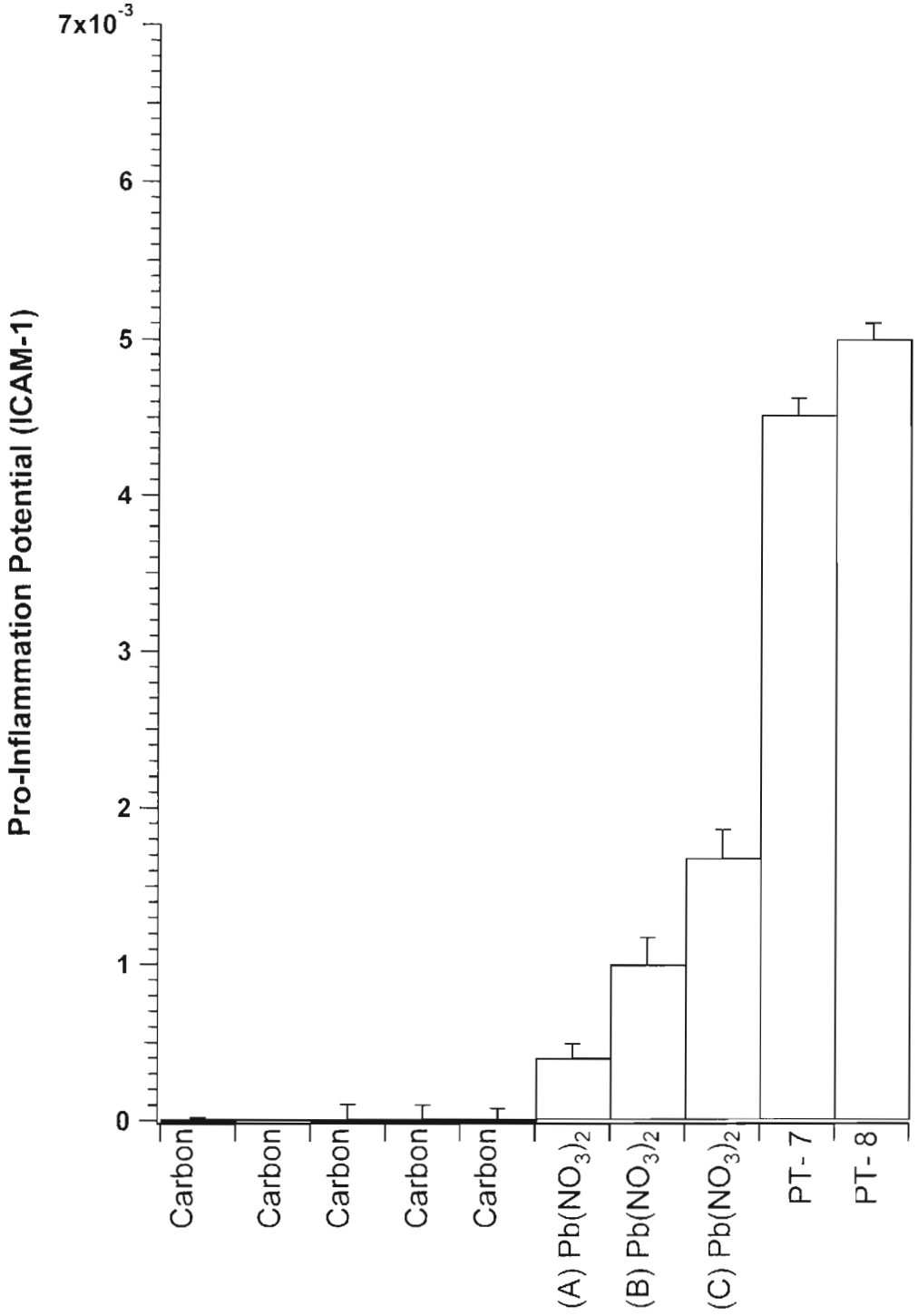

Figure 4-12: **Pro-inflammation potential (PIP) represented in terms of differential expression of ICAM-1 by A549 cells in response to 18 h incubation with particles of carbon, C + $Pb(NO_3)_2$, PT- 7, or PT- 8. The amounts of Pb were: (A) 2.7 x 10^{-4} fmol, (B) 1.6 x 10^{-3} fmol, and (C) 1.6 x 10^{-2} fmol.**

Table 4-6: Relative pro-inflammation potential (PIP) increase for each metal nitrate added to the multi-compound particle, and the same PIP value normalized to the number of moles of metal nitrate salt added.

	PT-4 to PT-5	PT-5 to PT-6	PT-6 to PT-7	PT-7 to PT-8
Metal nitrate added	Al^{3+}	Fe^{3+}	Zn^{2+}	Pb^{2+}
Relative PIP increase	$5.0x10^{-4}$	$4.0x10^{-4}$	$6.0x10^{-4}$	$5.0x10^{-4}$
Mole of metal added (fmol)	41	22	10	$1.6x10^{-3}$
Normalized relative PIP increase based on mole metal added	$1.2x10^{10}$	$1.8x10^{10}$	$6.0x10^{10}$	$3.1x10^{14}$
Log_{10}(Normalized relative PIP increase)	10.1	10.3	10.8	14.5

4.8 Discussion

A previous study measured the pro-inflammation potential (differential expression of ICAM-1) of EHC-93 particle mimics having different diameters but the same average composition of inorganic compounds.[185] In that study, each particle type contained several cations, in addition to three anions, sulphate, nitrate, and chloride. In this follow-up study, the differential expression of ICAM-1 by lung alveolar epithelial cells (A549) in response to different inorganic compounds in these particle types was measured. To facilitate inter-comparison of pro-inflammation potential of particles in this study, the anion content of each particle type was restricted to nitrate, and the size of all particle types investigated was 2.7 ± 0.5 μm.

The use of an alternating current (ac) trap enabled the creation of different particle types having different mole fractions of inorganic compounds. The nitrate salts of sodium, magnesium, calcium and strontium were used in the preparation of PT-4, since these have been reported as major components of EHC-93 particles,[44] as well as several PM samples from different locations worldwide.[44, 300] Despite these compounds being present in large quantities in these PM samples,[44, 300] information regarding their potential to cause injury both *in vivo* and *in vitro* is lacking. The preparation of other multi-compound particle types was achieved by systematic addition of specific inorganic compounds to prepare other secondary starting solutions, using the same procedure as that used to prepare PT-4.

It was observed that the differential expression of ICAM-1 by A549 cells dosed with particles containing single inorganic compounds was greater than when several compounds were combined. For instance, the ICAM-1 expression by PT-8 due to $Pb(NO_3)_2$ (plus carbon), was less than that observed for particles containing only $Pb(NO_3)_2$ (plus carbon) (Fig. 4-12).

The levels of differential ICAM-1 expression varied among the different particles. For instance, PT- 4 was the least potent with regard to effecting differential ICAM-1 when compared to other multi-compound particles investigated. PT-4 contained only alkali and alkaline earth nitrates, while others, PT-5, PT-6, PT-7, PT-8, PT-13, contained in addition transition metals, with PT-13 containing the largest number. Metals are known to induce the expression of ICAM-1 in A549 cells through the activation of redox-

sensitive nuclear factor kappa B (NF-κB) pathway.[99, 286] The alkali and alkaline earth metals possess less activity with regard to (NF-κB) pathway activation.[199] While the transition metals have higher potency, there are differences in the their activity towards NF-κB activation.[314] Our data suggests that the intrinsic chemical properties of each additional metal within each multi-compound particle type were responsible for the measured increase in differential expression of ICAM-1. The results of the normalized PIPs for each multi-compound particle type based on the number of moles of metal added indicated that Pb^{2+} caused the greatest differential expression of ICAM-1, which was significantly greater than Al^{3+}, Fe^{3+}, and Zn^{2+} (Table 4-6).

It is known that lead effects its toxicity through the induction of oxidative damage leading to the depletion of glutathione, and protein-bound sulfhydryl groups.[315] The depletion of the biomolecules cause the generation of reactive oxygen species including superoxide ion, hydrogen peroxide, and hydroxyl radicals.[316] The consequence of this include DNA damage, and altered calcium and sulfhydryl homeostasis.[317] As such, the increased ICAM-1 expression by A549 cells in response to PT-8 to which lead was added may be due to the induction of oxidative damage .

4.9 Conclusion

An ac trap and associated levitation methodology was used to levitate multi-compound particles created by systematic addition of inorganic

compounds at constant, but different, mole fraction. The differential expression of ICAM-1 by A549 cells in response to 18 h incubation with multi-compound particles was measured. The mole-corrected PIPs, normalized by the number of moles of a different metal systematically added to each multi-compound particle (PT-5 through PT-8), each showed an increase in ICAM-1 expression due to that metal. In comparing the values for Al^{3+}, Fe^{3+}, Zn^{2+}, and Pb^{2+}, the Pb^{2+} caused the most differential ICAM-1 expression.

CHAPTER 5: The measurement of differential expression of ICAM-1 by A549 cells in response to incubation with < 100 particles having varied abundances of NaCl in either solid or liquid state

5.1 Context

While studying the pro-inflammation potential (differential ICAM-1 expression) of single-compound particles in previous chapter, it was found that particles comprising NaCl and carbon effected measurable differential expression of ICAM-1 on A549 cells. This result was investigated further herein using particles having varied moles of NaCl in either solid or liquid state at the instant of their deposition onto A549 cells. The downstream biological response measured was differential ICAM-1expression.

5.2 Abstract

Particles of sodium chloride (NaCl) are ubiquitous throughout the troposphere. Herein, an ac trap was used in creating particles having varied moles of NaCl and in different physical states. The aim herein was to measure the differential expression of ICAM-1 by A549 cells in response to 18 h incubation with particles having varied moles of NaCl and in different physical states at the instant of deposition. As this would provide new information regarding the potential adverse health effects that the particles may cause upon inhalation. The physical states studied included liquid mimicked with particles of NaCl and glycerol, and solid mimicked with

particles of NaCl only (no carbon), and those comprising NaCl plus carbon. Our data indicated that NaCl in different physical states at the instant of deposition caused measurable ICAM-1 expression on A549 cells. Among the three physical states, the normalized pro-inflammation potential indicated that particles comprising NaCl plus carbon possessed the greatest value for ICAM-1. Suggesting that particle's physical state at the instant of deposition onto A549 cells was important regarding ICAM-1 expression.

5.3 Introduction

It is approximated that ~10^{12} kg of sea salt aerosol is released from earth's oceans to the troposphere annually.[165, 318] Sea-salt aerosol is a major source of sodium chloride in the troposphere.[165-167] Evaporation of water from sea salt aerosol leads to formation of NaCl particles,[168] and emitted sodium chloride particles can adsorb water onto their surface, and potentially deliquesce, or dissolve to form aqueous droplets.[168-170] Anthropogenic activities are also responsible for introducing NaCl to the troposphere. For instance, in winter, sodium chloride is released during its application on roads.[165] Despite ubiquitous presence of sodium chloride in the environment, studies investigating its toxicity are few.[319]

In the previous chapter, it was found that particles comprising NaCl and carbon caused measurable ICAM-1 expression on A549 cells. The influence of NaCl physical state, solid or liquid, in effecting differential expression of ICAM-1 on A549 cells was addressed in this study. The different physical states studied included sodium chloride dissolved in glycerol:water, sodium

chloride particles (no carbon), and particles comprising sodium chloride and carbon.

5.4 Materials and methods

5.4.1 Starting solutions preparation

A NaCl stock solution was prepared using reagent grade $NaCl_{(s)}$. This stock solution was used in the preparation of solutions, referred to as starting solutions, each containing: (i) NaCl and glycerol, (ii) NaCl only, and (iii) NaCl and carbon black. The starting solution containing NaCl and glycerol was prepared by diluting 0.81 mL of $1.7x10^{-1}$ M NaCl solution to 9.50 mL with glycerol and water (1:9, vol/vol). The preparation of starting solution containing only NaCl (no carbon) was performed by diluting 0.81 mL of 1.7 $x10^{-1}$ M NaCl solution to 9.50 mL with distilled deionised water. Four different starting solutions of NaCl and carbon, having different concentrations of NaCl but the same amount of carbon were prepared in the following way. 2 mL India ink, calculated to contain 0.30 g of carbon black was added to 0.81 mL of $1.7x10^{-1}$ M, 0.05 mL of $1.4x10^{-4}$ M, 0.5 mL of 1.4 $x10^{-4}$ M, and 5 mL of $1.4x10^{-4}$ M NaCl solution. The resulting solutions were diluted to 9.50 mL with distilled deionised water.

The following solution preparation was used in creating carbon particles that served as a control. 2.0 mL India ink calculated to contain 0.30 g of carbon black was diluted with 9.5 mL of distilled deionised water. A 0.5 mL aliquot was diluted with 12.5 mL of distilled deionised water.

5.4.2 A549 cell culture

The human lung alveolar epithelial cells (A549) were provided by Dr. Stephan F. van Eeden (James C Hogg iCAPTURE Centre for cardiovascular and pulmonary research, University of British Columbia, Canada). Cells were seeded onto a 18 mm x 18 mm glass cover slip placed in each well of a six-well plate containing 2 mL of minimal essential medium (MEM), supplemented with 10 % heat inactivated fetal bovine serum (FBS) (vol/vol), 1 % MEM vitamin solution (vol/vol), and 1 % L-glutamine (vol/vol). Cells were grown to 95 % confluence at 37 ^{o}C, 5 % CO_2, and 100 % relative humidity.

Four sets of controls were used. One set of controls was cell cultures incubated with different numbers of carbon particles, or particles comprising glycerol and water (1:9, vol/vol) depending on the test particle composition. A negative control was cells bathed with 2 mL of MEM only. The positive control was cells bathed with 2 mL MEM, treated with 10 μL of 1 mg/mL tumour necrosis factor alpha (TNF)-α (Sigma-Aldrich, T6674-10UG) in water. All these controls were incubated for 18 hrs under the same conditions as cell cultures onto which test particles were deposited.

5.4.3 Droplet dispensing

A 0.5 mL aliquot of each starting solution was diluted to give secondary starting solutions (Table 5-1). Each secondary starting solution was delivered directly into the internal reservoir of the droplet dispenser.

Table 5-1: The concentrations of NaCl in secondary starting solutions for droplet dispensing. Each secondary starting solution was delivered directly into the droplet dispenser internal reservoir.

Secondary starting solution	Volume of aliquot diluted (L)	Volume of glycerol in distilled deionised water used for dilution(1:9,vol/vol) (L)	Concentration of NaCl in secondary starting solution (M)
NaCl and glycerol	$5.0x10^{-4}$	$1.0x10^{-3}$	$7.3x10^{-3}$
	$5.0x10^{-4}$	$5.0x10^{-3}$	$1.5x10^{-3}$
	$5.0x10^{-4}$	$1.0x10^{-2}$	$7.3x10^{-4}$
	$5.0x10^{-4}$	$1.3x10^{-2}$	$5.8x10^{-4}$
	$5.0x10^{-4}$	$5.0x10^{-2}$	$1.5x10^{-4}$
	$5.0x10^{-4}$	$7.5x10^{-2}$	$9.7x10^{-5}$
	$5.0x10^{-4}$	$1.0x10^{-1}$	$7.3x10^{-5}$
NaCl only (No carbon)	Volume of aliquot diluted (L)	Volume of distilled deionised water used for dilution (L)	Concentration of NaCl in secondary starting solution (M)
	$5.0x10^{-4}$	$1.0x10^{-3}$	$7.3x10^{-3}$
	$5.0x10^{-4}$	$5.0x10^{-3}$	$1.5x10^{-3}$
	$5.0x10^{-4}$	$1.0x10^{-2}$	$7.3x10^{-4}$
NaCl + carbon	Volume of aliquot diluted (L)	Volume of distilled deionised water used for dilution (L)	Concentration of NaCl in secondary starting solution (M)
	$5.0x10^{-4}$	$1.3x10^{-2}$	$5.8x10^{-4}$
	$5.0x10^{-4}$	$1.3x10^{-2}$	$2.9x10^{-6}$
	$5.0x10^{-4}$	$1.3x10^{-2}$	$2.9x10^{-7}$
	$5.0x10^{-4}$	$1.3x10^{-2}$	$2.9x10^{-8}$

A schematic diagram of an ac trap with its major components is shown in Fig. 5-1A. It is housed in a chamber placed inside a biological safety cabinet (Nuaire Inc. Model Nu-425-600, Plymouth, MN, USA). The nozzle of the droplet dispenser has an internal diameter of 60 μm. The droplet dispenser's reservoir was filled with an aliquot of solution to be dispensed,

termed a secondary starting solution using 10-µL pipette. For droplet creation, a cylindrical piezoceramic element bonded to the outside of the droplet dispenser was actuated by an electrical signal from the waveform generator for the droplet dispenser, causing a small volume of liquid to expelled as a jet from the dispenser nozzle (Fig. 5-1B). The droplets were generated at a rate 120 Hz. The droplet-dispensing period was 5 s or less. A 200 V dc potential applied to an induction electrode, which was positioned 2 mm below the dispenser nozzle caused ion mobility within this jet, such that, when the jet of liquid separates from dispenser nozzle, that volume of liquid in the jet had a net charge and it collapsed to as a single droplet.

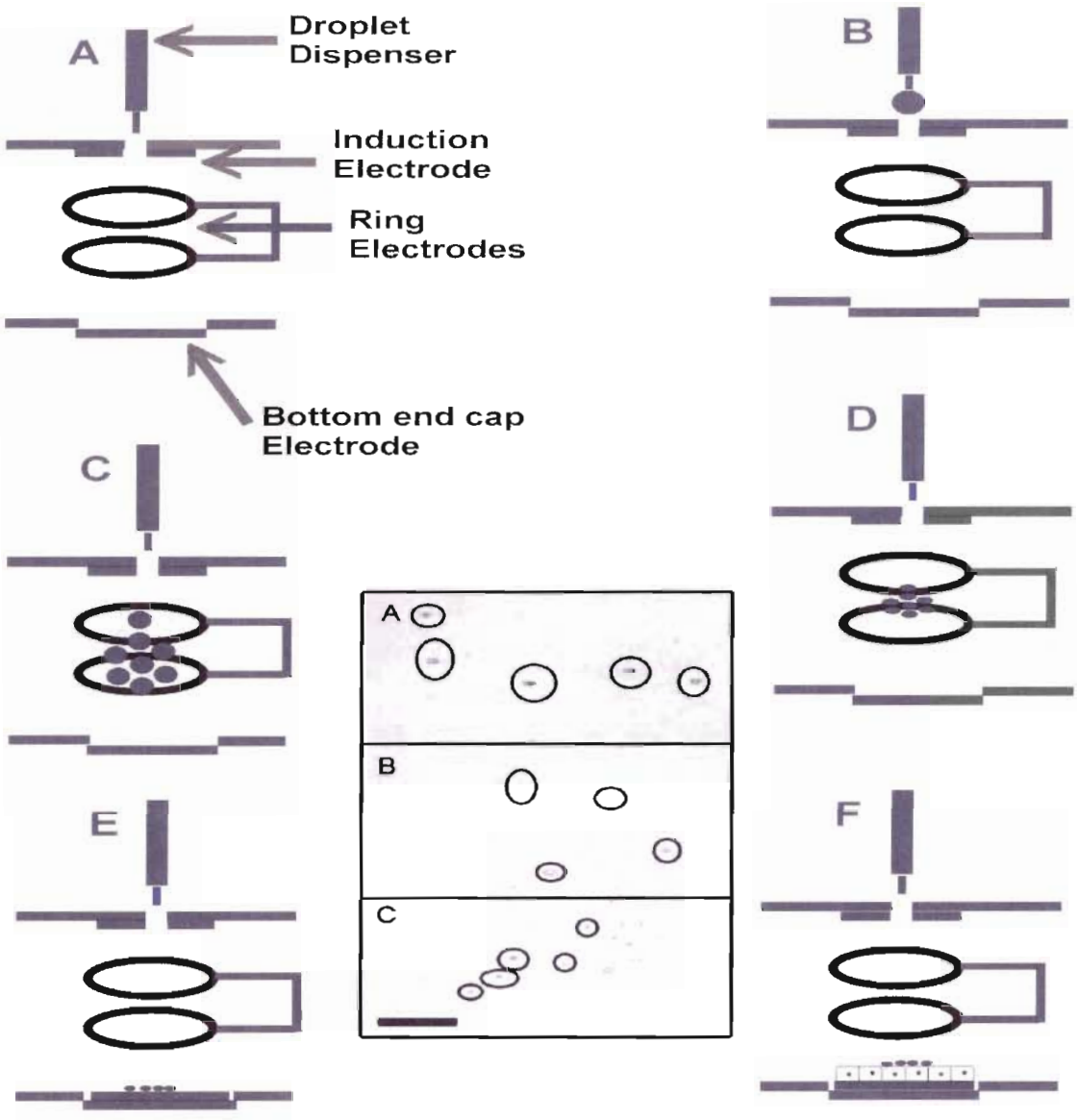

Figure 5-1: A representation of the levitation apparatus used in the creation and deposition of particles onto two different surfaces. (A) A schematic diagram of an ac trap with the major components indicated. A 10 µL aliquot of a multi-compound starting solution was used to load the internal reservoir of the droplet dispenser. (B) Dispensing of a droplet, (C) Levitation of a population of droplets while its volatile solvents evaporated, (D) Levitation of the resultant particles formed by the precipitation of the dissolved solids present in the droplets, (E) Particle deposition onto a glass slide for size characterization using optical microscopy, (F) Particle deposition onto a A549 cell culture. Note that any one cell was typically only in contact with one particle. Diagram not drawn to scale. Inserts are photomicrographs of NaCl particles having diameters of: (A) 1.9 µm, (B) 1.5 µm, and (C) 1.0 µm.

5.4.4 Particle levitation and deposition onto A549 cell culture

Each droplet passes through a 5-mm diameter hole cut on the induction electrode into an ac trap (Fig. 5-1C). Within the ac trap, each droplet is captured and levitated by an electric field having a sinusoidal waveform of 4.5 kV_{0-P} and frequency of 10 Hz applied to the ring electrodes of an ac trap. With the droplets captured, the frequency of this waveform generator was manually ramped to 920 Hz. The volatile solvents and water within each droplet evaporated quickly (i.e. within seconds), leaving behind a residue per droplet that is comprised of non-volatile solutes that precipitate/coagulate as a spherical solid referred to as particle. An attractive 500 V dc potential applied to the bottom electrode established the electric field enabling particle removal from the ac trap onto 75 mm x 25 mm glass slide for optical microscopy (Fig. 5-1E). Each residue was viewed under an optical microscope, had roughly a spherical shape and is referred to as a particle. The diameters of particles comprising NaCl only (no carbon) were 1.0 ± 0.1 μm, 1.5 ± 0.2 μm, and 1.9 ± 0.2 μm. The diameter of particles comprised of NaCl and carbon was 2.7 ± 0.5 μm. For particles containing NaCl and glycerol, the diameter was 28 ± 0.5 μm.

With a population of particles, between 5 to < 100 levitated in each trial, A549 cells were prepared for their deposition as follows. An 18 mm x 18 mm glass cover slip containing A549 cells was removed from the well of a six-well plate. The growth medium on the cover slip was drained for 2 s, and placed on 75 mm x 25 mm glass slide. The slide was placed on a mount at

the bottom electrode. An attractive 500 V dc potential applied to the bottom end cap electrode established the electric field enabling particle removal from the ac trap onto A549 cell culture (Fig. 5-1F).

For particles comprising either NaCl and glycerol, or NaCl only (no carbon), the number of particles deposited was not counted on the cell culture, rather particle accounting was performed as follows. First, the droplet dispenser was programmed to dispense a given number of droplets per trial. The droplets were captured and levitated within the ring electrodes of the ac trap, allowing water within each droplet to quickly evaporate (i.e. within seconds), leaving behind a single residue per droplet comprising either particles of NaCl and glycerol, or NaCl respectively. Each particle type was deposited onto a 75 mm x 25 mm glass slide and counted to ensure that, that number of particles was actually delivered. The site of particle deposition on a glass slide was marked using a pen. For deposition of particles (comprising either NaCl and glycerol, or NaCl only), onto A549 cells contained on 18 mm x 18 mm glass cover slip , each glass cover slip was placed on a mark on a glass slide. Following particle deposition, this site was marked on each cover slip using a mark pen to facilitate the identification of particle deposition site during fluorescence microscopy and image analysis. Each cover slip was removed from the glass slide and quickly placed in a 35 mm (diameter) and 10 mm (depth) tissue culture petri dish. Each petri dish was incubated at 37 ^{o}C, 5 % CO_2, and 100 % relative humidity for 18 hrs.

5.5 Immunocytochemistry assay

Labelling of ICAM-1 expressed on A549 cells resulting from 18 h incubation with NaCl particles was performed using immunocytochemistry assay. Each 18 mm x 18 mm cover slip containing A549 cells was twice rinsed with 1 mL phosphate buffered saline (PBS) solution, and fixed with 1 mL of 1 % acetone solution for 10 min. Acetone solution was drained after 10 min. Cells were then rinsed with 1 mL of PBS solution, followed by 1 mL of tris-buffered salt (TBS) solution.

Thereafter, cell culture was treated with 95 µL of serum-free protein block, noted to contain 0.25 % casein in PBS, stabilizing proteins and 0.015 M sodium azide by its manufacturer (DakoCytomation Inc., X0909, Carpinteria, CA, USA) for 30 min. After 30 min, 95 µL of 50 µg /0.5 mL primary antibody of mouse anti-human monoclonal CD-54 (Caltag Laboratories, LMHCD54F, Burlingham, CA, USA) was added and allowed to stay for 1 h.

Following a 1 h treatment with the primary antibody, cell culture was rinsed with 1 mL TBS solution. This was followed by treatment with 95 µL of 2 mg/mL solution of goat-antimouse secondary antibody conjugated to Alexa fluor 546 (Invitrogen Detection Technologies, 34779A, Eugene, OR, USA) for 30 min. At the end of this period, cells were rinsed four times with 1 mL TBS solution.

The control cell cultures incubated under the same conditions as cells dosed with test particles for 18 h, were labelled for ICAM-1 using primary and

secondary antibodies as described herein. Each cover slip was mounted on 75 mm x 25 mm glass slide prior to performing fluorescence microscopy and image analysis.

5.6 Fluorescence microscopy and image analysis

The acquisition of images of emission signal from fluorescently labelled goat anti-mouse secondary antibodies bound to ICAM-1 expressed on A549 cells was performed with an inverted fluorescent microscope fitted with an epi-fluorescent filter block (filter block model MG-1, EP-FI, microscope model AE31, Motic Instruments Inc., Richmond, BC, Canada). The particle deposition site was located through optical microscopy as follows. Light from optical microscope's light source was focused on each cover slip. This light was used to locate particles on cell culture through the eyepiece's field-of-view. For particles comprising NaCl (no carbon), or NaCl in glycerol, the deposition site was a mark on each glass cover slip. This mark was located through the field-of-view of the eyepiece. Following the location of the deposition site, the microscope's fluorescence module was used to acquire fluorescence emission signal.

The intensity of fluorescence emission signal at each pixel from each scan of cell culture was used to calculate differential ICAM-1 expression using Image J software (National Institute of Health, Bethesda, MD, USA). The numerical values of the pixel signal were summed with Microsoft Excel. The summed value of ICAM-1 for each cell culture is reported as total signal intensity normalised using fluorescent signal emission from cell cultures

treated with TNF-α positive control. The total fluorescent signal intensity from cell cultures that were respectively deposited with carbon particles, glycerol: water particles, and the negative controls were normalized to the positive controls and the relative expression of ICAM-1 measured in those was ~0.4.

5.7 Results

The diameter of each particle type was measured through optical microscopy. The numerical value of fluorescent signal intensity of labelled antibodies indicative of ICAM-1 expression on A549 cell cultures as a function of number of particles deposited was plotted (Fig 5-2 to 5-9). These data were fitted using least squares linear regression. The value of the fitted slope for each particle type is termed a pro-inflammation potential (PIP) for ICAM-1.

The PIPs for particles comprising NaCl in glycerol: water are shown in Fig. 5-10. These particles showed a levelling-off regarding differential expression of ICAM-1 at NaCl > 525 fmol. NaCl amounts above this threshold effected small incremental differential ICAM-1 expression. For particles containing NaCl at 131 fmol, 87 fmol, and 65 fmol, that are below this threshold, resulted in linear decreases in differential ICAM-1 expression.

The pro-inflammation potential of A549 cells incubated with NaCl particles (no carbon) having diameters of 1.0 μm, 1.5 μm, 1.9 μm, showed that particle having diameter of 1.0 μm caused the greatest ICAM-1 expression (Fig. 5-11). The differential expression of ICAM-1 (PIP) for

particles comprising sodium chloride and carbon, at diameter of 2.7 μm, but varied moles of NaCl is indicated in Fig. 5-12. At 0.0265 fmol of NaCl, the differential expression of ICAM-1 on A549 cells was $2.9 \times 10^{-4} \pm 3.2 \times 10^{-4}$ (slope + error). When this amount was increased by 10X (NaCl = 0.265 fmol), it resulted in ICAM-1 expression increase by 3.3X. With a further increase in amount of NaCl by 100X (NaCl = 2.65 fmol), the differential ICAM-1 expression was increased by 3.9X. At 525 fmol (i.e.1981x increase in NaCl amounts), an increase of 6.5X in differential ICAM-1 expression was observed.

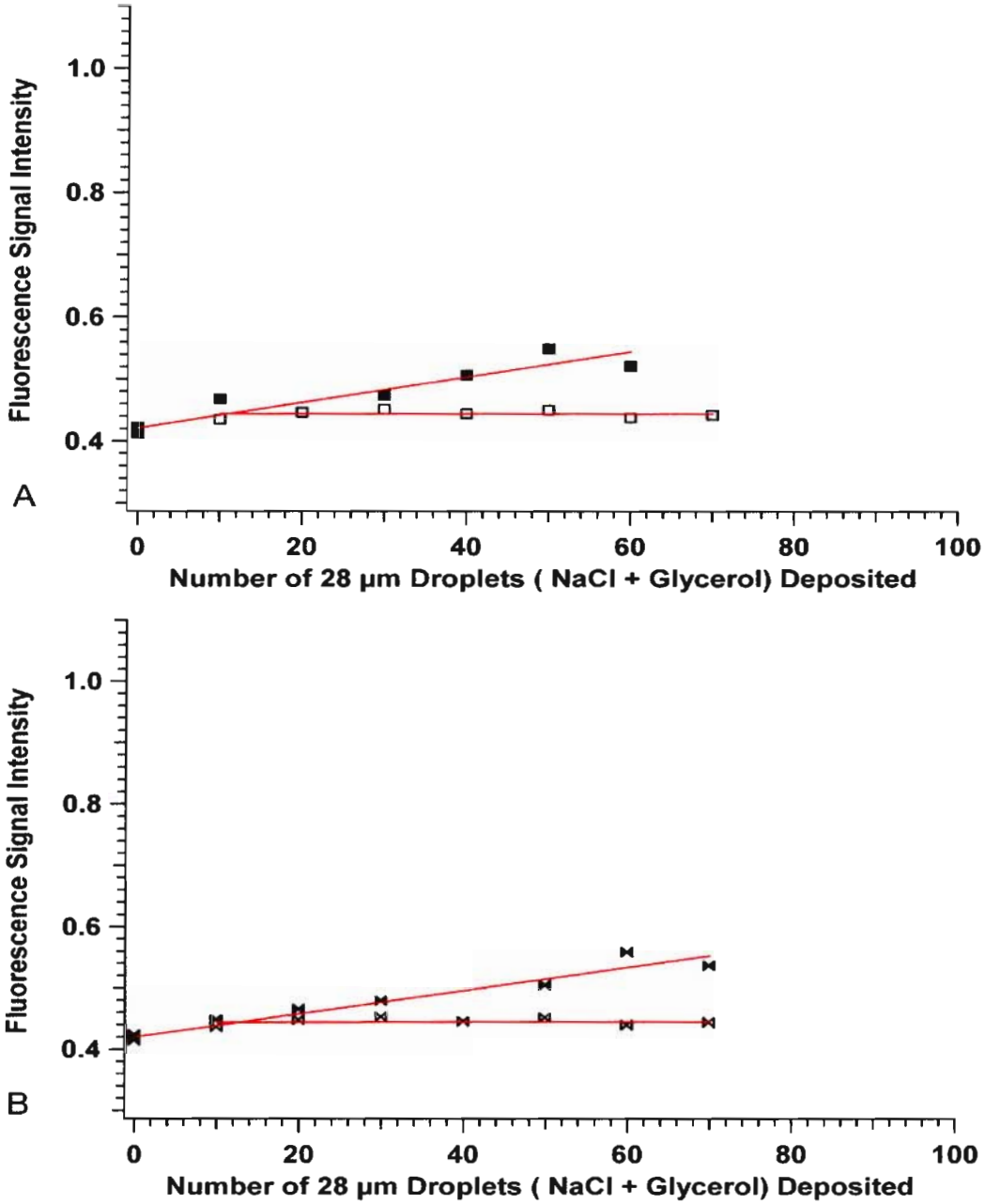

Figure 5-2: **Relative fluorescence signal intensity of ICAM-1 expressed on A549 cell culture after 18 h incubation with particles having diameter of 28 µm comprising sodium chloride (NaCl) and glycerol. Bottom x-axis indicates the number of particles deposited onto the cell culture. Filled symbols in (A) and (B), represent NaCl and glycerol particles. Open symbols represent particles containing glycerol:water. The fluorescence signal intensity was collected from 1.07 mm^2 area centred over the site of particle deposition. The R^2 coefficients from the linear least squares fit to the fluorescence signal intensity versus the number of particles deposited (filled symbols) was: (A) 0.9149 and (B) 0.9566. The amount of NaCl per particle was: (A) 6561 fmol, (B) 1312 fmol.**

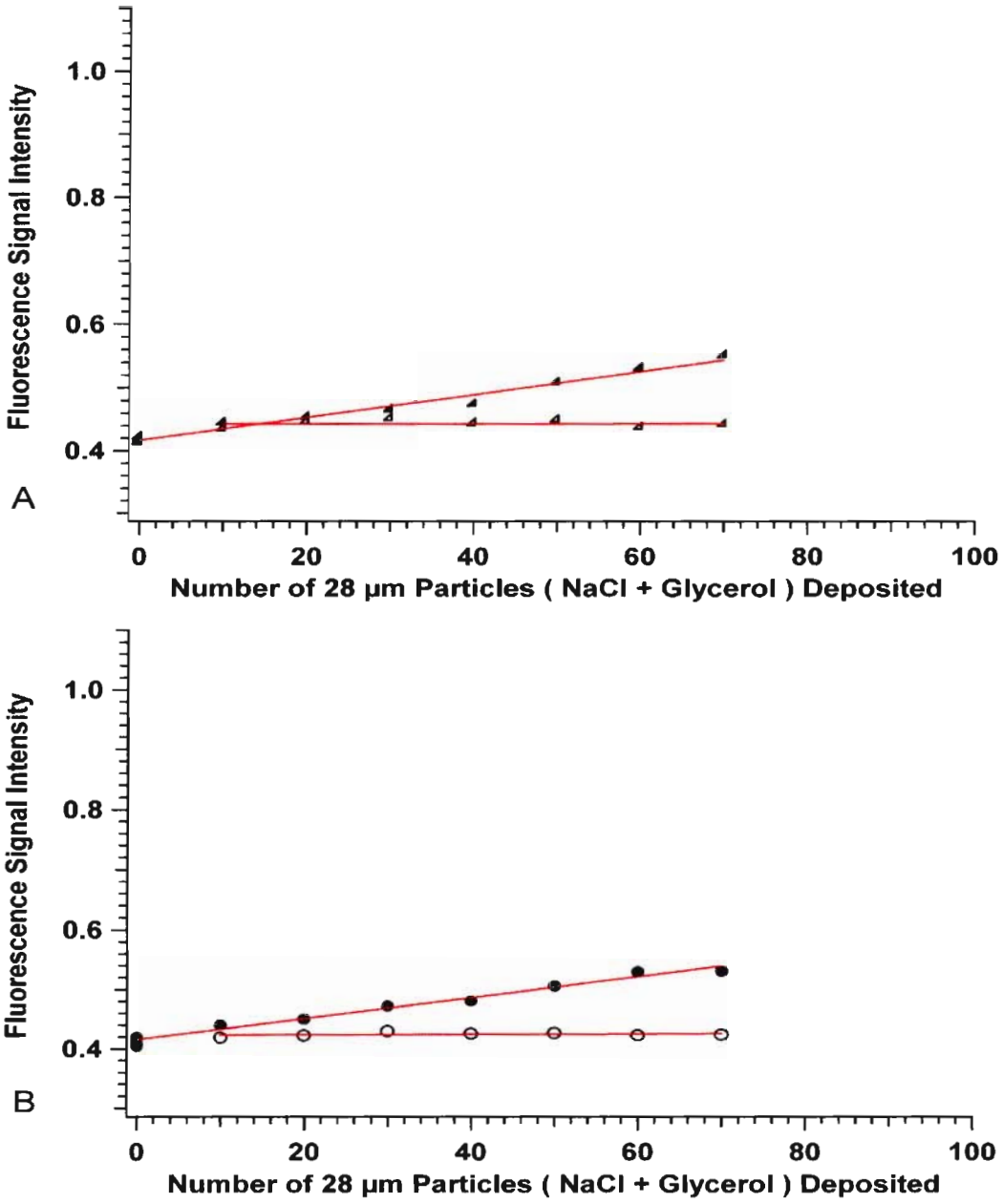

Figure 5-3: **Relative fluorescence signal intensity of ICAM-1 expressed on A549 cell culture after 18 h incubation with particles having diameter of 28 µm comprising sodium chloride (NaCl) and glycerol . Bottom x-axis indicates the number of particles deposited onto the cell culture. Filled symbols in (A) and (B), represent NaCl and glycerol particles. Open symbols represent particles containing glycerol:water. The fluorescence signal intensity was collected from 1.07 mm^2 area centred over the site of particle deposition. The R^2 coefficients from the linear least squares fit to the fluorescence signal intensity versus the number of particles deposited (filled symbols) was: (A) 0.9808, and (B) 0.9819. The amount of NaCl per particle was: (A) 656 fmol, and (B) 525 fmol.**

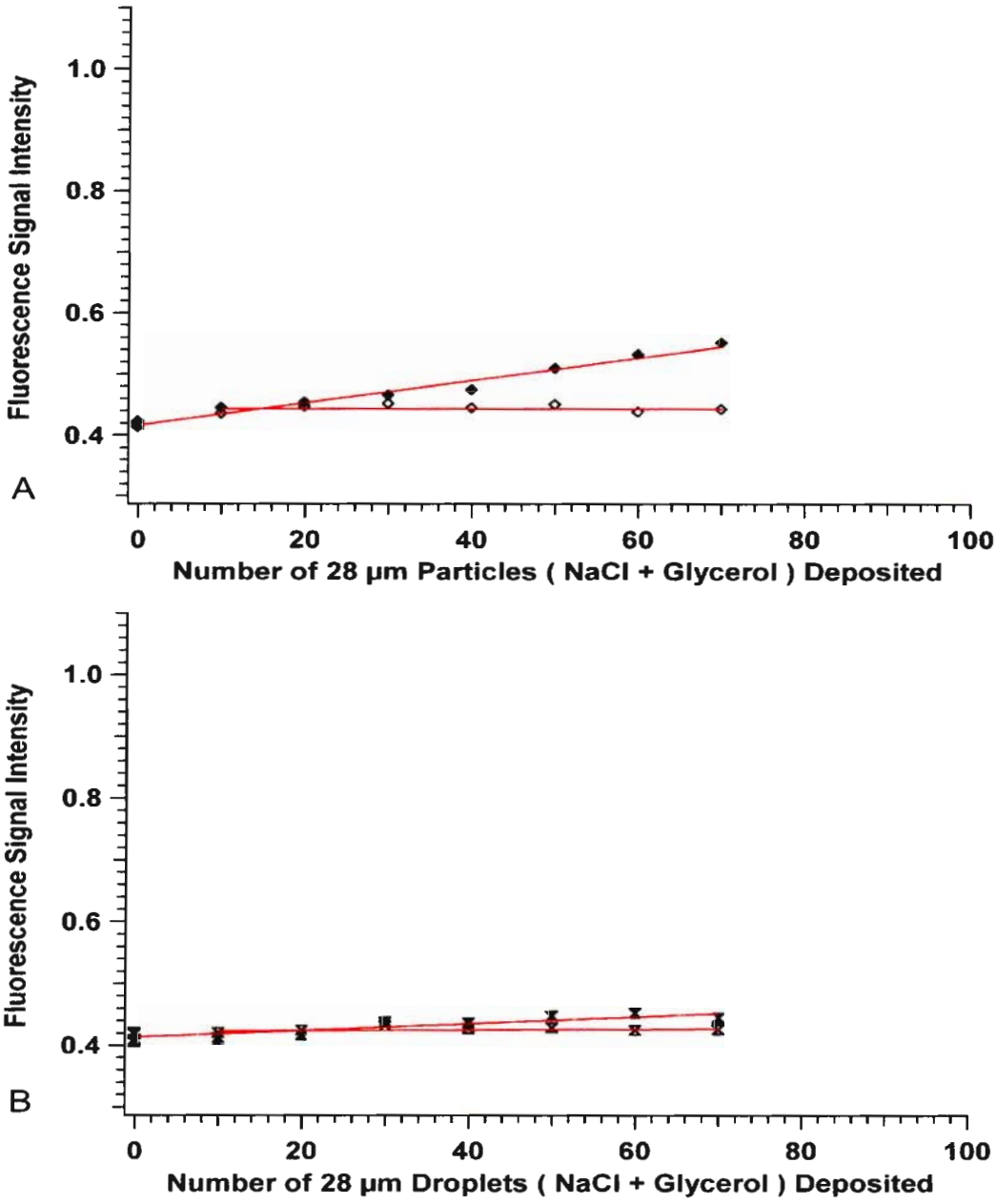

Figure 5-4: **Relative fluorescence signal intensity of ICAM-1 expressed on A549 cell culture after 18 h incubation with particles having diameter of 28 µm comprising sodium chloride (NaCl) and glycerol. Bottom x-axis indicates the number of particles deposited onto the cell culture. Filled symbols in (A) and (B), represent NaCl and glycerol particles. Open symbols represent particles containing glycerol:water. The fluorescence signal intensity was collected from 1.07 mm^2 area centred over the site of droplet deposition. The R^2 coefficients from the linear least squares fit to the fluorescence signal intensity versus the number of particles deposited (filled symbols) was: (A) 0.9804, and (B) 0.8183. The amount of NaCl per particle was: (A) 131 fmol, and (B) 87 fmol.**

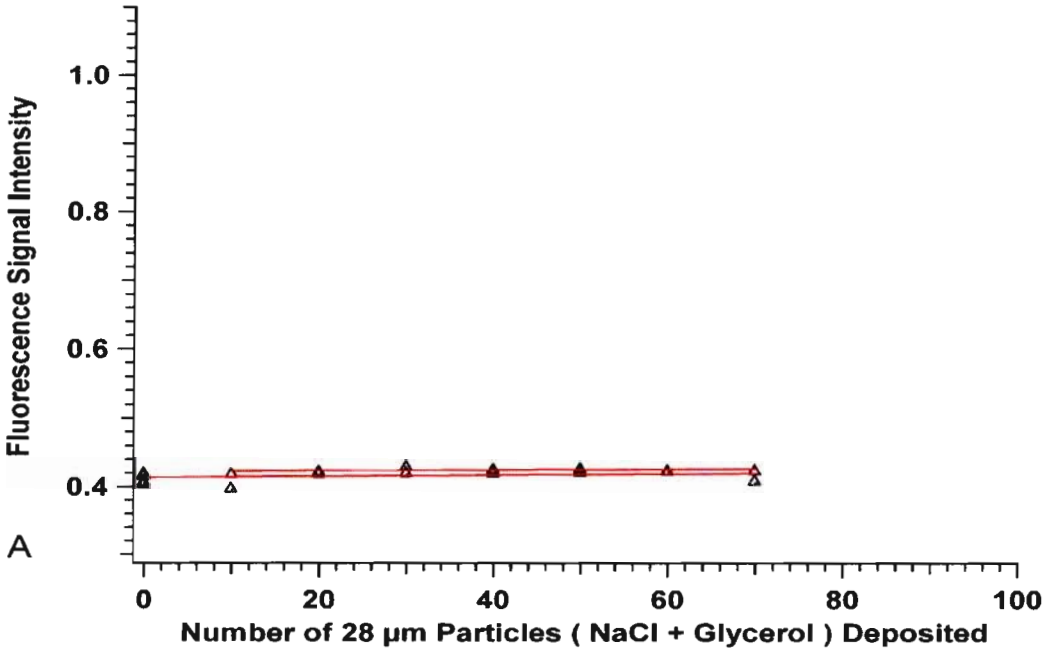

Figure 5-5: **Relative fluorescence signal intensity of ICAM-1 expressed on A549 cell culture after 18 h incubation with particles having diameter of 28 µm comprising sodium chloride (NaCl) and glycerol. Bottom x-axis indicates the number of particles deposited onto the cell culture. Filled symbols in (A), represent NaCl in glycerol particles. Open symbols represent particles containing glycerol:water. The fluorescence signal intensity was collected from 1.07 mm^2 area centred over the site of particle deposition. The R^2 coefficient from the linear least squares fit to the fluorescence signal intensity versus the number of particles deposited (filled symbols) was: (A) 0.8722. The amount of NaCl per particle was: (A) 65 fmol.**

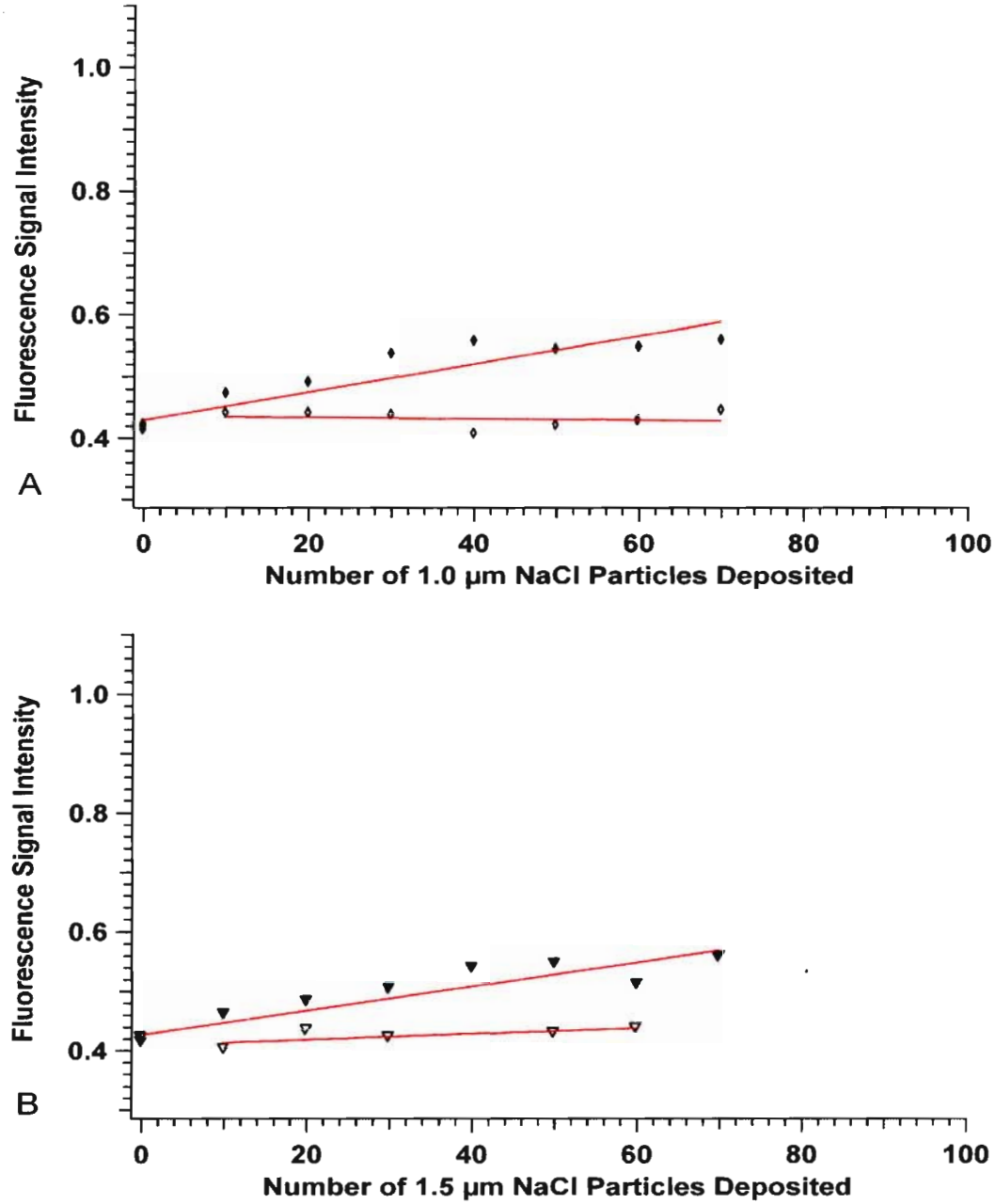

Figure 5-6: **Relative fluorescence signal intensity of ICAM-1 expressed on A549 cell culture after 18 h incubation with particles comprising sodium chloride (NaCl) (no carbon) at diameters: (A) 1.0 µm , and (B) 1.5 µm. Bottom x-axis shows the number of NaCl particles deposited onto the cell culture. Filled symbols in (A) and (B), represent NaCl particles. Open symbols represent carbon particles. The fluorescence signal intensity was collected from 1.07-mm^2 area centred over the site of particle deposition. The R^2 coefficients from the linear least squares fit to the fluorescence signal intensity versus the number of particles deposited (filled symbols) was: (A) 0.9469, and (B) 0.8824. The amount of NaCl in each particle was: (A) 656 fmol, and (B) 1312 fmol.**

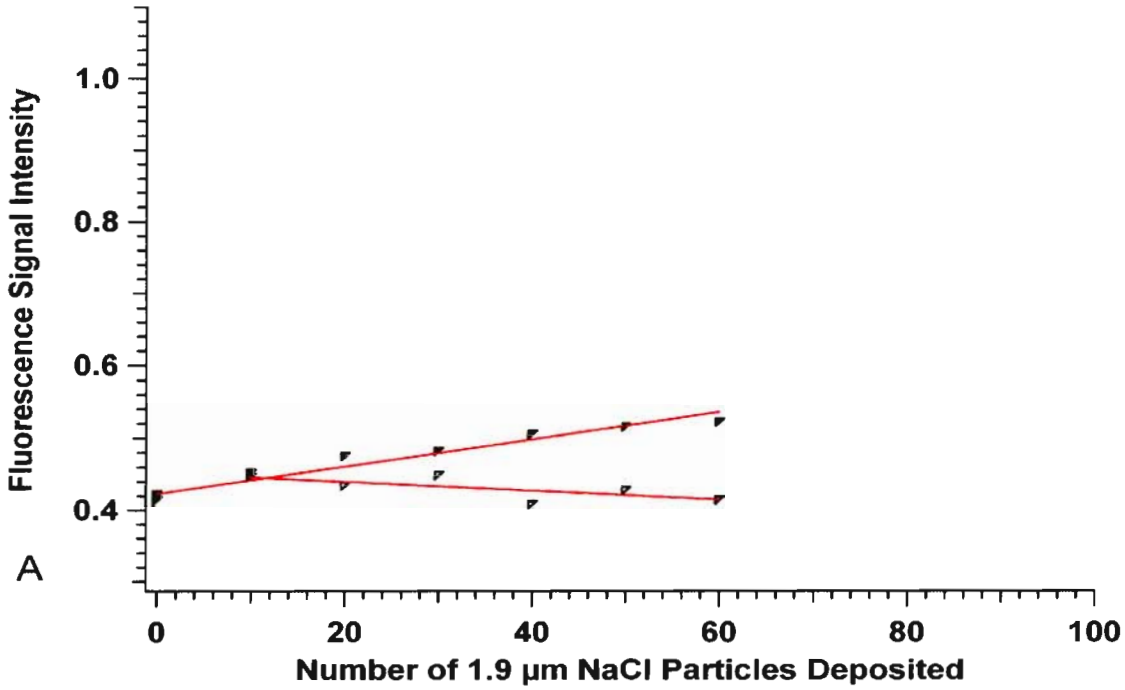

Figure 5-7: **Relative fluorescence signal intensity of ICAM-1 expressed on A549 cell culture after 18 h incubation with particles comprising sodium chloride (NaCl) (no carbon) at diameter: (A) 1.9 µm. Bottom x-axis shows the number of NaCl particles deposited onto the cell culture. Filled symbols in (A), represents NaCl particles. Open symbols represent carbon particles. The fluorescence signal intensity was collected from 1.07-mm^2 area centred over the site of particle deposition. The R^2 coefficient from the linear least squares fit to the fluorescence signal intensity versus the number of particle deposited (filled symbols) was: (A) 0.9626. The amount of NaCl in particle was: (A) 6561 fmol.**

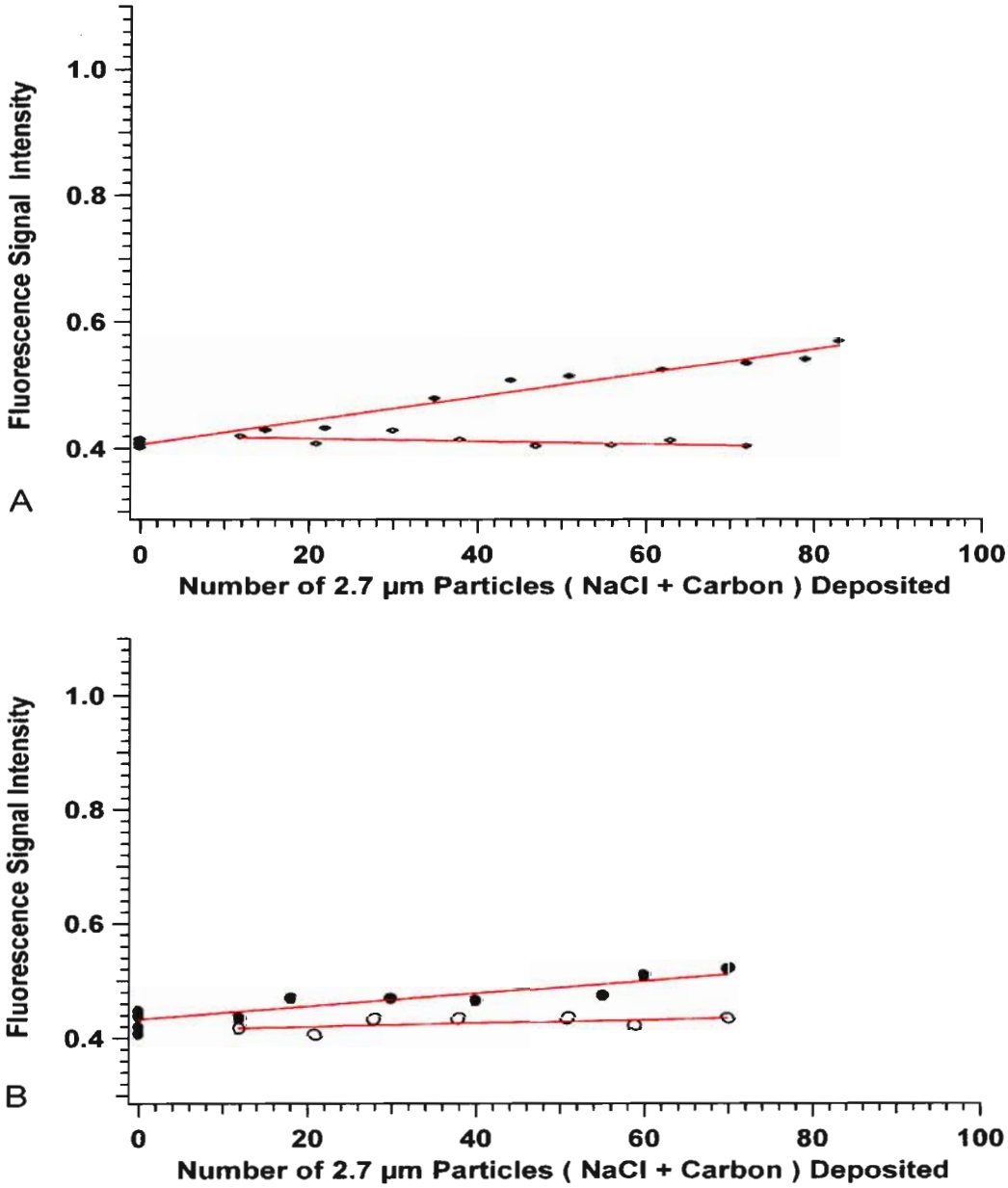

Figure 5-8: **Relative fluorescence signal intensity of ICAM-1 expressed on A549 cell culture after 18 h incubation with 2.7 µm particles containing sodium chloride and carbon: (A) and (B). Bottom x-axis shows the number particles comprising sodium chloride and carbon deposited onto the cell culture. Filled symbols in (A) and (B), represent particles comprising NaCl and carbon. Open symbols represent carbon particles. The fluorescence signal intensity was collected from 1.07-mm^2 area centred over the site of particle deposition. The R^2 coefficients from the linear least squares fit to the fluorescence signal intensity versus the number of particles deposited (filled symbols) was : (A) 0.9755, and (B) 0.8117. The amount of NaCl per particle was: (A) 525 fmol, C (India ink) = 3.3 x 10^4 fmol, and (B) 2.65 fmol, C (India ink) = 3.3 x 10^4 fmol.**

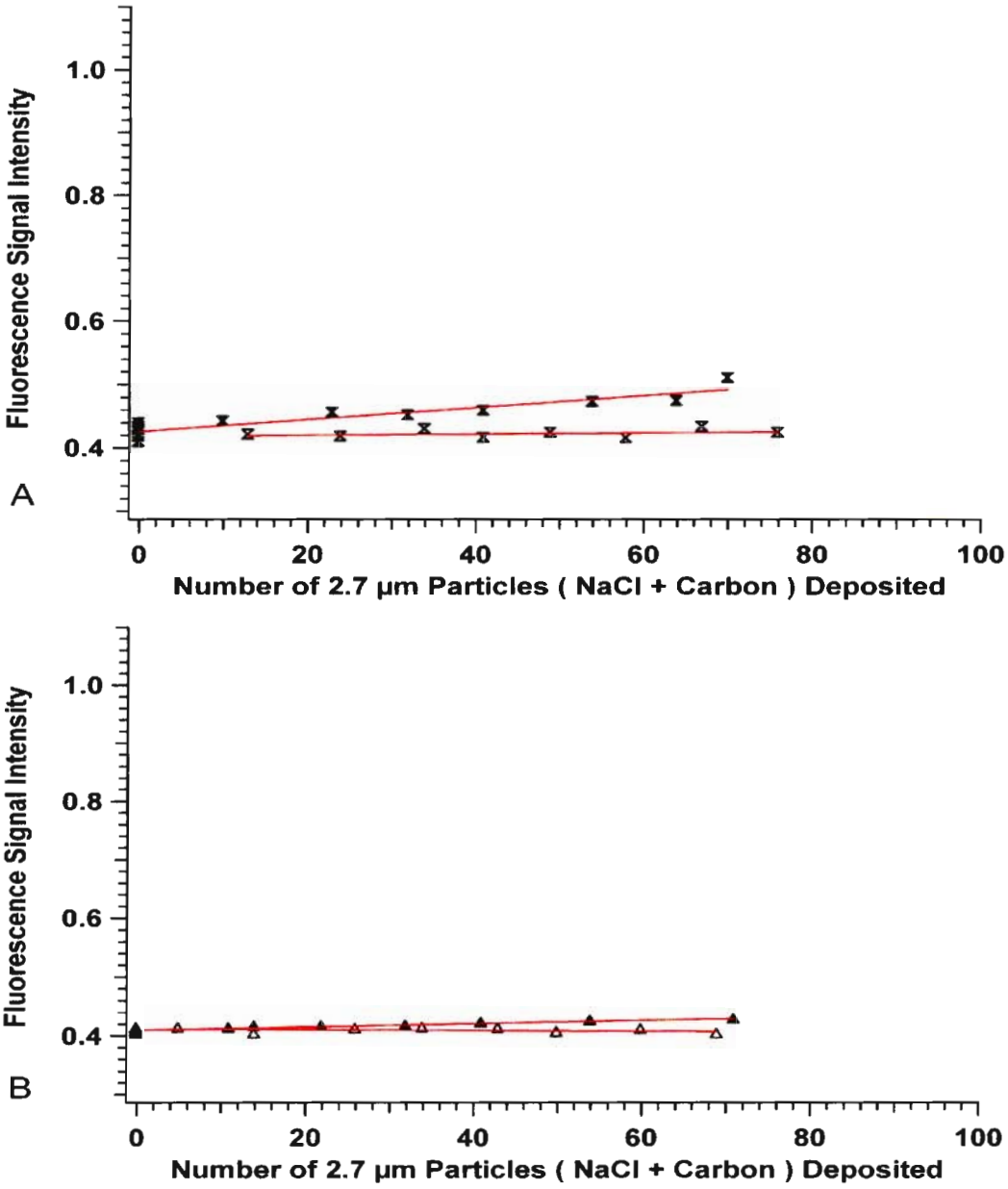

Figure 5-9: **Relative fluorescence signal intensity of ICAM-1 expressed on A549 cell culture after 18 h incubation with 2.7 µm particles comprising sodium chloride and carbon: (A) and (B). Bottom x-axis indicates the number of particles comprising sodium chloride and carbon deposited onto the cell culture. Filled symbols in (A) and (B), represent particles comprising NaCl and carbon. Open symbols represent carbon particles. The fluorescence signal intensity was collected from 1.07-mm^2 area centred over the site of particle deposition. The R^2 coefficient from the linear least squares fit to the fluorescence signal intensity versus the number of particles deposited (filled symbols) was: (A) 0.8495, and (B) 0.8692. The amount of NaCl per particle was: (A) 0.265 fmol, C (India ink) = 3.3 x 10^4 fmol, and (B) 0.0265 fmol, C (India ink) = 3.3 x 10^4 fmol.**

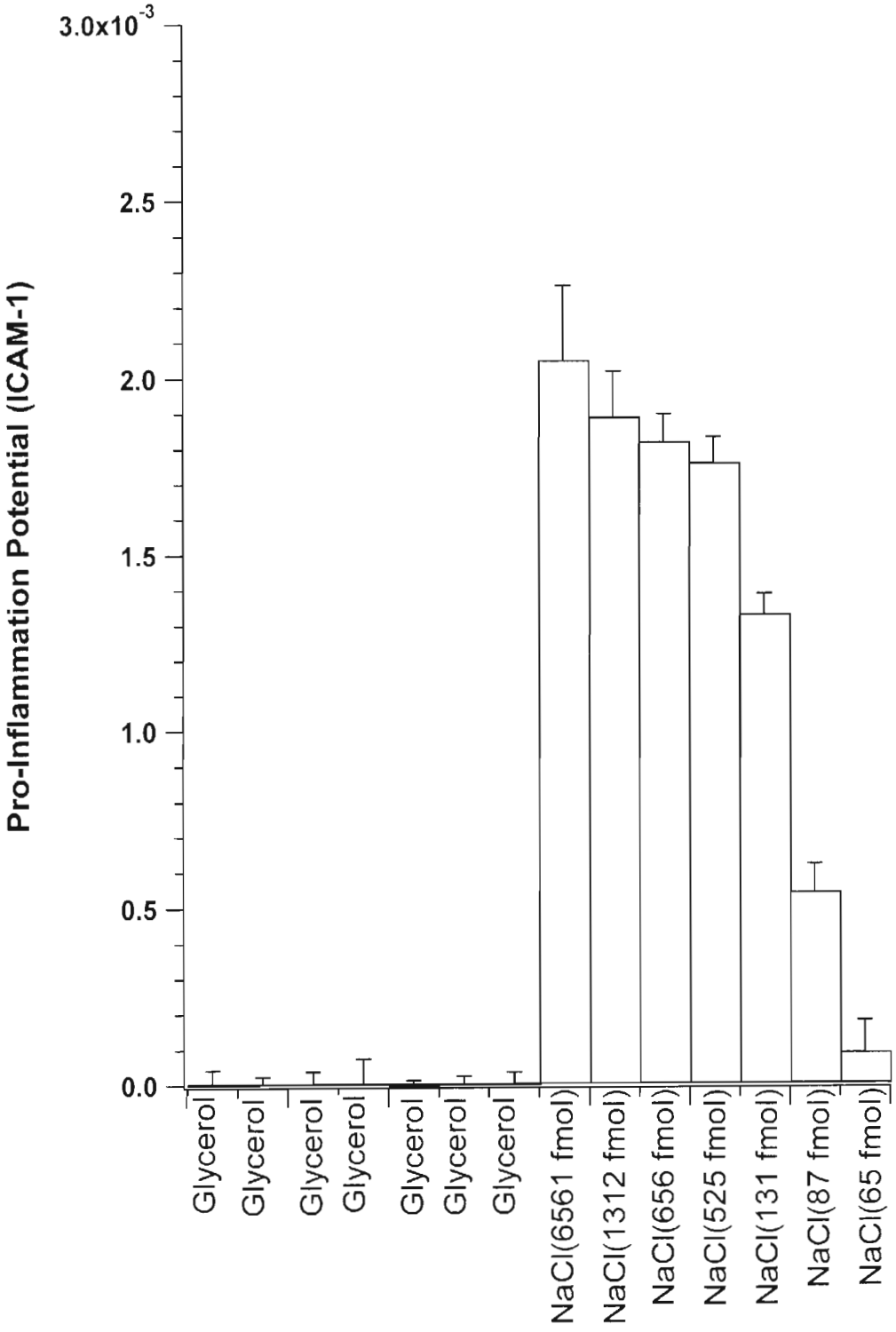

Figure 5-10: **Pro-inflammation potential (PIP) represented in terms of differential expression of ICAM-1 by A549 cells in response to 18 h incubation with glycerol and NaCl, at the moles of NaCl indicated. The glycerol mole per particles was 18 pmol, and is valid for all particles.**

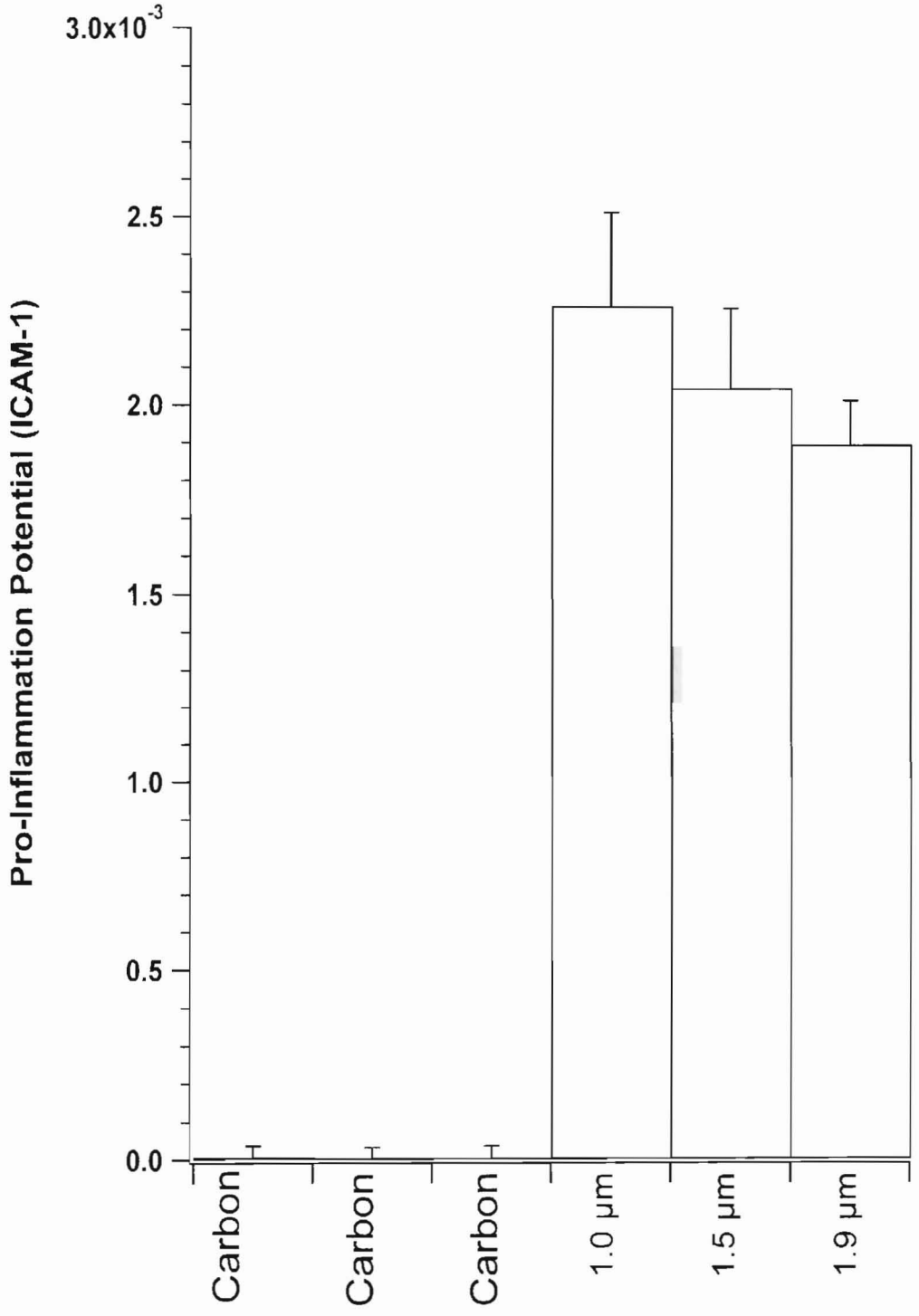

Figure 5-11: **Pro-inflammation potential (PIP) represented in terms of differential expression of ICAM-1 by A549 cells in response to 18 h incubation with carbon particles, and particles comprising NaCl (no carbon) of diameters of 1.0 µm, 1.5 µm, and 1.9 µm, having 656, 1312, and 6561 fmol of NaCl, respectively.**

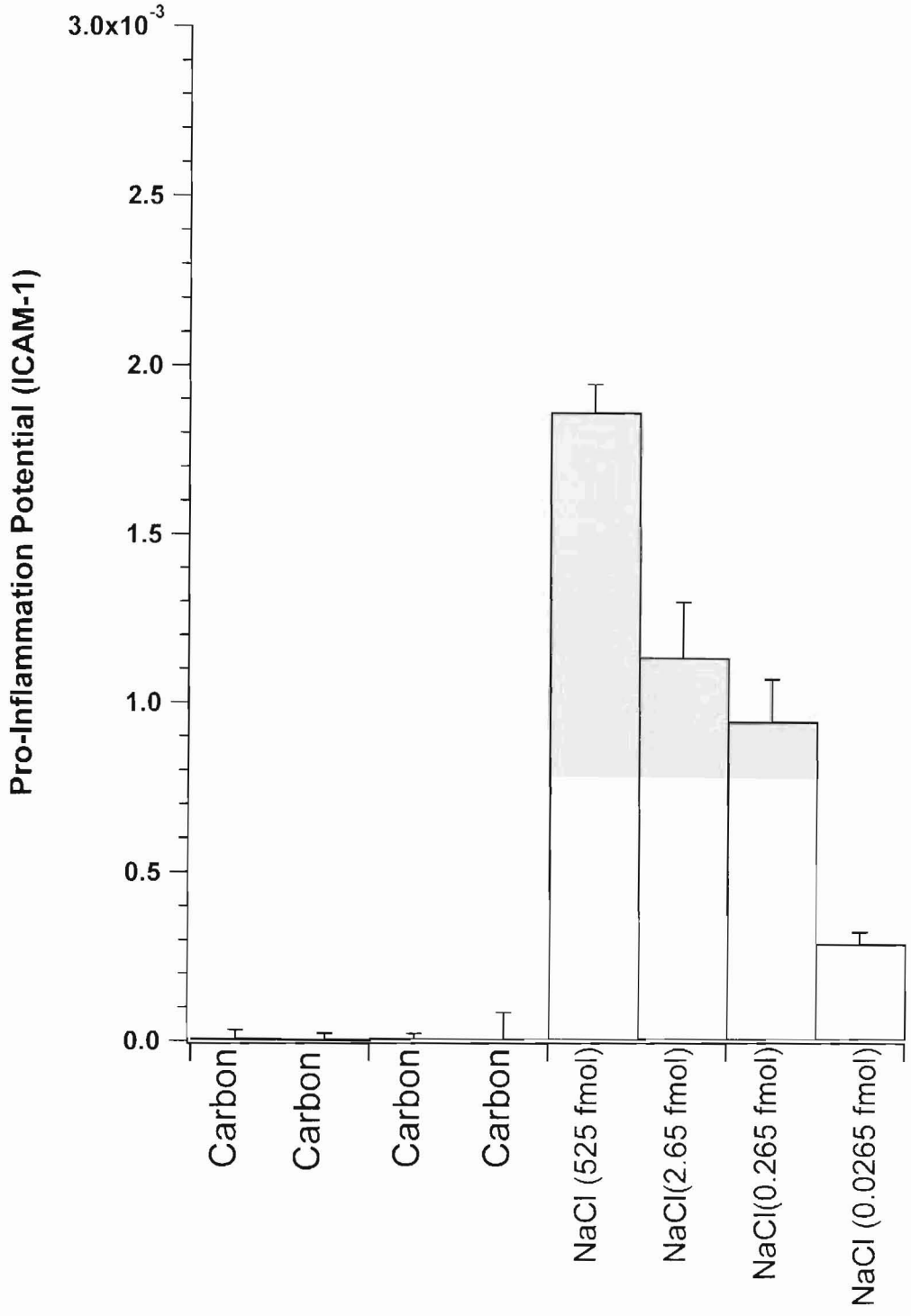

Figure 5-12: **Pro-inflammation potential (PIP) represented in terms of differential expression of ICAM-1 by A549 cells in response to 18 h incubation with carbon particles, and particles comprising carbon and NaCl. The particles had 525 fmol, 2.65 fmol, 0.265 fmol, and 0.0265 fmol of NaCl respectively. The size of the particles is the same, and is 2.7 μm.**

Table 5-2: The pro-inflammation potential (PIP) due to sodium chloride in each particle type, and the same PIP value normalized to the number of moles of sodium chloride contained in that particle.

Particle type	Mole of NaCl in particle (fmol)	PIP (ICAM-1)	Error	Normalized PIP based on mole NaCl added
NaCl + glycerol	6561	2.0×10^{-3}	$\pm 2.1\times10^{-4}$	3.0×10^{8}
	1312	1.9×10^{-3}	$\pm 1.3\times10^{-4}$	1.4×10^{8}
	656	1.8×10^{-3}	$\pm 7.7\times10^{-5}$	2.7×10^{9}
	525	1.7×10^{-3}	$\pm 7.2\times10^{-5}$	3.2×10^{9}
	131	1.3×10^{-3}	$\pm 5.7\times10^{-5}$	9.9×10^{9}
	87	5.4×10^{-4}	$\pm 7.7\times10^{-5}$	6.2×10^{9}
	65	9.1×10^{-5}	$\pm 8.9\times10^{-5}$	1.4×10^{9}
NaCl only (no carbon)	6561	1.9×10^{-3}	$\pm 2.5\times10^{-4}$	2.9×10^{8}
	1312	2.0×10^{-3}	$\pm 2.1\times10^{-4}$	1.5×10^{9}
	656	2.3×10^{-3}	$\pm 1.2\times10^{-4}$	3.5×10^{9}
NaCl + carbon	525	1.9×10^{-3}	$\pm 8.2\times10^{-5}$	3.6×10^{9}
	2.65	1.1×10^{-3}	$\pm 1.6\times10^{-4}$	4.1×10^{11}
	0.265	9.4×10^{-4}	$\pm 1.3\times10^{-4}$	3.5×10^{12}
	0.0265	2.9×10^{-4}	$\pm 3.2\times10^{-4}$	1.1×10^{13}

5.8 Discussion

We have previously shown that particles comprising NaCl and carbon caused measurable expression of ICAM-1 on A549 cells. Herein, the influence of NaCl physical states, namely solid or liquid, in causing differential ICAM-1 expression on A549 cells was measured. The particles studied herein mimicked various physical states in which NaCl could be found in the troposphere. For instance, NaCl particles (no carbon) mimicked particles that can be formed by evaporation of water from sea sprays.[165, 166] NaCl that have dissolved in organic:water forming aqueous droplets was mimicked with particles containing NaCl in glycerol.[169] Particles of NaCl plus carbon could

mimic NaCl particles potentially contaminated with carbon from combustion of biological materials.

The effect of NaCl on ICAM-1 expression by A549 cells is not well documented in literature. A549 cells possess characteristics similar to type-II cells of lung alveolar epithelium.[163] As such, these results can provide new information regarding the potential toxicity of this compound upon inhalation. Our data indicate that all the physical states of NaCl, following an 18 h incubation period with A549 cells, effected a small, but measurable, differential ICAM-1 expression. For instance, particles containing carbon and NaCl (0.0265 fmol NaCl) per particle effected differential expression of ICAM-1 on A549 cells; which comparable levels was effected by particles comprising only NaCl (no carbon), or by those containing NaCl and glycerol, at NaCl amounts of 1312 fmol, and 6561 fmol respectively. The normalized pro-inflammation potential (PIP) due to the number of moles of sodium chloride contained in each particle indicated that particles comprising NaCl and carbon clearly caused the highest normalized PIP.

The small differences in the levels ICAM-1 expression resulting from NaCl in different physical states studied herein could be due to differences in their rates of endocytosis by A549 cells.[196] It is speculated that particle uptake by the cells may have resulted in osmotic stress on the lysosomes. This stress on the lysosomes may have triggered the production of TNF-α.[312] ICAM-1 expression on A549 cells is known to be induced by TNF-α through the activation of the nuclear factor kappa B (NF-κB) pathway.[99, 198] In

consideration of this data, it is speculated that the differential ICAM-1 expression on A549 cells following incubation with NaCl particles could be due to an initiation of osmotic stress.

5.9 Conclusion

The ac trap was used in creating NaCl particles having different physical states. The pro-inflammation potential (ICAM-1) of A549 cells following 18 h incubation with NaCl particles was measured. NaCl particles caused small but measurable differential ICAM-1 expression on A549 cells, and the physical state of NaCl at the instant of deposition was important.

Chapter 6: Conclusion and future directions

An ac trap and associated levitation methodology facilitated the creation and deposition of ambient particle mimics onto A549 cells *in vitro*. The measured differential ICAM-1 expression by A549 cells after 18 h incubation with particles was reported. For particles at diameters of 6.8, 3.8, and 2.6 μm, but whose bulk or average inorganic compound composition mimicked EHC-93, our data indicated that particle having diameter of 2.6 μm effected the greatest differential expression of ICAM-1 on A549 cells. When the relative contribution of inorganic compounds namely aluminium nitrate, iron nitrate, zinc nitrate, and lead nitrate systematically added to PT-5, PT-6, PT-7, and PT-8 to the e differential ICAM-1 expression was measured, it was found that lead nitrate caused the most differential ICAM-1 expression. A549 cells incubated with NaCl particles having different physical states, solid or liquid, at the instant of deposition effected measurable ICAM-1 expression. However, among the three physical states studied: NaCl particles, NaCl and glycerol particles, or particles of NaCl plus carbon, the normalized pro-inflammation potential indicated that particles comprising NaCl plus carbon possessed the greatest value for ICAM-1. The data suggest that particle's physical state at the instant of deposition onto A549 cells was important regarding ICAM-1 expression.

Ambient PM is complex and comprises several classes of organic compounds. It would be interesting to further investigate, the influence of the different oxidation states of metals used herein to effecting differential ICAM-1 expression. It is also suggested that other studies measure the pro-inflammation potential of particles comprising inorganic compounds investigated herein, and organic compounds including acids, aldehydes or ketones, that are present in the troposphere. Such studies, in addition, could investigate the effects of organic compounds chain lengths in particles to differential expression of ICAM-1.

The study involving NaCl particles found that they caused measurable ICAM-1 expression on A549 cells, suggesting that they possess the potential to effect lung inflammation upon inhalation. ICAM-1 expression by A549 cells is known to be complex, involving several cytokines including interleukin (IL)-1,8,13 that participate in effecting an inflammatory response. It is suggested that further studies be done on particle comprising NaCl plus carbon. In addition, it would be interesting to learn how lysosomes are affected by the NaCl. Such studies will involve staining A549 cells incubated with particles using acridine orange and using phase contrast microscopy to observe changes in lysosomal size that would indicate whether the cells are shrinking or expanding due to osmotic stress.

References

(1) Breuer, G. Air in danger: ecological perspectives of the atmosphere; Cambridge university press: London, **1980**.

(2) Finlayson-Pitts, B. J.; Pitts, J. N. Chemistry of the upper and lower atmosphere. Theory, experiments, and applications. 2nd ed.; Academic press: New York, **2000**.

(3) Butler, J. D. Air pollution chemistry; Academic press: New York, 1979.

(4) Kan, H. D.; Chen, B. H. Sci Total Environ **2004**, 322, 71-79.

(5) Lei, H. C.; Tanner, P. A.; Huang, M. Y.; Shen, Z. L.; Wu, Y. X. Atmos Environ **1997**, 31, 851-861.

(6) Sheppard, L.; Levy, D.; Norris, G.; Larson, T. V.; Koenig, J. Q. Epidemiol **1999**, 10, 23-30.

(7) Lipsett, M.; Hurley, S.; Ostro, B. Environ Health Persp **1997**, 105, 216-222.

(8) Brimblecombe, P. History and early air pollution; Methuen press: New York, **1987**.

(9) Arndt, R. L.; Carmichael, G. R.; Streets, D. G.; Bhatti, N. Atmos Environ **1997**, 31, 1553-1572.

(10) Akimoto, H.; Narita, H. Atmos Environ **1994**, 28, 213-225.

(11) Doherty, G. M.; Newell, R. E.; Reichle, H. G. J Geophys Res-Atmos **1986**, 91, 9827-9839.

(12) Brook, R. D.; Franklin, B.; Cascio, W.; Hong, Y. L.; Howard, G.; Lipsett, M.; Luepker, R.; Mittleman, M.; Samet, J.; Smith, S. C.; Tager, I. Circulation **2004**, 109, 2655-2671.

(13) Bardini, C. J Econ Hist **1997**, 57, 633-653.

(14) Howard, P. H.; Datta, R. S.; Hanchett, A. Fuel **1977**, 56, 346.

(15) Morris, S. C.; Moskowitz, P. D.; Sevian, W. A.; Silberstein, S.; Hamilton, L. D. Science **1979**, 206, 654-662.

(16) Billings, C. E.; Matson, W. R. Science **1972**, 176, 1232-1233.

(17) Mcelroy, M. W.; Carr, R. C.; Ensor, D. S.; Markowski, G. R. Science **1982**, 215, 13-19.

(18) Firket, J. T Faraday Soc **1936**, 32, 1192-1197.

(19) Logan, W. P. D. Brit Med J **1956**, 1, 722-725.

(20) Glasser, M.; Greenbur, L.; Field, F. Arch Environ Health **1967**, 15, 684-694.

(21) Begeman, C. R.; Colucci, J. M. Science **1968**, 161, 271.

(22) Schultz, M. G.; Diehl, T.; Brasseur, G. P.; Zittel, W. Science **2003**, 302, 624-627.

(23) Vogel, G. Science **2004**, 305, 967.

(24) Service, R. F. Science **2004**, 305, 962-963.

(25) Schwartz, J.; Dockery, D. W. Am Rev Respir Dis **1992**, 145, 600-604.

(26) Pope, C. A.; Thun, M. J.; Namboodiri, M. M.; Dockery, D. W.; Evans, J. S.; Speizer, F. E.; Heath, C. W. Am J Resp Crit Care **1995**, 151, 669-674.

(27) Dockery, D. W.; Pope, C. A.; Xu, X. P.; Spengler, J. D.; Ware, J. H.; Fay, M. E.; Ferris, B. G.; Speizer, F. E. N Eng J Med **1993**, 329, 1753-1759.

(28) Greenbur, L.; Field, F.; Erhardt, C. L.; Glasser, M.; Reed, J. I. Arch Environ Health **1967**, 15, 430-454.

(29) Mcdonald, J. C.; Drinker, P.; Gordon, J. E. Am J Med Sci **1951**, 221, 325-342.

(30) Mccarrol, J.; Bradley, W. Am J Public Health **1966**, 56, 1933-1942.

(31) Heimann, H. Arch Environ Health **1970**, 20, 230-251.

(32) Bell, M. L.; Davis, D. L.; Fletcher, T. Environ Health Persp **2004**, 112, 6-8.

(33) Pope, C. A.; Dockery, D. W.; Spengler, J. D.; Raizenne, M. E. Am Rev Respir Dis **1991**, 144, 668-674.

(34) McGranahan, G. M.F. Air pollution and health in rapidly developing countries; Earthscan publication: London, **2003**.

(35) Davis, T. W. W.; Wark, K.F. Air pollution: its origin and control; Addison Wesley Longman Inc.: California, **1998**.

(36) Kennedy, H. W. W. Air pollution control; Oceana publications, Inc.: New York, **1969**.

(37) Meyer, W. B.; Turner, B. L. Annu Rev Ecol Syst **1992**, 23, 39-61.

(38) Hendersonsellers, A.; Gornitz, V. Clim Change **1984**, 6, 231-257.

(39) Keyfitz, N. Sci Amer **1989**, 261, 118-126.

(40) Riley, K. Popul Environ **2002**, 23, 479-494.

(41) Chan, C. C.; Ozkaynak, H.; Spengler, J. D.; Sheldon, L. Environ Sci Technol **1991**, 25, 964-972.

(42) Chan, C. C.; Spengler, J. D.; Ozkaynak, H.; Lefkopoulou, M. J Air Waste Manag Assoc **1991**, 41, 1594-1600.

(43) Morris, D. L.; Barker, P. J.; Legator, M. S. Arch Environ Health **2004**, 59, 160-165.

(44) Vincent, R.; Goegan, P.; Johnson, G.; Brook, J. R.; Kumarathasan, P.; Bouthillier, L.; Burnett, R. T. Fund Appl Toxicol **1997**, 39, 18-32.

(45) Biran, R.; Tang, Y. Z.; Brook, J. R.; Vincent, R.; Keeler, G. J. Int J Environ Anal Chem **1996**, 63, 315-322.

(46) Hoppel, W. A.; Frick, G. M.; Fitzgerald, J.; Larson, R. E. J Geophys Res-Atmos **1994**, 99, 14443-14459.

(47) Pirjola, L.; Laaksonen, A.; Aalto, P.; Kulmala, M. J Geophys Res-Atmos **1998**, 103, 8309-8321.

(48) Kulmala, M.; Hameri, K.; Aalto, P. P.; Makela, J. M.; Pirjola, L.; Nilsson, E. D.; Buzorius, G.; Rannik, U.; Dal Maso, M.; Seidl, W.; Hoffman, T.; Janson, R.; Hansson, H. C.; Viisanen, Y.; Laaksonen, A.; O'Dowd, C. D. Tellus B **2001**, 53, 324-343.

(49) Schroder, F.; Strom, J. Atmos Res **1997**, 44, 333-356.

(50) Pryor, S. C.; Sorensen, L. L. J Appl Meteorol **2000**, 39, 725-731.

(51) Galindo, I.; Ivlev, L. S.; Gonzalez, A.; Ayala, R. J Volcanol Geoth Res **1998**, 83, 197-217.

(52) Delfino, R. J.; Zeiger, R. S.; Seltzer, J. M.; Street, D. H.; Matteucci, R. M.; Anderson, P. R.; Koutrakis, P. Environ Health Persp **1997**, 105, 622-635.

(53) Huffman, G. P.; Huggins, F. E.; Shah, N.; Huggins, R.; Linak, W. P.; Miller, C. A.; Pugmire, R. J.; Meuzelaar, H. L. C.; Seehra, M. S.; Manivannan, A. J Air Waste Manag Assoc **2000**, 50, 1106-1114.

(54) bin Abas, M. R.; Oros, D. R.; Simoneit, B. R. T. Chemosphere **2004**, 55, 1089-1095.

(55) Raes, F.; Van Dingenen, R.; Vignati, E.; Wilson, J.; Putaud, J. P.; Seinfeld, J. H.; Adams, P. Atmos Environ **2000**, 34, 4215-4240.

(56) Poschl, U. Angew Chem Int 2005, 44, 7520-7540.

(57) Hinds, W. C. Aerosol technology: properties, behaviour, and measurement of ambient particles; Wiley-interscience: New York, **1982**.

(58) Napari, I.; Noppel, M.; Vehkamaki, H.; Kulmala, M. J Chem Phys **2002**, 116, 4221-4227.

(59) Raes, F.; Vandingenen, R. J Geophys Res-Atmos **1992**, 97, 12901-12912.

(60) Korhonen, P.; Kulmala, M.; Laaksonen, A.; Viisanen, Y.; McGraw, R.; Seinfeld, J. H. J Geophys Res-Atmos **1999**, 104, 26349-26353.

(61) Kulmala, M.; Pirjola, U.; Makela, J. M. Nature **2000**, 404, 66-69.

(62) Yu, F. Q.; Turco, R. P. J Geophys Res-Atmos **2001**, 106, 4797-4814.

(63) Yu, F. Q.; Turco, R. P. Geophys Res Lett **2001**, 28, 155-158.

(64) Chow, J. C.; Watson, J. G.; Fujita, E. M.; Lu, Z. Q.; Lawson, D. R.; Ashbaugh, L. L. Atmos Environ **1994**, 28, 2061-2080.

(65) Chan, Y. C.; Simpson, R. W.; Mctainsh, G. H.; Vowles, P. D.; Cohen, D. D.; Bailey, G. M. Atmos Environ **1997**, 31, 3773-3785.

(66) Behrendt, H.; Becker, W. M.; Fritzsche, C.; SliwaTomczok, W.; Tomczok, J.; Friedrichs, K. H.; Ring, J. Int Arch Allergy Immunol **1997**, 113, 69-74.

(67) Councell, T. B.; Duckenfield, K. U.; Landa, E. R.; Callender, E. Environ Sci Technol **2004**, 38, 4206-4214.

(68) Osornio-Vargas, A. R.; Bonner, J. C.; Alfaro-Moreno, E.; Martinez, L.; Garcia-Cuellar, C.; Rosales, S. P. D.; Miranda, J.; Rosas, I. Environ Health Persp **2003**, 111, 1289-1293.

(69) Chow, J. C.; Watson, J. G.; Lu, Z. Q.; Lowenthal, D. H.; Frazier, C. A.; Solomon, P. A.; Thuillier, R. H.; Magliano, K. Atmos Environ **1996**, 30, 2079-2112.

(70) Laden, F.; Neas, L. M.; Dockery, D. W.; Schwartz, J. Environ Health Persp **2000**, 108, 941-947.

(71) Yeh, H. C.; Cuddihy, R. G.; Phalen, R. F.; Chang, I. Y. Aerosol Sci Technol **1996**, 25, 134-140.

(72) Phalen, R. F.; Schum, G. M.; Oldham, M. J. J Aerosol Med **1990**, 3, 271-282.

(73) Shoji, T.; Huggins, F. E.; Huffman, G. P.; Linak, W. P.; Miller, C. A. Energ Fuel **2002**, 16, 325-329.

(74) Kleeman, M. J.; Schauer, J. J.; Cass, G. R. Environ Sci Technol **1999**, 33, 3516-3523.

(75) Rogge, W. F.; Hildemann, L. M.; Mazurek, M. A.; Cass, G. R.; Simoneit, B. R. T. Environ Sci Technol **1993**, 27, 636-651.

(76) Jang, M. S.; Kamens, R. M. Environ Sci Technol **2001**, 35, 3626-3639.

(77) Bates, D. V.; Kaneko, K.; Henderso,J.A.; Milicemi.J.; Anthonis.N.R.; Dollfuss, R.; Dolovich, M. Scand J Respir Dis **1966**, S, 15-23.

(78) Krogh, A.; Lindhard, J. J Physiol-London **1914**, 47, 431-445.

(79) Wilkey, D. D.; Lee, P. S.; Hass, F. J.; Gerrity, T. R.; Yeates, D. B.; Lourenco, R. V. Arch Environ Health **1980**, 35, 294-303.

(80) Garrard, C. S.; Gerrity, T. R.; Yeates, D. B. Clin Res **1980**, 28, A780-A780.

(81) Knowles, M. R.; Boucher, R. C. J Clin Invest **2002**, 109, 571-577.

(82) Adamson, I. Y. R.; Bowden, D. H. Lab Invest **1974**, 30, 35-42.

(83) Adamson, I. Y. R.; Bowden, D. H. Lab Invest **1975**, 32, 736-745.

(84) Evans, M. J.; Cabral, L. J.; Stephens, R. J.; Freeman, G. Exp Mol Pathol **1975**, 22, 142-150.

(85) Witschi, H. Toxicol **1976**, 5, 267-277.

(86) Williams, M. C. P Natl Acad Sci-Biol **1984**, 81, 6054-6058.

(87) Kuroki, Y.; Voelker, D. R. J Biol Chem **1994**, 269, 25943-25946.

(88) Hamm, H.; Fabel, H.; Bartsch, W. Clin Invest **1992**, 70, 637-657.

(89) Ikegami, M.; Ueda, T.; Woods, E.; Jobe, A. Am Rev Respir Dis **1993**, 147, A143-A143.

(90) Johansson, J.; Curstedt, T.; Robertson, B. Eur Respir J **1994**, 7, 372-391.

(91) Burns, A. R.; Takei, F.; Doerschuk, C. M. J Immunol **1994**, 153, 3189-3198.

(92) Kang, B. H.; Crapo, J. D.; Wegner, C. D.; Letts, L. G.; Chang, L. Y. Am J Resp Cell Mol **1993**, 9, 350-355.

(93) Gadient, R. A.; Patterson, P. H. Stem Cells **1999**, 17, 127-137.

(94) Movat, H. Z. Inflammation, immunity and hypersensitivity; Harper and Row press: New York, **1971**.

(95) Ebert, R. H. The inflammatory process; Academic press: New York, **1965**.

(96) Marchand, F. Virchows Arch A **1922**, 237, 303-323.

(97) Korhonen, K.; Soukka, H.; Halkola, L.; Peuravuori, H.; Aho, H.; Pulkki, K.; Kero, P.; Kaapa, P. O. Pediatr Res **2003**, 54, 192-197.

(98) Ishii, H.; Hayashi, S.; Hogg, J. C.; Fujii, T.; Goto, Y.; Sakamoto, N.; Mukae, H.; Vincent, R.; van Eeden, S. F. Resp Res **2005**, 6,87-96.

(99) Holden, N. S.; Catley, M. C.; Cambridge, L. M.; Barnes, P. J.; Newton, R. Eur J Biochem **2004**, 271, 785-791.

(100) Gehr, P.; Geiser, M.; Hoffmann, V. I.; Church, S.; Waber, U.; Baumann, M. Microsc Res Techniq **1993**, 26, 423-436.

(101) Griese, M. Eur Respir J **1999**, 13, 1455-1476.

(102) Bennett, W. D. Jpn J Pharmacol **2002**, 88, 50.

(103) Mukherjee, T. K.; Mishra, A. K.; Mukhopadhyay, S.; Hoidal, J. R. J Immunol **2007**, 178, 1835-1844.

(104) Rahman, I. Biochem Pharmacol **2000**, 60, 1041-1049.

(105) Elder, A.; Johnston, C.; Gelein, R.; Finkelstein, J.; Wang, Z.; Notter, R.; Oberdorster, G. Exp Lung Res **2005**, 31, 527-546.

(106) Donaldson, K.; Stone, V.; Seaton, A.; MacNee, W. Environ Health Persp **2001**, 109, 523-527.

(107) Donaldson, K.; MacNee, W. Int J Hyg Environ Health **2001**, 203, 411-415.

(108) Stadnyk, A. W. Faseb J **1994**, 8, 1041-1047.

(109) Whicher, J. T.; Evans, S. W. Clin Chem **1990**, 36, 1269-1281.

(110) Brown, D. M.; Donaldson, K.; Borm, P. J.; Schins, R. P.; Dehnhardt, M.; Gilmour, P.; Jimenez, L. A.; Stone, V. Am J Physiol-Lung C **2004**, 286, L344-L353.

(111) Resnick, N.; Gimbrone, M. A. Faseb J **1995**, 9, 874-882.

(112) Read, M. A.; Whitley, M. Z.; Williams, A. J.; Collins, T. J Exp Med **1994**, 179, 503-512.

(113) Beg, A. A.; Baldwin, A. S. Gene Dev **1993**, 7, 2064-2070.

(114) Thompson, J. E.; Phillips, R. J.; Erdjumentbromage, H.; Tempst, P.; Ghosh, S. Cell **1995**, 80, 573-582.

(115) Rahman, I.; MacNee, W. Thorax **1998**, 53, 601-612.

(116) Stacey, K. J.; Sweet, M. J.; Hume, D. A. J Immunol **1996**, 157, 2116-2122.

(117) Hou, J. Z.; Baichwal, V.; Cao, Z. D. P Natl Acad Sci USA **1994**, 91, 11641-11645.

(118) Jahnke, A.; Johnson, J. P. Febs Letters **1994**, 354, 220-226.

(119) Yuo, A.; Kitagawa, S.; Ohsaka, A.; Saito, M.; Takaku, F. Biochem Bioph Res 1990, 171, 491-497.

(120) Khwaja, A.; Carver, J. E.; Linch, D. C. Blood **1992**, 79, 745-753.

(121) Yong, K. L.; Rowles, P. M.; Patterson, K. G.; Linch, D. C. Blood **1992**, 80, 1565-1575.

(122) Schmal, H.; Shanley, T. P.; Jones, M. L.; Friedl, H. P.; Ward, P. A. J Immunol **1996**, 156, 1963-1972.

(123) Dustin, M. L.; Springer, T. A. J Cell Biol **1988**, 107, 321-331.

(124) Dustin, M. L.; Carpen, O.; Springer, T. A. J Immunol **1992**, 148, 2654-2663.

(125) Springer, T. A. Cell **1994**, 76, 301-314.

(126) Osborn, L. Cell **1990**, 62, 3-6.

(127) Mccullou, J.; Carter, S. J.; Quie, P. G. J Lab Clin Med **1972**, 79, 886-894.

(128) Huber, H.; Fudenber,H. Int Arch Allergy Immunol **1968**, 34, 18-27.

(129) Babior, B. M. N Eng J Med **1978**, 298, 659-668.

(130) Badwey, J. A.; Karnovsky, M. L. Annu Rev Biochem **1980**, 49, 695-726.

(131) Hirsch, J. G.; Strauss, B. J Immunol **1964**, 92, 145-154.

(132) Karnovsky, M. L.; Sbarra, A. J. Fed Proc **1959**, 18, 257-257.

(133) Sbarra, A. J.; Karnovsky, M. L. J Biol Chem **1959**, 234, 1355-1362.

(134) Hirsch, J. G.; Cohn, Z. A. Fed Proc **1964**, 23, 1023-1027.

(135) Baldridge, C. W.; Gerard, R. W. Am J Physiol **1933**, 103, 235-236.

(136) Babior, B. M. N Eng J Med **1978**, 298, 1478-1478.

(137) Iyer, G. Y. N.; Quastel, J. H. Can J Biochem Phys **1963**, 41, 427-434.

(138) Patriarc, P.; Cramer, R.; Moncalvo, S.; Rossi, F.; Romeo, D. Arch Biochem Biophys **1971**, 145, 255-263.

(139) Babior, B. M.; Curnutte, J. T.; Mcmurrich, B. J. J Clin Invest **1976**, 58, 989-996.

(140) Babior, B. M.; Curnutte, J. T.; Mcmurrich, B. J. Clin Res **1976**, 24, A436-A436.

(141) Takanaka, K.; Obrien, P. J. Arch Biochem Biophys **1975**, 169, 428-435.

(142) Takanaka, K.; Obrien, P. J. Arch Biochem Biophys **1975**, 169, 436-442.

(143) Klebanof, S. J. J Exp Med **1967**, 126, 1063-1078.

(144) Klebanof, S. J. J Clin Invest **1967**, 46, 1078-1081.

(145) Klebanof, S. J. J Bacteriol **1968**, 95, 2131-2138.

(146) Harrison, J. E. Schultz, J. J Biol Chem **1976**, 251, 1371-1374.

(147) Lawrence, E. Henderson's Dictionary of biological terms. 11 ed.; Longman scientific and technical :Singapore, **1995**.

(148) Stearns,R.C.;Pauluskis,J.D.; Audus,K.L. J. Am J Respir Cell Mol Biol **2001**,24,108-115.

(149) Forster, K. A.; Yazdanian, M.; Audus,K. L. J Pharm Pharmacol **2001**,53,57-66.

(150) Goldfischer,S.;Kikkawa,Y.;Hoffman,L. J Histochem Cytochem **1968**,16,102-109.

(151) Williams, M.C. Proc Natl Acad Sci USA **1984**,81, 6054-6058.

(152) Schnitzler, N.; Haase, G.; Podbielski, A.; Lutticken, R.; Schweizer, K. G. Nature Med **1999**, 5, 231-235.

(153) Humlicek, A. L.; Pang, L. Y.; Look, D. C. Am J Physiol-Lung C **2004**, 287, L598-L607.

(154) Vanseventer, G. A.; Shimizu, Y.; Horgan, K. J.; Shaw, S. J Immunol **1990**, 144, 4579-4586.

(155) Tsukada, N.; Miyagi, K.; Matsuda, M.; Yanagisawa, N. Ann Neurol **1993**, 33, 646-649.

(156) Chihara, J.; Yamamoto, T.; Kurachi, D.; Nakajima, S. Lancet **1994**, 343, 1108-1108.

(157) Marlin, S. D.; Staunton, D. E.; Springer, T. A.; Stratowa, C.; Sommergruber, W.; Merluzzi, V. J. Nature **1990**, 344, 70-72.

(158) Martin, S.; Martin, A.; Staunton, D. E.; Springer, T. A. Antimicrob Agents Chemother **1993**, 37, 1278-1285.

(159) Fakler, C. R.; Wu, B.; McMicken, H. W.; Geske, R. S.; Welty, S. E. Inflamm Res **2000**, 49, 63-72.

(160) Piedboeuf, B.; Frenette, J.; Petrov, P.; Welty, S. E.; Kazzaz, J. A.; Horowitz, S. Am J Resp Cell Mol **1996**, 15, 71-77.

(161) Vincent, R.; Bjarnason, S. G.; Adamson, I. Y. R.; Hedgecock, C.; Kumarathasan, P.; Guenette, J.; Potvin, M.; Goegan, P.; Bouthillier, L. Am J Pathol **1997**, 151, 1563-1570.

(162) Biran, R.; Tang, Y. Z.; Brook, J.; Vincent, R.; Keeler, G. Int J Environ Anal Chem **1996**, 63, 315-322.

(163) Lieber, M.; Smith, B.; Szakal, A.; Nelsonrees, W.; Todaro, G. Int J Cancer **1976**, 17, 62-70.

(164) Speit, G.; Bonzheim, I. Mutagenesis **2003**, 18, 545-548.

(165) Finlayson-Pitts, B. J.; Ezell, M. J.; Pitts, J. N. Nature **1989**, 337, 241-244.

(166) Prospero, J. M.; Charlson, R. J.; Mohnen, V.; Jaenicke, R.; Delany, A. C.; Moyers, J.; Zoller, W.; Rahn, K. Rev Geophy **1983**, 21, 1607-1629.

(167) Blanchard, D. C.; Woodcock, A. H. B Am Meteorol Soc **1979**, 60, 1257.

(168) Hoffman, R. C.; Laskin, A.; Finlayson-Pitts, B. J. J Aerosol Sci **2004**, 35, 869-887.

(169) Weis, D. D.; Ewing, G. E. J Geophys Res-Atmos **1999**, 104, 21275-21285.

(170) Dai, D. J.; Peters, S. J.; Ewing, G. E. J Phys Chem **1995**, 99, 10299-10304.

(171) Sloane, C. S.; Elmoursi, A. A. Ieee T Ind Appl **1989**, 25, 711-719.

(172) Chung, S. K.; Trinh, E. H. J Cryst Growth **1998**, 194, 384-397.

(173) Rhim, W. K.; Chung, S. K. J Cryst Growth **1991**, 110, 293-301.

(174) Mund, C.; Zellner, R. Chemphyschem **2003**, 4, 638-645.

(175) Ashkin, A.; Dziedzic, J. M. Science **1975**, 187, 1073-1075.

(176) Musick, J.; Popp, J.; Kiefer, W. J Raman Spectrosc **2000**, 31, 217-219.

(177) Seaver, M.; Galloway, A.; Manuccia, T. J. Rev Sci Instrum **1989**, 60, 3452-3459.

(178) Davis, E. J.; Rassat, S. D.; Foss, W. J. Aeosol Sci **1992**, 23.

(179) Cao, Y. M.; Xie, W. J.; Sun, J.; Wei, B. B.; Lin, S. J Appl Polym Sci **2002**, 86, 84-89.

(180) Vehring, R.; Aardahl, C. L.; Davis, E. J.; Schweiger, G.; Covert, D. S. Rev Sci Instrum **1997**, 68, 70-78.

(181) Olsen, A. P.; Flagan, R. C.; Kornfield, J. A. Rev Sci Instrum **2006**, 77, 73901-73907.

(182) Hoffmann, G. G.; Lentz, E.; Schrader, B. Rev Sci Instrum **1993**, 64, 823-824.

(183) Millikan, R. A. The electron, its isolation, measurement and determination of some its properties; University of Chicago press: Chicago, **1971**.

(184) Haddrell, A. E.; van Eeden, S. F.; Agnes, G. R. Toxicol *in Vitro* **2006**, 20, 1030-1039.

(185) Eleghasim, N. M.; Haddrell, A. E.; van Eeden, S.F.; Agnes, G. R. Int. J Mass Spect **2006**, 258, 134-141.

(186) Vincent, R.; Bjarnason, S. G.; Adamson, I. Y.; Hedgecock, C.; Kumarathasan, P.; Guenette, J.; Potvin, M.; Goegan, P.; Bouthillier, L. Am. J. Path. **1997**, 151, 1563-1570.

(187) Harrison, R. G. P Soc Exp Biol Med **1907**, 4, 140-143.

(188) Harrison, R. G. J Exp Zool **1910**, 9, 787-U727.

(189) Harrison, R. G. Arch Entwicklung Org **1910**, 30, 15-33.

(190) Carrel, A. J Exp Med **1912**, 15, 516-U530.

(191) Glinos, A. D.; Gey, G. O. Cancer Res **1952**, 12, 265-265.

(192) Eagle, H. Science **1955**, 122, 501-504.

(193) Buonassisi, V.; Cohen, A. I.; Sato, G. P Natl Acad Sci USA **1962**, 48, 1184-1190.

(194) Yaffe, D. P Natl Acad Sci USA **1968**, 61, 477-483.

(195) Bottenstein, J. E.; Sato, G. H. P Natl Acad Sci USA **1979**, 76, 514-517.

(196) Stearns, R. C.; Paulauskis, J. D.; Godleski, J. J. Am J Resp Cell Mol **2001**, 24, 108-115.

(197) Mulligan, M. S.; Vaporciyan, A. A.; Warner, R. L.; Jones, M. L.; Foreman, K. E.; Miyasaka, M.; Todd, R. F.; Ward, P. A. J Immunol **1995**, 154, 1350-1363.

(198) Limper, A. H. Am J Resp Cell Mol **1997**, 16, 110-111.

(199) Pelletier, M.; Lavastre, V.; Girard, D. Toxicol Sci **2002**, 69, 210-216.

(200) Chang, C. H.; Huang, Y.; Issekutz, A. C.; Griffith, M.; Lin, K. H.; Anderson, R. J Virol **2002**, 76, 427-431.

(201) Reilly, P. L.; Woska, J. R.; Jeanfavre, D. D.; Mcnally, E.; Rothlein, R.; Bormann, B. J. J Immunol **1995**, 155, 529-532.

(202) Morgan, T. E. N Eng J Med **1971**, 284, 1185-1195.

(203) Bost, F.; McKay, R.; Dean, N.; Mercola, D. Clin Chem **1997**, 43, 56.

(204) Jiang, F. N.; Liu, D. J.; Neyndorff, H.; Chester, M.; Jiang, S. Y.; Levy, J. G. J Natl Cancer Inst **1991**, 83, 1218-1225.

(205) Vangipuram, S. D.; Sheele, J.; Atkinson, R. L.; Holland, T. C.; Dhurandhar, N. V. Obes Res **2004**, 12, 770-777.

(206) Eagle, H. Science **1959**, 130, 432-437.

(207) Rose, W. C.; Haines, W. J.; Warner, D. T. J Biol Chem **1954**, 206, 421-430.

(208) Tozer, B. T.; Pirt, S. J. Nature **1964**, 201, 375-377.

(209) Rose, W. C.; Leach, B. E.; Coon, M. J.; Lambert, G. F. J Biol Chem **1955**, 213, 913-922.

(210) Rose, W. C.; Coon, M. J.; Lockhart, H. B.; Lambert, G. F. J Biol Chem **1955**, 215, 101-110.

(211) Rose, W. C.; Eades, C. H.; Coon, M. J. J Biol Chem **1955**, 216, 225-234.

(212) Eagle, H.; Oyama, V. I.; Levy, M.; Freeman, A. E. J Biol Chem **1957**, 226, 191-205.

(213) Freshney, R. I. Culture of animal cells: A manual of basic techniques; Wiley-Liss publisher: New Tork, **2005**.

(214) Eagle, H.; Oyama, V. I.; Levy, M.; Freeman, A. Science **1956**, 123, 845-847.

(215) Eagle, H. J Exp Med **1955**, 102, 595-600.

(216) Vogt, A.; Mishell, R. I.; Dutton, R. W. Exp Cell Res **1969**, 54, 195-201.

(217) Guilbert, L. J.; Iscove, N. N. Nature **1976**, 263, 594-595.

(218) Iscove, N. N.; Melchers, F. J Exp Med **1978**, 147, 923-933.

(219) Yamada, K. M.; Geiger, B. Curr Opin Cell Biol **1997**, 9, 76-85.

(220) Hynes, R. O. Cell **1992**, 69, 11-25.

(221) Fisher, H. W.; Puck, T. T.; Sato, G. P Natl Acad Sci USA **1958**, 44, 4-10.

(222) Devonne, T. L.; Mouray, H. Clin Chim Acta **1978**, 90, 83-85.

(223) Maciag, T.; Cerundolo, J.; Ilsley, S.; Kelley, P. R.; Forand, R. P Natl Acad Sci USA **1979**, 76, 5674-5678.

(224) Stiles, C. D.; Capone, G. T.; Scher, C. D.; Antoniades, H. N.; Vanwyk, J. J.; Pledger, W. J. P Natl Acad Sci USA **1979**, 76, 1279-1283.

(225) Joukov, V.; Kaipainen, A.; Jeltsch, M.; Pajusola, K.; Olofsson, B.; Kumar, V.; Eriksson, U.; Alitalo, K. J Cell Physiol **1997**, 173, 211-215.

(226) Folkman, J.; Haudenschild, C. C.; Zetter, B. R. P Natl Acad Sci USA **1979**, 76, 5217-5221.

(227) Kelley, D. S.; Becker, J. E.; Vanpotter, R. Cancer Res **1978**, 38, 4591-4600.

(228) Ballard, P. L.; Tomkins, G. M. Nature **1969**, 224, 344-345.

(229) Fredin, B. L.; Seifert, S. C.; Gelehrter, T. D. Nature **1979**, 277, 312-313.

(230) Guner, M.; Freshney, R. I.; Morgan, D.; Freshney, M. G.; Thomas, D. G. T.; Graham, D. I. Brit J Cancer **1977**, 35, 439-447.

(231) Mclean, J. S.; Freshney, R. I. Eur J Cell Biol **1986**, 42, 27-27.

(232) Ham, R. G.; Mckeehan, W. L. In Vitro Cell Dev B **1978**, 14, 11-22.

(233) Sternberger, L. A. Immunocytochemistry; Prentice-Hall, Inc.: New Jersey, **1974**.

(234) Reiner, L. Science **1930**, 72, 483-484.

(235) Heidelberger, M.; Kendall, F. E. J Exp Med **1934**, 59, 519-528.

(236) Marrack, J. Nature **1934**, 133, 292-293.

(237) Coons, A. H.; Creech, H. J.; Jones, R. N. P Soc Exp Biol Med **1941**, 47, 200-202.

(238) Coons, A. H.; Snyder, J. C.; Cheever, F. S.; Murray, E. S. J Exp Med **1950**, 91, 31-38.

(239) Hill, A. G. S.; Deane, H. W.; Coons, A. H. J Exp Med **1950**, 92, 35-44.

(240) Coons, A. H.; Leduc, E. H.; Connolly, J. M. J Exp Med **1955**, 102, 49-60.

(241) van Kuppevelt, T. H.; Dennissen, M. A. B. A.; van Venrooij, W. J.; Hoet, R. M. A.; Veerkamp, J. H. J Biol Chem **1998**, 273, 12960-12966.

(242) Dowsett, M.; Bartlett, J.; Ellis, I. O.; Salter, J.; Hills, M.; Mallon, E.; Watters, A. D.; Cooke, T.; Paish, C.; Wencyk, P. M.; Pinder, S. E. J Pathol **2003**, 199, 418-423.

(243) Wang, H.; Pevsner, J. Cell Tissue Res **1999**, 296, 511-516.

(244) Than, G. N.; Sumegi, B.; Szekeres, G.; Bellyei, S.; Than, N. G.; Szigeti, A.; Bohn, H. J Obstet Gynaecol Res **2002**, 28, 8-12.

(245) Prikk, K.; Maisi, P.; Pirila, E.; Sepper, R.; Salo, T.; Wahlgren, J.; Sorsa, T. J Pathol **2001**, 194, 232-238.

(246) Dulbecco, R.; Vogt, M. J Exp Med **1954**, 99, 183-199.

(247) Wang, K.; Feramisco, J. R.; Ash, J. F. Method Enzymol **1982**, 85, 514-562.

(248) Horie, T.; Mizuma, T.; Kasai, S.; Awazu, S. Am J Physiol **1988**, 254, G465-G470.

(249) Tacha, D. E.; Mckinney, L. J Histotechnol **1992**, 15, 127-132.

(250) Simmons, D.; Makgoba, M. W.; Seed, B. Nature **1988**, 331, 624-627.

(251) Panchuk-Voloshina, N.; Haugland, R. P.; Bishop-Stewart, J.; Bhalgat, M. K.; Millard, P. J.; Mao, F.; Leung, W. Y. J Histochem Cytochem **1999**, 47, 1179-1188.

(252) Burnett, R. T.; Dales, R.; Krewski, D.; Vincent, R.; Dann, T.; Brook, J. R. Am J Epidemiol **1995**, 142, 15-22.

(253) Samet, J. M.; Dominici, F.; Curriero, F. C.; Coursac, I.; Zeger, S. L. N Eng J Med **2000**, 343, 1742-1749.

(254) Bates, D. V.; Sizto, R. Environ Res **1987**, 43, 317-331.

(255) Schwartz, J.; Slater, D.; Larson, T. V.; Pierson, W. E.; Koenig, J. Q. Am Rev Respir Dis **1993**, 147, 826-831.

(256) Bates, D. V.; Bakeranderson, M.; Sizto, R. Environ Res **1990**, 51, 51-70.

(257) Libby, P. Nature **2002**, 420, 868-874.

(258) Pope, C. A.; Burnett, R. T.; Thurston, G. D.; Thun, M. J.; Calle, E. E.; Krewski, D.; Godleski, J. J. Circulation **2004**, 109, 71-77.

(259) Brunekreef, B. Occup Environ Med **1997**, 54, 781-784.

(260) Hetland, R. B.; Cassee, F. R.; Refsnes, M.; Schwarze, P. E.; Lag, M.; Boere, A. J. F.; Dybing, E. Toxicol *in Vitro* **2004**, 18, 203-212.

(261) Gilmour, P. S.; Rahman, I.; Hayashi, S.; Hogg, J. C.; Donaldson, K.; MacNee, W. Am J Physiol-Lung **2001**, 281, L598-L606.

(262) Nel, A. Science **2005**, 308, 804-806.

(263) Zmirou, D.; Deloraine, A.; Balducci, F.; Boudet, C.; Dechenaux, J. J Occup Environ Med **1999**, 41, 847-856.

(264) Delucchi, M. A.; Murphy, J. J.; McCubbin, D. R. J Environ Manag **2002**, 64, 139-152.

(265) Zaim, K. K. Environ Manag **1999**, 23, 271-277.

(266) Anjilvel, S.; Asgharian, B. Fund Appl Toxicol **1995**, 28, 41-50.

(267) Cassee, F. R.; Muijser, H.; Duistermaat, E.; Freijer, J. J.; Geerse, K. B.; Marijnissen, J. C. M.; Arts, J. H. E. Arch Toxicol **2002**, 76, 277-286.

(268) Gilmour, P. S.; Brown, D. M.; Lindsay, T. G.; Beswick, P. H.; MacNee, W.; Donaldson, K. Occup Environ Med **1996**, 53, 817-822.

(269) Dye, J. A.; Lehmann, J. R.; McGee, J. K.; Winsett, D. W.; Ledbetter, A. D.; Everitt, J. I.; Ghio, A. J.; Costa, D. L. Environ Health Persp **2001**, 109, 395-403.

(270) Schins, R. P. F.; Lightbody, J. H.; Borm, P. J. A.; Shi, T. M.; Donaldson, K.; Stone, V. Toxicol Appl Pharmacol **2004**, 195, 1-11.

(271) Guo, H.; Lee, S. C.; Ho, K. F.; Wang, X. M.; Zou, S. C. Atmos Environ **2003**, 37, 5307-5317.

(272) Burrell, R.; Rylander, R. Environ Res **1982**, 27, 325-336.

(273) Helander, I.; Saxen, H.; Salkinojasalonen, M.; Rylander, R. Infect Immunol **1982**, 35, 528-532.

(274) Baseler, M. W.; Fogelmark, B.; Burrell, R. Infect Immunol **1983**, 40, 133-138.

(275) Donaldson, K.; Stone, V.; Tran, C. L.; Kreyling, W.; Borm, P. J. A. Occup Environ Med **2004**, 61, 727-728.

(276) Brown, D. M.; Wilson, M. R.; MacNee, W.; Stone, V.; Donaldson, K. Toxicol Appl Pharmacol **2001**, 175, 191-199.

(277) Ghio, A. J.; Huang, Y. C. T. Inhal Toxicol **2004**, 16, 53-59.

(278) Omara, F. O.; Fournier, M.; Vincent, R.; Blakley, B. R. J Toxicol Environ Health A **2000**, 59, 67-85.

(279) Fujii, T.; Hayashi, S.; Hogg, J. C.; Vincent, R.; Van Eeden, S. F. Am J Resp Cell Mol **2001**, 25, 265-271.

(280) Travis, S. M.; Singh, P. K.; Welsh, M. J. Curr Opin Immunol **2001**, 13, 89-95.

(281) Look, D. C.; Rapp, S. R.; Keller, B. T.; Holtzman, M. J. Am J Physiol **1992**, 263, L79-L87.

(282) Infeld, M. D.; Brennan, J. A.; Davis, P. B. Am J Physiol **1992**, 262, L535-L541.

(283) Schauer, J. J. J Expo Anal Environ Epidemiol **2003**, 13, 443-453.

(284) Goto, Y.; Hogg, J. C.; Shih, C. H.; Ishii, H.; Vincent, R.; van Eeden, S. F. Am J Physiol-Lung **2004**, 287, L79-L85.

(285) Catley, M. C.; Cambridge, L. M.; Nasuhara, Y.; Ito, K.; Chivers, J. E.; Beaton, A.; Holden, N. S.; Bergmann, M. W.; Barnes, P. J.; Newton, R. J Biol Chem **2004**, 279, 18457-18466.

(286) Hoare, G. S.; Chester, A. H.; Yacoub, M. H.; Marczin, N. Int J Mol Med **2002**, 9, 35-44.

(287) Haddrell, A. E.; Ishii, H.; van Eeden, S. F.; Agnes, G. R. Anal. Chem. **2005**, 77, 3623-3628.

(288) March, R. E. Rapid Commun Mass Spectrom **1998**, 12, 1543-1554.

(289) Davis, E. J.; Buehler, M. F.; Ward, T. L. Rev Sci Instrum **1990**, 61, 1281-1288.

(290) Davis, E. J. Aerosol Sci Technol **1997**, 26, 212-254.

(291) Turnbull, A. B.; Harrison, R. M. Atmos Environ **2000**, 34, 3129-3137.

(292) Monn, C.; Becker, S. Toxicol Appl Pharmacol **1999**, 155, 245-252.

(293) Nel, A.; Xia, T.; Madler, L.; Li, N. Science **2006**, 311, 622-627.

(294) Schwarze, P. E.; Hetland, R. B.; Refsnes, M.; Lag, M.; Becher, R. Int J Hyg Environ Health **2002**, 204, 327-331.

(295) Wilson, W. E.; Chow, J. C.; Claiborn, C.; Wei, F. S.; Engelbrecht, J.; Watson, J. G. Chemosphere **2002**, 49, 1009-1043.

(296) Zelikoff, J. T.; Schermerhorn, K. R.; Fang, K. J.; Cohen, M. D.; Schlesinger, R. B. Environ Health Persp **2002**, 110, 871-875.

(297) Gavett, S. H.; Haykal-Coates, N.; Copeland, L. B.; Heinrich, J.; Gilmour, M. I. Environ Health Persp **2003**, 111, 1471-1477.

(298) Schaumann, F.; Borm, P. J. A.; Herbrich, A.; Knoch, J.; Pitz, M.; Schins, R. P. F.; Luettig, B.; Hohlfeld, J. M.; Heinrich, J.; Krug, N. Am J Resp Crit Care **2004**, 170, 898-903.

(299) Schwarze, P. E.; Ovrevik, J.; Lag, M.; Refsnes, M.; Nafstad, P.; Hetland, R. B.; Dybing, E. Hum Exp Toxicol **2006**, 25, 559-579.

(300) Goldman, L. R. Environ Health Persp **1998**, 106, 857-862.

(301) London, S. J.; Romieu, I. Lancet **2000**, 356, 946-946.

(302) Smith, L. E.; Denissenko, M. F.; Bennett, W. P.; Li, H. Y.; Amin, S.; Tang, M. S.; Pfeifer, G. P. J Natl Cancer Inst **2000**, 92, 803-811.

(303) Lan, Q.; Mumford, J. L.; Shen, M.; DeMarini, D. M.; Bonner, M. R.; He, X. Z.; Yeager, M.; Welch, R.; Chanock, S.; Tian, L. W.; Chapman, R. S.; Zheng, T. Z.; Keohavong, P.; Caporaso, N.; Rothman, N. Carcinogenesis **2004**, 25, 2177-2181.

(304) Oortgiesen, M.; Veronesi, B.; Eichenbaum, C.; Kiser, P. F.; Simon, S. A. Am J Physiol-Lung C **2000**, 278, L683-L695.

(305) Brewer, R.; Belzer, W. Atmos Environ **2001**, 35, 5223-5233.

(306) Adamson, I. Y. R.; Prieditis, H.; Hedgecock, C.; Vincent, R. Toxicol Appl Pharmacol **2000**, 166, 111-119.

(307) Campen, M. J.; Nolan, J. P.; Schladweiler, M. C. J.; Kodavanti, U. P.; Evansky, P. A.; Costa, D. L.; Watkinson, W. P. Toxicol Sci **2001**, 64, 243-252.

(308) Salnikow, K.; Li, X. M.; Lippmann, M. Toxicol Appl Pharmacol **2004**, 196, 258-265.

(309) Costa, D. L.; Dreher, K. L. Environ Health Persp **1997**, 105, 1053-1060.

(310) Merolla, L.; Richards, R. J. Exp Lung Res **2005**, 31, 671-683.

(311) Dybing, E.; Lovdal, T.; Hetland, R. B.; Lovik, M.; Schwarze, P. E. Toxicology **2004**, 198, 307-314.

(312) Huntzicker, J. J.; Heyerdahl, E. K.; Mcdow, S. R.; Rau, J. A.; Griest, W. H.; Macdougall, C. S. J Air Pollut Control Assoc **1986**, 36, 705-709.

(313) Gray, H. A.; Cass, G. R.; Huntzicker, J. J.; Heyerdahl, E. K.; Rau, J. A. Environ Sci Technol **1986**, 20, 580-589.

(314) Stohs, S. J.; Bagchi, D. Free Radical Bio Med **1995**, 18, 321-336.

(315) Klaunig,J.M.;Xu,Y.;Isenberg,J.S.;Bochowski,S.;Kolaja,K.L.;Jiang,J.K. Environ Health Perspect **1998**,106,289-295.

(316) Stohs,S.; Bagchi, D. Free Radical Biol Med **1995**,18,321-336.

(317) Sugawara,E.;Nakamura,K.; Miyake,T.; Fukumura, A.;Seki,Y. Br J Ind Med **1995**,18,321-336.

(318) Mankin, W. G.; Coffey, M. T. Science **1984**, 226, 170-172.

(319) Umeno, E.; Mcdonald, D. M.; Nadel, J. A. J Clin Invest **1990**, 85, 1905-1908.

(320) Takeuchi, M.; Okura, T.; Mori, T.; Akita, K.; Ohta, T.; Ikeda, M.; Ikegami, H.; Kurimoto, M. Cell Tissue Res **1999**, 297, 467-473.